



FTS THESIS
629.252 COS
30001007614367
Cosic, Ivan
Development and testing of a
variable valve timing system
(VVT) for a twincam

ACKNOWLEDGEMENT

I would like to gratefully thank my supervisor, Kevin Hunt and my co-supervisor Mark Armstrong for their valuable guidance, patience and advice. Without their support this project would not have been possible.

I am grateful to Professor Geoffrey Lleonart for his patience and advice in the correction of my thesis.

I wish to thank the technical staff at the School of Built Environment, especially Laurance Martin and Harry Friedrich for constructing the cylinder head test rig and practical assistance.

I wish to thank Bruce Cameron from Holden Australia for his kind donation of a Holden Vectra 2.0 litre twincam engine for the project.

I am thankful to MSC Software for their support and advice in ADAMS software.

Finally, I would like to thank my entire family for their support.

TABLE OF CONTENTS

ABSTRACT	v
1. INTRODUCTION	1
1.1 Background	1
1.2 Variable Valve Timing	3
1.3 Aim	4
1.4 Approach	4
2. LITERATURE REVIEW	5
2.1 Introduction	5
2.2 Phase Changing	5
2.3 Cam Changing	10
2.4 Intake Valve Closing	15
2.5 Lost Motion Valves	18
2.6 Electrically Actuated Valves	19
2.7 Hydraulically Actuated Valves	20
2.8 Valves Actuated by Two Cams in Parallel	21
2.9 Literature Review Summary	22
3. METHODS AND EQUIPMENT	23
3.1 Introduction	23
3.2 Engine Specification	23
3.3 Cylinder Head Test Rig	24
3.4 Laser Displacement Sensor	25
3.5 DTVEE Software	28

3.6 Vectra Engine Cylinder Head Valve Profile	29
3.7 Hertzian Contact Theory	30
4. RESULTS AND DISCUSSION	33
4.1 Computer Simulation	33
4.2 DVC Components	33
4.2.1 Constraints	39
4.3 Dynamic Valve Control	47
4.4 Simulation Results	51
4.4.1 DVC Valve Profile	52
4.4.2 Valve Velocity and Acceleration Results	69
4.5 Force and Stress Analysis of Components	81
4.5.1 Forces Acting on DVC Components	82
4.5.2 Stress Analysis	93
4.5.3 Hertz Contact Pressure	99
5. CONCLUSIONS AND RECOMMENDATIONS	100
5.1 Conclusions	100
5.2 Recommendations	101
6. REFERENCES	102
APPENDIX A	107
APPENDIX B	111
APPENDIX C	112

ABSTRACT

Variable valve timing (VVT) is an innovative design that enhances automotive engine performance and is important in addressing fuel consumption and emission output concerns. The purpose of the research reported here was to examine the concept of a VVT system because it had the promise of application in the advancement of engine technology.

In this study, a new VVT system, termed the dynamic valve control (DVC) system was developed. The DVC system was modeled using the computer simulation software package ADAMS, which determined the forces acting on the principal components at operational speeds, as well as the valve timing and lift profile of the system. Stress analysis of the rocker arm was carried out using Cosmos/DesignStar software. The valve timing and lift characteristics of the DVC system were compared to an existing standard production engine.

The results of the study showed that the proposed DVC system can essentially realise closure of its valves and achieve variable valve lift. In addition, the DVC system valve timing and lift profile showed better characteristics when compared with those of an existing Holden Vectra 2.0 litre twincam engine.

1. INTRODUCTION

1.1 Background

Resources of fossil fuels are finite and if they are to be used to provide energy for transport they must be used efficiently. There are also strong pressures to make automotive vehicles less environmentally polluting and one of the most important factors in reducing global warming is the increased use of vehicles with better fuel economy. The U.S Department of Energy (1998) concluded that for every litre of fuel burnt in a vehicle, 9 kilograms of carbon dioxide, a greenhouse gas pollutant, is transferred into the atmosphere. By choosing a vehicle with a fuel consumption of 50 kilometres rather than 40 kilometres per litre can prevent approximately 10000 kilograms of carbon dioxide from being released over the lifetime of a vehicle.

About 15% of the energy in the fuel is used to propel a vehicle, the rest of the energy is lost to atmosphere. Automobiles need energy to accelerate, and to overcome air resistance and the friction from tires, wheels and axles. Fuel provides the needed energy in the form of chemicals that can be combusted to release heat. Engines transform heat released in combustion into useful work that ultimately turns the vehicle wheels, propelling it along the road, see U.S Department of Energy (2001).

Over the last decade there has been a significant improvement in the fuel consumption of vehicles and as a result they have become less polluting. The most effective way to increase horsepower and /or efficiency is to increase an engine's ability to process air. Since the engine valves play a major role in controlling the flow of air/fuel mixture into and out of the cylinders, it is important to study the role of engine valve systems in relation to improving the efficiency of automotive engines.

Valves activate the airflow of an automotive engine. The timing of air-intake and exhaust is controlled by the shape and phase angle of cams. To optimise the air-flow, engines require different valve timings at different speeds, and it has been found beneficial to open the inlet valve earlier and close the exhaust valve later. In other words, the overlapping between the

intake and exhaust periods should be increased as the engine speed increases.

Overlap refers to the period when both the intake and exhaust valves are open at the same time. When the intake valve is opened before the exhaust valve closes, a scavenging effect occurs, in which the rush of the exhaust out of the cylinder draws in a little more of the intake charge into the cylinder.

The valves of an engine do not open and close exactly when the piston reaches the top and bottom of its cycle. The intake valve begins to open before the piston reaches top dead centre (TDC), and closes after the piston reaches bottom dead centre (BDC). The exhaust valve begins to open as the piston reaches the bottom, and begins to close as the piston reaches the top. As the engine's speed increases, air in the manifold gains momentum, and even when the piston reaches BDC, air continues to be drawn into the cylinder. Thus, to obtain as much air as possible in the cylinder without causing inefficiencies from inertial forces, it is desirable to have the valve timing change with the engine speed.

Previously, manufacturers have used one or more camshafts to open and close an engine's valves. The camshaft is turned by a timing chain connected to the crankshaft and as the engine speed increases or decreases, the crankshaft and camshaft rotate to keep the valve timing close to that needed for engine operation. Increased valve duration (the length of time that the valves are held open) yields greater power at high speed but reduces torque at low speed. While a greater valve lift (distance that the valves are opened, usually expressed in millimetres) without increasing duration, yields more power without much change in the nature of the power curve. Generally it is impractical to optimise the valve timing for both high and low engine speed with a simple crankshaft-driven valve train. As a result, engine designers have to compromise timing in the specification of the camshaft. For example, an ordinary sedan has its valve timing optimized for mid-range engine speed so that both low speed driving ability and high-speed output do not significantly suffer. However, this compromise results in wasted fuel and reduced performance beyond the optimized speed range, see Brauer (1999).

1.2 Variable Valve Timing

As technology has advanced, so too has the development of engine design and nowadays it is normal for modern vehicles to have multi-valve technology. Variable valve timing (VVT) is seen as the next step to enhance engine efficiency.

Variable valve timing was first introduced as an innovative design that increased engine torque and output while addressing environmental issues, such as pollutants emitted from automotive engines. The variable valve timing system uses an electronic system, known as the engine control unit (ECU) to electronically control the operation of the engine valves. The system is able to detect the engine speed and adjust the valve timing accordingly. As a consequence, more oxygen can be supplied through the air intake valve as more fuel is injected into the combustion chamber. Greater fuel and oxygen in the combustion chamber leads to increased power and torque.

Most variable valve timing systems are combined with lift control, which varies the lift of the intake and exhaust valves while the engine is operating at high speed. As the intake and exhaust valve lift increases, a larger volume of air/fuel mixture is introduced, along with ejection of a greater volume of exhaust gas. This results in the engine producing higher output power while operating at high speeds. The variable valve timing system allows the valve timing of an automotive engine to be ideally fixed by increasing the valve lift when the engine speed is high, which results in improved fuel economy.

In principle, variable valve timing improves fuel efficiency and performance because it adjusts the valve timing between high and low engine speeds for optimum performance, thus efficiency throughout the entire speed range can be improved.

The variable valve timing system proposed in this study called the dynamic valve control system (DVC) is a unique system based on the concept of varying the degree of valve lift, the duration of valve opening and capable of virtual closure of the valves.

1.3 Aim

The aim of the research program reported here was to develop a computer based model of a variable valve timing system, developed by my co-supervisor Mark Armstrong, called dynamic valve control (DVC) for automotive engines.

1.4 Approach

The present study represents the initial stage of a research and development program involving the design and construction on an experimental DVC system to be fitted to an existing automotive engine.

To achieve this aim a computer simulation model showing the operation of the DVC system was constructed using ADAMS software. This virtual model was used to establish a geometry that improves engine performance. The forces acting on the rocker arm of the DVC system were analysed, enabling the design of this component to be refined. In addition, the valve timing and lift characteristics of a current production engine were compared to the DVC system's valve timing sequencing.

2. LITERATURE REVIEW

2.1 Introduction

Many mechanisms have been proposed to produce variable valve timing systems. Each mechanism varies the valve timing either in duration, phase, or both. There are numerous versions of VVT mechanisms in production today, and these VVT systems can be basically classified into seven VVT models, which are reviewed below.

2.2 Phase Changing

Cam phasing VVT is the simplest, cheapest and most common mechanism used presently. Basically, it varies the valve timing by shifting the phase angle of camshafts relative to the crankshaft. Wilson et al. (1993), concluded that intake and exhaust camshafts can be simultaneously varied with notable improvements in fuel economy and emission reduction, this was also confirmed by Ashley (1995).

The phase angle can be shifted either by the use of a phasing actuator, whereby the change in phase angle is produced by adjusting the hydraulic flows in and out of the actuator chambers or with the camshaft drive being connected to the camshaft through a helical spline. The latter mechanism was employed by Maekawa (1989). The phase angle between the driveshaft and the camshaft was changed as the idler gear was moved axially along the camshaft or vice-versa.

Wilson et al. concluded that high performance double overhead cam (DOHC) engines had a long valve open duration, high valve lift and produced maximum power output. However, the large valve overlap caused poor idle stability and also reduced engine torque at low speeds.

Moriya et al. (1996) developed the Intelligent Variable Valve Timing (VVT-I), as depicted in Figure 2.1. The VVT-I system varies the valve timing by shifting the phase angle of camshafts and only responds when the valves open and close in relation to engine speed. It basically consists of three parts:

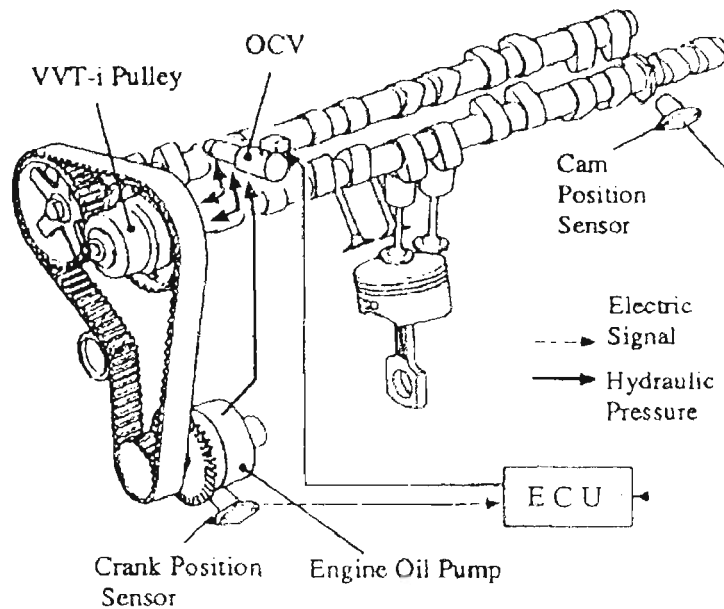


Figure 2.1 – VVT- I system

- (1) VVT-I Pulley - Located at the front end of the intake camshaft, it produces a timing difference between the intake camshaft and the crankshaft by a hydraulic actuator.
- (2) Oil Control Valve (OCV) - Controls oil pressure to the VVT-I pulley according to ECU command and continually controlling oil feeding and draining between the VVT-I Pulley and OCV achieves continual phasing.
- (3) Engine Control Unit (ECU) - Computes optimal valve timing based on the engine operating condition and drives the OCV. The OCV control current is determined by comparing the target advance angle, according to the engine operating condition, with actual advance angle.

Titolo (1991) investigated the use of a Fiat VVT system for use in a V8 engine. The VVT device comprised :

(1) A multi-dimensional cam-follower assembly

(2) An actuator regulator assembly

The multi-dimensional cam follower varies the valve opening/closing, both in phase and in lifting. The actuator regulator assembly changes the cam-follower position by means of an axial displacement of the camshaft, which takes place continuously as a function of engine speed.

When the engine is running, the rotation of the camshaft begins to open the intake or the exhaust valve. At the beginning of valve opening, an oscillating plate is in a nearly horizontal position. As the valve lift increases, the plate changes its inclination until it assumes the maximum inclination at maximum lift. During the valve-closing phase, the maximum plate inclination returns to a horizontal position.

Steinberg et al. (1998) developed a fully continuous variable camshaft timing (VCT) system which can be applied to both intake and exhaust camshafts. The VCT system is shown in Figure 2.2.

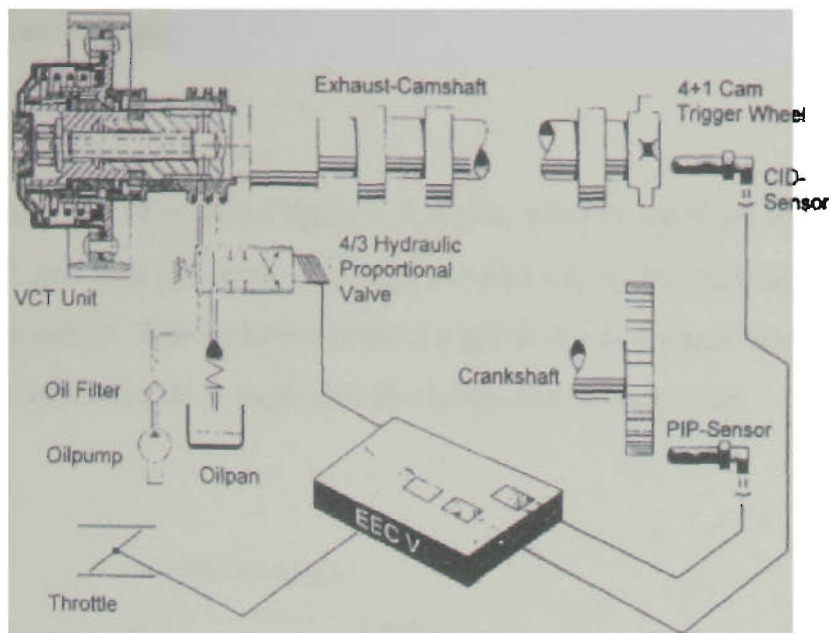


Figure 2.2 – VCT system

Sensors and triggerwheels are used to measure the camshaft position relative to Top Dead Centre (TDC). The engine management system processes these data to continuously control the cam position via an electric current to the solenoid.

A cylindrical component, which has helical gears on its exterior and interior surface, is fitted between the camshaft pulley and the camshafts end. The gear on the exterior surface meshes with a corresponding gear in the bore of the camshaft pulley, while the interior gear meshes with a gear mounted on the end of the camshaft. Opposite the camshaft, a piston is moved axially by oil pressure depending on the camshaft position. The axial movement is transformed into a rotation of the camshaft relative to the timing pulley. Leone et al. (1996) concluded that there were three benefits to the VCT system. Firstly, NO_x is reduced due to the increased internal residual, secondly, unburned Hydrocarbons are reduced because they were drawn back into the cylinder to be “reburnt” during the next combustion cycle, and thirdly, the intake stroke pumping work was reduced.

Griffiths et al. (1988) developed their own phase changing VVT mechanism called the

Mitchell mechanical variable valve timing system. The system exploits angular velocity to change valve timing.

The system can be seen in Figure 2.3, and it is the eccentricity of the driveshaft axis to the camshaft axis that generates a change in valve timing by imposing a variable angular velocity on the camshaft. The variation creates a phase lag and phase lead of the camshaft in relation to the drive shaft that is exploited to change the valve timing.

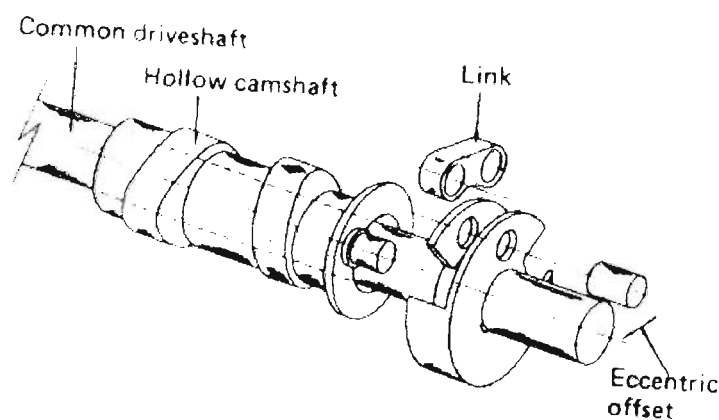


Figure 2.3 – Mitchell VVT system

The Mitchell system can be applied to single or multi-cylinder engines with single or twin camshaft configurations.

Yagi (1992) et al. developed a variable valve actuation mechanism called the shuttle cam. The system, shown in Figure 2.4, uses a gear-train-driven valve system with a rocker arm that activates the valve. The cam gears rotate around the idler gear and the camshafts move along the rocker-arm surface that are concentric with the idler gear. This enables variation of lift by the alternation of the rocker-arm lever ratio and the cam phasing changes simultaneously with the degree of rotation of the cam gears.

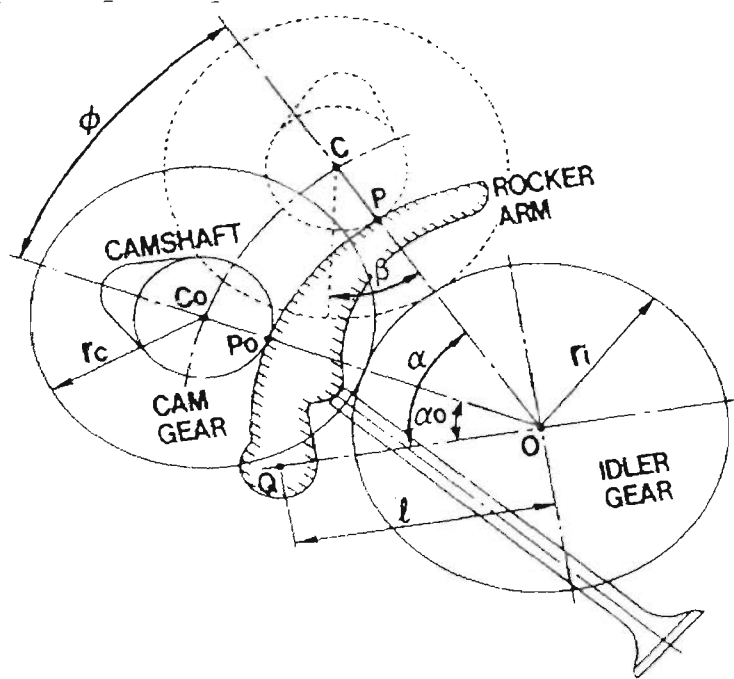


Figure 2.4 – Shuttle cam

A variable valve timing system called the VAST, was developed by Hannibal et al. (1998), the system enabled the variable control of the intake and exhaust valves. It was possible to vary the valve opening, up to approximately 50° crankshaft angle, continuously for each valve lift movement. As a result, fuel consumption and emissions were reduced.

Cam phasing VVT systems, are simple and compact mechanisms that have minimal wear and energy loss. However to date, they cannot vary the duration of valve opening, thus allowing only earlier or later valve opening.

2.3 Cam Changing

Cam changing systems are the most efficient VVT systems in production presently, since

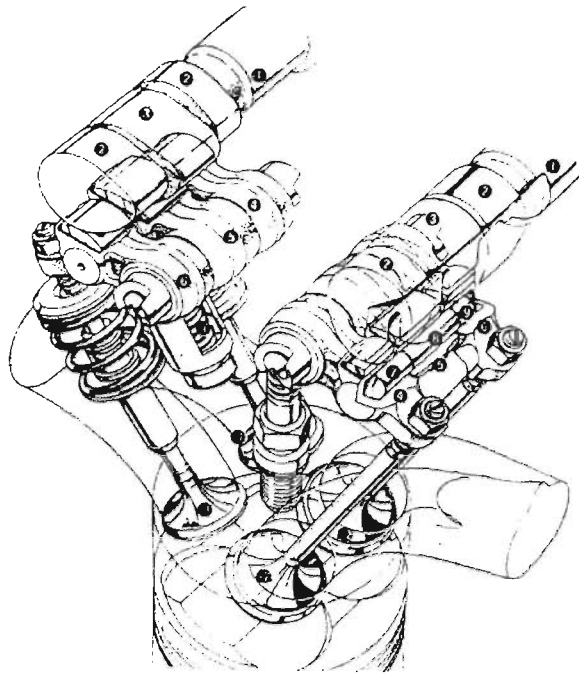
they allow variability in the duration of valve opening as well as the lift of the valves. They can also switch between completely different cam profiles, unlike other systems which can only basically vary the timing by advancing and retarding a standard set of cams.

In 1989, Hosaka et al. (1991) introduced the valve timing electronic control (VTEC) engine system, which was able to maintain a high output throughout the entire engine speed range. Thus enabling the high speed performance of a racing engine without sacrificing low and medium speed performance.

Heywood (1988) stated that to develop a high performance engine it is necessary to increase the volumetric efficiency and reduce friction. A racing engine requires wider valve overlap and increased valve lift to obtain optimum performance at high engine speed. However in a conventional engine, the valve timing and degree of valve lift is set for optimum performance at low and medium engine speeds.

Hosaka et al. (1991) identified that by designing for higher valve lift, wider valve timing and larger valve diameter, it was possible to obtain a higher volumetric efficiency to cope with high output engine speeds. With VTEC, the valve timing and lift can be adjusted at low engine rotation to increase torque and prevent air from being forced back through the intake.

A diagrammatic view of the VTEC system is shown in Figure 2.5. The cam has three separate profiles located at the intake and exhaust of each cylinder. The centre profile is used exclusively for high speed and the two identical outside profiles for low speed.



- | | |
|---------------------------------|----------------------|
| ① Camshaft | ⑦ Hydraulic Piston A |
| ② Cam Lobe for Low Speed Range | ⑧ Hydraulic Piston B |
| ③ Cam Lobe for High Speed Range | ⑨ Stopper Pin |
| ④ Primary Rocker Arm | ⑩ Lost-motion Spring |
| ⑤ Mid Rocker Arm | ⑪ Exhaust Valve |
| ⑥ Secondary Rocker Arm | ⑫ Intake Valve |

Figure 2.5 – VTEC system

The rocker arm assembly comprises a mid rocker arm with primary and secondary rocker arms on each side. The changeover mechanism is composed of two hydraulic pistons that are located within the rocker arm, a stopper pin and a return spring. A lost motion spring is located within the mid-rocker arm, so that the valve can open and close at high speeds. The whole system is operated by a hydraulic actuator, which is controlled by the engine control unit (ECU).

The VTEC has a four valve per cylinder valve arrangement. The VTEC camshaft has a low-speed and high-speed cam profile. While in lower speed mode, the valve timing goes along with the low-speed cam and once the engine reaches high speed, the outer rocker arm lifts off

the low-speed cam and follows the high speed cam. This effectively allows the high-speed cam to control the two valve timings. Hosaka et al. concluded that since the high-speed cam was able to control the two valve settings, the engine was able to get sufficient air at both low and high speeds. As a result, the engine was able to perform better with an even torque band, and more than adequate power at the high end.

Matsuki et al. (1996) conducted further research of the VTEC system by developing a three stage VTEC lean burn engine. The mechanism developed was based on the previous VTEC system but included modifications to the valve train, intake port and combustion chamber configurations. The three-stage VTEC system had the same the valve timing and lift switching mechanism as its predecessor, the VTEC.

As illustrated in Figure 2.6, it can be seen that the three stage VTEC system's camshaft has three cam lobes per valve pair and rocker arms for primary, secondary and middle cam profiles. The three profiles are for valve inactivity, low and medium engine speeds and high engine speed. The rocker arm integrates two hydraulic passages, which can be switched to and from each other by a spool valve setting.

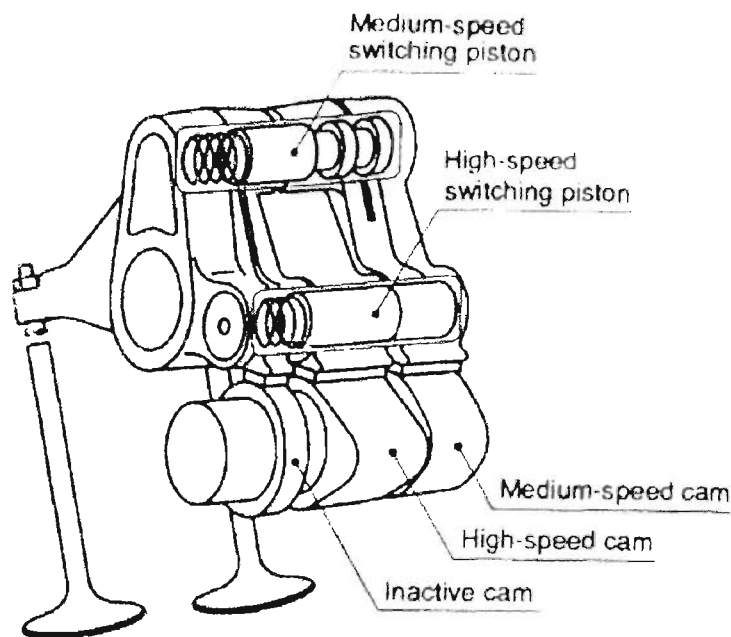


Figure 2.6 – 3-Stage VTEC system

At medium-speed range, the hydraulic passage opens as a result of the electronic control unit (ECU) signal, providing hydraulic pressure to the switching piston. The primary and secondary rocker arms are connected to each other and lift the valve using the medium-speed cam profile. The valve timing and lift at this stage are set so that they ensure an appropriate charging efficiency and less valve drive friction.

While in the high-speed range, the ECU allows the other hydraulic passage to open, providing hydraulic pressure to the high-speed switching piston. As a result, both the primary and secondary rocker arms are connected to the middle rocker arm. Consequently accessing the high-speed cam profile, the valve timing and lift are optimized to generate a high power output.

They concluded that the three-stage VTEC system can generate approximately 40% more engine power than the original VTEC engine that Hosaka et al. (1991) developed, while maintaining the same fuel consumption. Nakayame et al. (1994) concluded that because the VTEC systems alter the valve timing and lift according to various driving conditions, it was able to use a leaner mixture than existing engines. As a result, the VTEC systems reduce Hydrocarbon emissions considerably due to the improvement in engine combustion.

Hatano et al. (1993), developed a VVT system featuring a multi-mode valve system, it was called Mitsubishi Innovative Valve Timing and Lift Electronic Control (MIVEC). The system enables deactivation of unnecessary cylinders during low speed cruise and improved the engine output performance under all engine speed ranges by selecting optimum cam profiles depending on the engine speed, as shown in Table 2.1.

○ ACTIVATED ● DEACTIVATED

MODE	CYLINDER	CAM FOLLOWER	
		LOW - SPEED CAM	HIGH - SPEED CAM
I	NO. 1, 4 CYLINDERS	●	●
	NO. 2, 3 CYLINDERS	○	●
II	ALL CYLINDERS	○	●
III	ALL CYLINDERS	●	○

Table 2.1 – MIVEC valve operation

Hara and Kumaga (1989) developed a VVT lift and timing control system (VLTC), which varied the lift timing by changing the fulcrum of the rocker arm. The fulcrum was varied according to the inclination of a lever that engages with a control cam. The control cam was driven by an actuator mechanism to provide control over valve lift and timing. They concluded that their system reduced valve train noise and delivered stable valve operation throughout the high-speed range.

Although cam changing VVT systems can vary the lift of the valves, they cannot fully close the valves to zero lift, as well, additional cams are required to vary the lift from low-speed to high-speed.

2.4 Intake Valve Closing

Intake valve closing is a practical concept applicable to engines in which the intake valves can be phased relative to each other to extend the total intake opening period. Bassett et al. (1997) studied the use of a late intake valve closing (LIVC) mechanism as a means to

eliminate most of the pumping losses (pumping loss represents the power required to pump charge into and out of the cylinders) and conserve fuel. They identified that the problem of pumping losses must be addressed, because as the engine was throttled, pumping losses progressively increased until no useful output was generated at idle speed.

Their proposed system consists of an intake camshaft, which causes late closing of the intake valve at all times. At high loads a reed valve situated in the intake manifold prevented the charge from being rejected from the cylinder. At low loads, the reed valve was deactivated to allow the charge to return to the inlet manifold. They asserted that the LIVC system allowed the engine to operate with wider than normal throttle settings at low speed, thus enabling the reduction of pumping losses.

Ma (1988) and Saunders et al. (1989) agreed with Bassett's research by also concluding that there was better fuel consumption with the LIVC. Lenz and Wichart (1989) stated that with a late intake valve closing mechanism, a torque increase of 8% can be achieved, fuel consumption can be improved by 4%, along with and a 20%-50% reduction in pumping losses.

Payri et al. (1984) compared pumping losses between a standard engine and an engine fitted with a VVT system. Their conclusion was that pumping losses would be significantly reduced with a VVT system and the efficiency of an engine would improve. They found that there was a strong pressure drop in the throttle valve of the carburetor when the engine runs at a partial load rate, this decreased the mean pressure along the intake and as a result, pumping losses were increased. With a VVT system, the throttle valve was eliminated and load regulation was achieved by means of the total opening time of the intake valve. The pressure drop during the intake process was minimal and the fluid inside the cylinder expands from the moment that the intake valve was closed until the piston reached bottom dead centre (BDC) and afterwards was compressed during the compression stroke.

On the other hand, Tuttle (1982) investigated the use of an early intake valve closing (EIVC) mechanism as a means for controlling the load of a spark-ignition engine. The engine was operated unthrottled, with load controlled by closing the intake valve during the intake stroke

of the engine after the required amount of charge has been induced into the cylinder. He found that compared to a conventional throttled engine operating at part load, the EIVC had lower pumping loss, fuel consumption and NO_x emissions. On the other hand, Hara et al. (1989) found that even though pumping losses were reduced with intake valve closing mechanisms, improvement in fuel economy equivalent to the reduction in pumping losses were not obtained. They concluded that the major contributing factor to this phenomenon was the deterioration of the combustion. The cause of combustion deterioration was the drop in cylinder gas temperature and pressure due to a decrease in the compression ratio.

Urata et al. (1993) found a solution to the combustion deterioration problem by developing a hydraulic variable valve train (HVT), which could vary the intake valve closing timing freely. Due to the fact that conventional engine management systems are not applicable for non-throttling operation, they designed the HVT system, which could minimise pumping losses and reduce fuel consumption.

A solenoid valve, was connected to the oil path, which linked the intake valve and cam to block and release oil pressure. The valve lifted along its cam profile once the solenoid valve was activated. When the solenoid-valve was activated to close during cam lift, the valve was lifted along the cam profile as in conventional engines. When the solenoid-valve was deactivated to open at a specific time during cam lift, oil pressure was released to let the valve spring close the intake-valve, regardless of the cam lift. Adjusting the time at which the solenoid-valve opens, controlled the intake-valve closing timing.

Vogel et al. (1996) investigated implementing variable valve timing systems using a secondary valve in the intake tract, which would act in accordance with the conventional poppet valve of the engine. They found that there were two beneficial uses of the secondary valve. Firstly, it enabled the control of valve overlap, thus improving low speed and low end performance. Secondly, to use it as a load control mechanism, i.e., it would replace the conventional throttle and reduce pumping losses that were associated with conventional throttling. Ohyama and Fujieda (1995) stated that by substituting the throttle with direct fuel injection, increases the air/fuel ratio limit, thus reducing nitrogen oxide emissions.

2.5 Lost Motion Valves

Lost motion valves are operated directly by conventional cams and the timing variation is produced by varying the length of the pushrod to produce an adjustable lash in the valve mechanism. The rocker fulcrum or the camshaft is moved to vary the valve lash. Since these mechanisms convey output motion during only part of the cam lift, they are called “lost-motion” mechanisms. Lost motion mechanisms are very simple to implement and can be used to attain very ranges of valve opening. Systems can be designed that automatically vary duration with engine speed to provide near-optimum full throttle fuel efficiency and torque.

Herrin and Pozniak (1984) found that their lost motion mechanism, termed a variable timing lifter (VTL), can vary the timing of engine valve opening and closing, was durable and precise in its control. When applied to a high specific output engine, the mechanism allowed much lower idle speeds and reduced idle fuel consumption without compromising high-speed power. The VTL can minimise the effects of fixed valve timing compromise by providing a reduction in valve open duration and valve overlap at low engine speeds to allow a slow and stable idle, which reduced idle fuel consumption. The device however, responds only to engine speed and cannot optimize valve timing for changes in load.

Lee et al. (1995) developed the electronic valve timing (EVT) system that operated with a lost motion hydraulic actuator linked to a high flow electromagnetic solenoid valve. Valve control was provided by an electronic control unit, which acted upon the solenoid.

When the solenoid was closed, a hydraulic lock was created and the valve motion was forced to follow the cam profile. If the solenoid was opened during the valve event, the valve lift and duration were modified depending on when the solenoid was opened. They also obtained similar results to Herrin and Pozniak. They concluded that by advancing the intake valve closing timing, torque can be improved at low speed condition by about 10%, fuel consumption can be decreased by 10% and NO_x emissions by 30%.

Hu (1996) applied electronic control to shape valve lift. Cams with hydraulic linkages actuated the engine intake and exhaust valves. The fluid was vented (venting was controlled

by electronic triggering of the solenoid valves) from the linkages to effect lost motion between the cams and the engine valves. This allowed optimization of valve timing, lift and duration for retarding and for positive power.

Lost motion systems are one of the simplest mechanisms for obtaining a large range of valve durations, however, the valve lift off and seating impacts of valves can cause high valve stresses and engine speeds are limited by the seating impacts.

2.6 Electrically Actuated Valves

Electrically actuated valves are operated directly by electric actuators, usually solenoids. Varying the time of energizing and de-energizing the solenoids produces variation in the timing.

Schechter and Llevin (1996) introduced a camless engine with independent and continuously variable control of valve timing, lift and duration. The engine valve opening and closing was controlled by two solenoid valves that were connected to high and low pressure plenums. Valve opening was controlled by the solenoid valve connected to the high pressure plenum, while valve closing was controlled by the solenoid valve connected to the low pressure plenum.

Douglas (1997) developed an electromagnetic valve actuator (EVA) system that controls valves electronically, without the need for a camshaft, rocker assembly, pulley or timing belt. The EVA system had one actuator at each valve chamber with two opposing spring coils fitted at each valve chamber providing the necessary force to open and close the valves. The spring forces were supplemented by electromagnetic force from the EVA coils. The intake and exhaust valves were independently computer controlled and timed, making it possible to fine tune air/fuel and exhaust flows to engine needs.

Electrically actuated systems have a high energy consumption with restricted valve duration range and engine speed range.

2.7 Hydraulically Actuated Valves

Hydraulically actuated valves are operated directly by hydraulic actuators, usually hydraulic cylinders and the fluid is metered through either mechanical or solenoid valves.

Desantes et al. (1988) investigated the use of a hydraulically controlled variable valve timing system, which utilised a hydraulic mechanism to open and close the valves. The system was based on an axial lifting of the intake valve by a hydraulic plunger. The degree of early intake valve closing depended on the engine running conditions, which were controlled by a microprocessor. The microprocessor controlled an electrovalve, which discharged the oil stocked under the plunger through the driven valve. The plunger was located at one end of the rocker arm, which pivoted around the cam contact point as fixed centre. The variable closing of the intake valve depended on the moment at which the microprocessor ordered the electrovalve opening and closure. The system is illustrated in Figure 2.7.

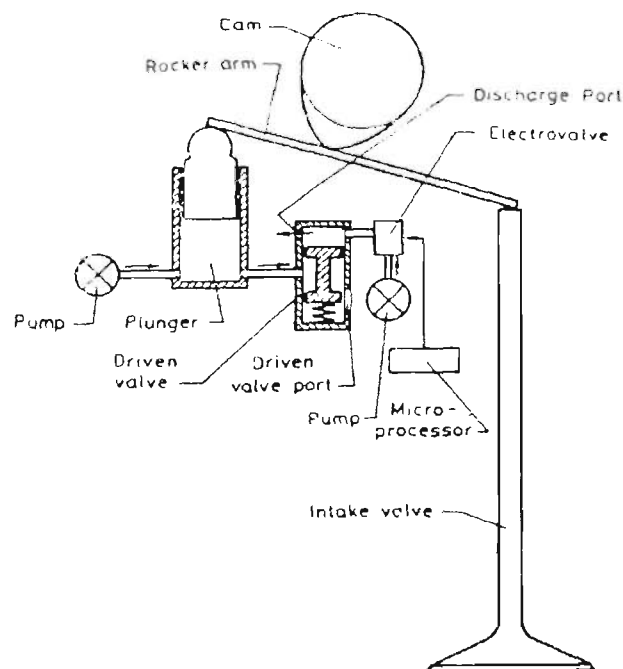


Figure 2.7 – Hydraulically controlled VVT system

Crohn et al. (1990) were able to adjust the intake valve timing by the use of a hydraulic – mechanical acting camshaft adjuster. The timing was adjusted, dependent on the load and engine speed, by turning the intake camshaft using a hydraulic adjuster. The camshaft adjuster was controlled in line with the engine speed and load by the fuel injection control unit.

Hydraulically actuated systems are simple in their operation and have fewer mechanical elements than most standard valve trains, however, they are prone to high fuel consumption and limited maximum engine speed.

2.8 Valves Actuated by Two Cams in Parallel

In these systems, the valves are operated by two cams in parallel in such a way that the valve displacement equals the larger effective displacement of either cam. Timing is varied by changing the phase angle between each cam and the crankshaft. The most common implementation of this concept employs a single cam profile, which is actually made up of two separate cams that can be rotationally shifted relative to each other. Two concentric shafts usually drive the two cams. The outer camshaft drives one set of cams while slots in it allow the second set of cams to project through from the inner shaft.

Kreuter (1998) developed a similar system called the Meta VVH. It had two camshafts, which operate as opening and closing camshafts that rotated at the same speed and acted on the intake valves via a follower and a transmission element. The opening camshaft was driven directly by the crankshaft while the opening cam drove the closing camshaft via a gear drive. The gear drive allows a phasing between both camshafts in a range necessary to vary lift and duration of the valves from zero to maximum. The valve lift function corresponded to the sum of the displacements of the two cams. These systems have large valve duration ranges but are mechanically rather complex.

2.9 Literature Review Summary

The literature review indicates that variable valve timing systems presently available have shortcomings. Principally, cam phasing mechanisms cannot vary the duration of valve opening and cam changing systems cannot achieve zero lift. Other mechanisms suffer from high fuel consumption, high valve stresses and are complex systems.

3. METHODS AND EQUIPMENT

3.1 Introduction

This chapter describes the experimental procedure involved in obtaining the valve lift profile of a cylinder head and the actual valve lift results. The measurement of the standard Vectra valve lift provided a profile from which maximum valve velocity and acceleration could be estimated. These estimations provided input for setting upper limits for the DVC system. The standard production engine selected was a Holden Vectra 2.0 litre twincam engine. To obtain the valve lift profile of the Vectra engine, the Vectra cylinder head was removed from the engine and fitted to a specially designed cylinder head test rig. The cylinder head test rig, was built in the School of Built Environment at Victoria University of Technology. A future DVC prototype will be trialed on the Vectra cylinder head test rig.

To obtain the Vectra's valve lift profile, data acquisition software, DTVEE and a LB-12/72 laser displacement sensor were used to evaluate the valve lift characteristics of the standard Vectra cylinder head. The engine specifications, the details of the construction of the test rig, the description of the data acquisition and the laser displacement sensor and valve lift results of the Vectra cylinder head are presented.

3.2 Engine Specification

The engine specification is shown in Table 3.1

Model	Holden Vectra
Displacement	1998 cm ³
Stroke	86 mm
Intake Valve Diameter	32 mm
Exhaust Valve Diameter	29 mm
Output	100 kW
Torque	185 Nm
Firing Order	1, 3, 4, 2
Compression Ratio	9.6: 1
Engine Management	Simtec 5.5
Fuel	Premium Unleaded Fuel

Table 3.1 – Holden Vectra engine specifications.

3.3 Cylinder Head Test Rig

The test rig is shown in Figure 3.1. The cylinder head was removed from the Holden Vectra engine and bolted to the test rig's railings. A variable speed motor, located at the bottom of the test rig drives the valve gear of the cylinder head. The variable speed motor specifications are given in Table 3.2.



Figure 3.1 – Cylinder head test rig.

Type	Vari Speed Motor Control
Model	WW 2SS
Input	230 V
Output	0.7 kW
Maximum Amperes	5.5

Table 3.2 – Specifications for the variable speed motor.

3.4 Laser Displacement Sensor

Once the Vectra cylinder head was fitted to the test rig, to attain the valve lift profile of the Vectra engine, an LB-12/72 laser displacement sensor was used to sample the

analog signals as the valves opened and closed. The laser displacement sensor is illustrated in Figure 3.2. To accurately sample signals, the reference point of the sensor needs to be positioned within 30 to 50 mm of the intended target. If the sensor is positioned within the acceptable measuring range, the LED indicator will indicate an orange colour. If the sensor is not positioned within range, the LED indicator will show a red colour. The sensor specifications can be seen in Table 3.3.

The reference position of the sensor was positioned approximately 40 mm from the valve seat. Once the reference position was positioned within the acceptable range of the valve seat, the sensor was switched on and as the valve opened and closed the sensor sampled the analog signals.

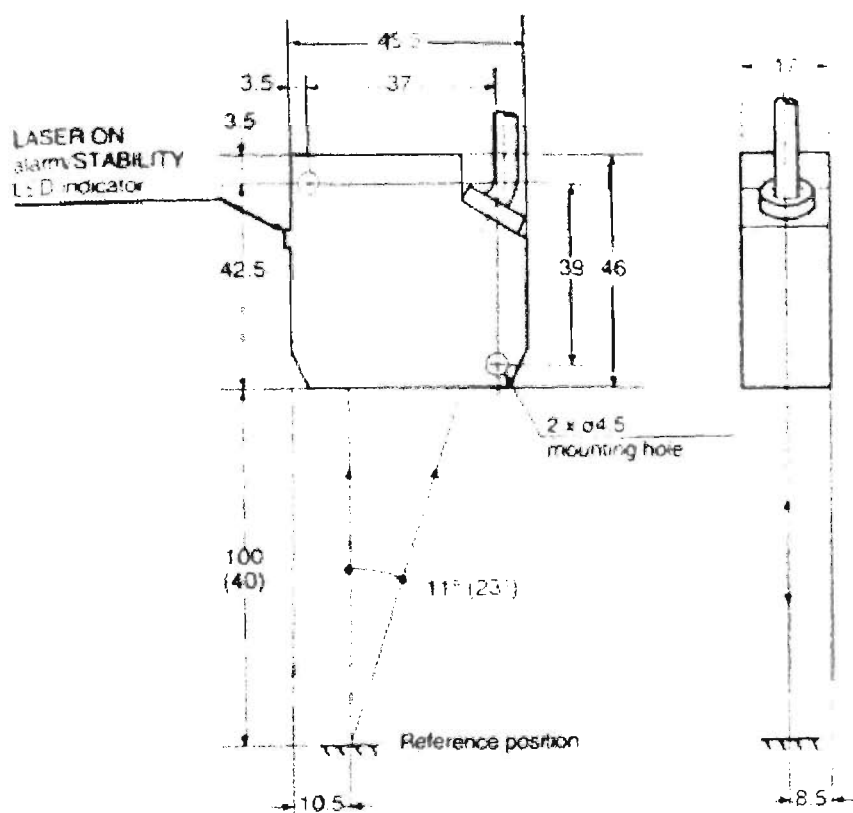


Figure 3.2 – LB – 12/72 Laser Displacement Sensor.

Type	High – Resolution
Model	LB – 12/72
Reference Distance	40 mm
Measuring Range	± 10 mm
Light Source	Infrared Semi-Conductor Laser
Wavelength	780 nm
Spot Diameter	1.0 mm
Linearity	1% of F.S
Resolution	2 μ m (at 60 ms) / 15 μ m (at 2 ms) / 50 μ m (at 0.15 ms)
Analog Voltage	± 4 V (0.4 V/mm)
Analog Impedance	100 Ω
Zero – Point Adjustment Range	30 to 50 mm
Response Frequency	DC to 3 kHz (at 0.15 ms) (-3 dB) / DC to 200 Hz (at 2 ms) (-3 dB) / DC to 6Hz (at 60 ms)
Power Supply	12 to 24 VDC $\pm 10\%$
Current Consumption	120 mA maximum

Table 3.3 – Specifications of the Laser Displacement Sensor.

3.5 DTVEE Software

After the laser displacement sensor sampled the analog signals as the Vectra valves opened and closed, the data acquisition software, DTVEE was used to show the digital readout from the analog signal of the laser. A computer program was written to acquire, process and save the data gathered from the laser measurements of the valve lift of the cylinder head.

Prior to the cylinder head test, the user has to enter to the program:

- (1) The analogue to digital configuration information,
- (2) Data panel information

The DTVEE program basically consists of three parts, analogue to digital conversion, data panel box and the analogue to digital sample results, which is the cam displacement box as seen in Figure 3.3. In the analogue to digital conversion box, one specifies the channel to be read, the gain and the rate of data acquisition. The information from the analogue to digital configuration box and the data panel box is then processed and the digital readout of the measurement of the valve lift is presented on the screen.

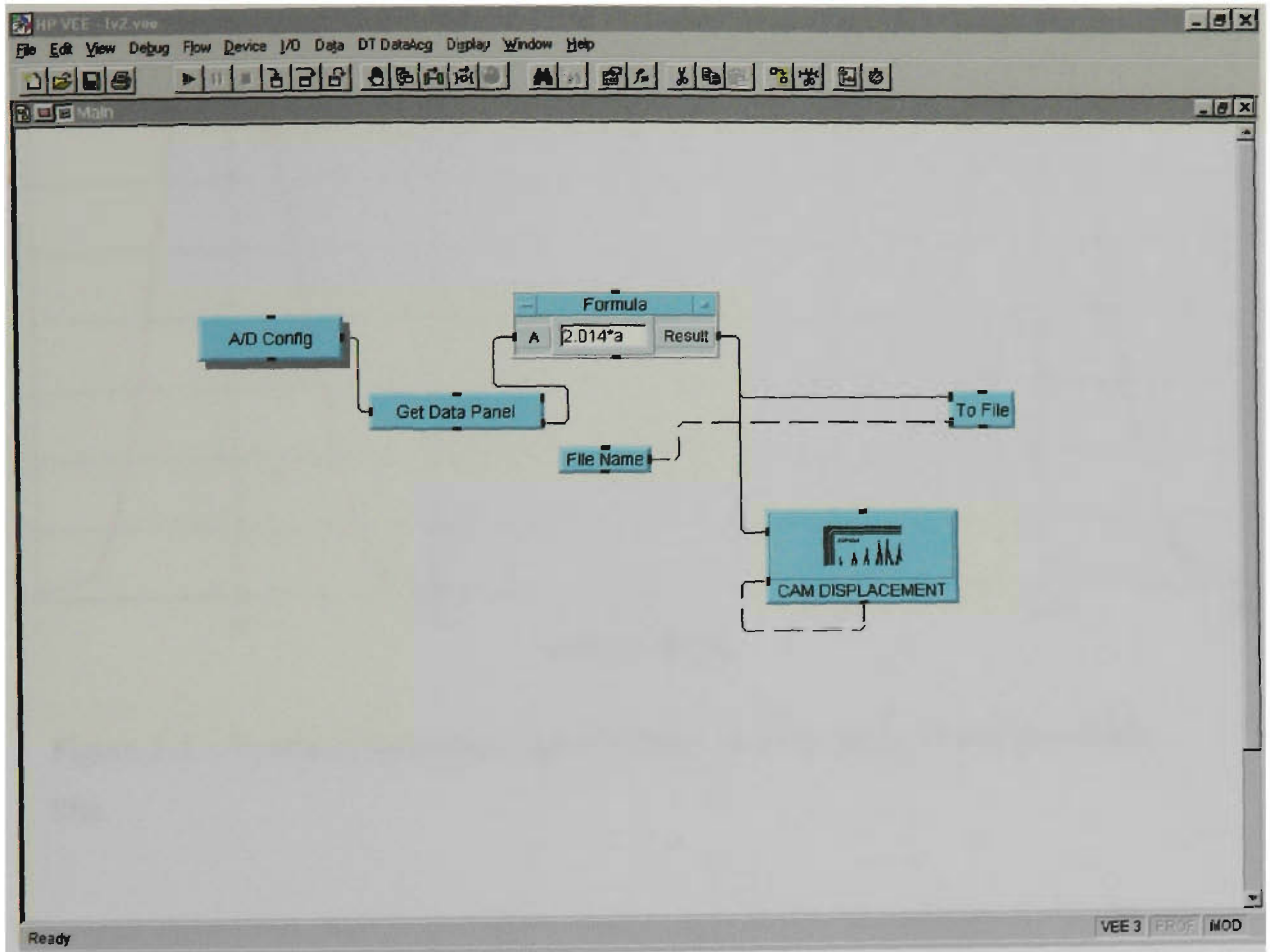


Figure 3.3 – DTVEE Data Acquisition Program

3.6 Vectra Engine Cylinder Head Valve Profile

The valve lift data was saved as an ASCII file in DTVEE, and then processed in Microsoft Excel.

As illustrated in Figure 3.4, the maximum valve lift of the standard Vectra engine was 9 mm with a valve duration of 130 degrees of camshaft rotation.

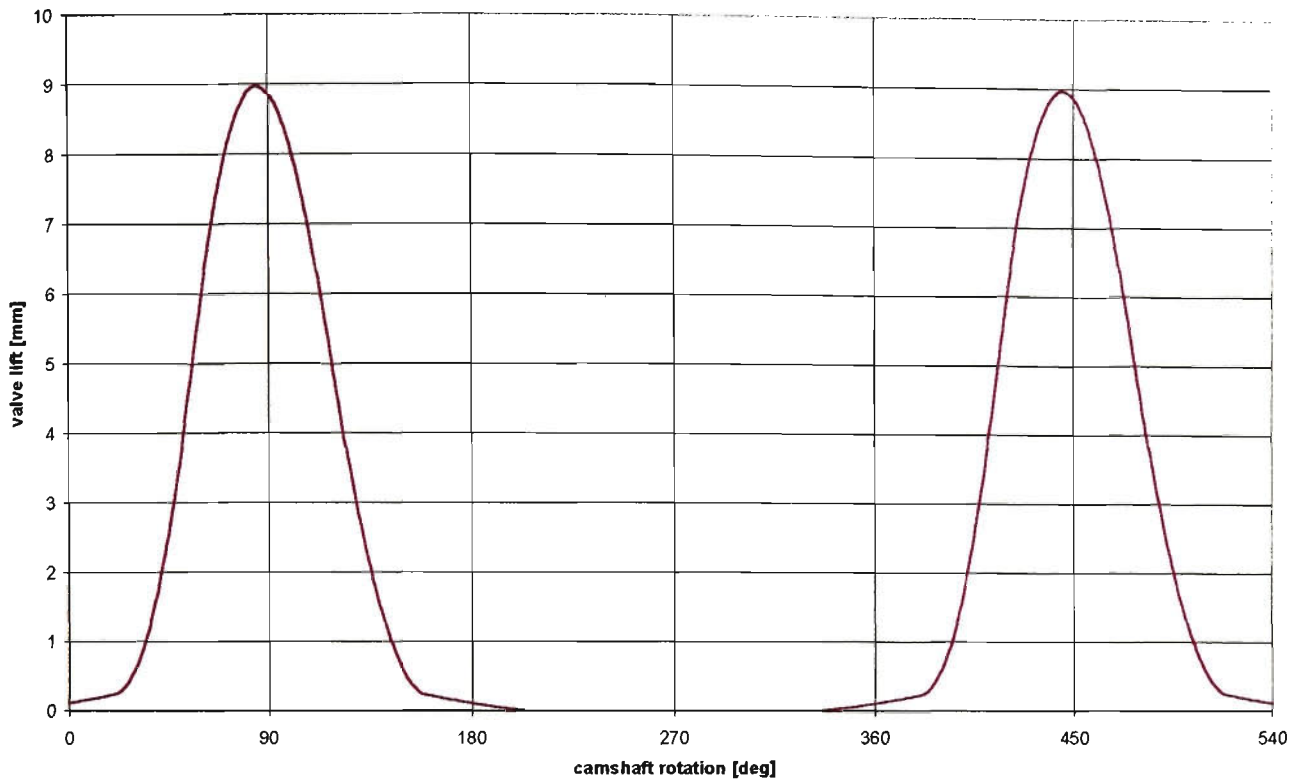


Figure 3.4 – Vectra cylinder head valve lift and valve duration of two successive lifts.

The result shows that the Vectra engine has no variable lift capability by which the valve can be operated to suit engine speed. Its speed range is a compromise between high and low rpm. This is due to the fact that the Vectra engine uses two camshafts, which are turned by a timing chain connected to the crankshaft, to open and close its valves. Therefore, as the speed of the engine increases and decreases, the crankshaft to camshaft synchronisation is maintained to keep valve timing relatively close to what is needed for engine operation. As can be seen from the figure the maximum valve lift of the Vectra engine is 9 mm.

3.7 Hertzian Contact Theory

To guard against the possibility of surface failure, it is necessary to investigate the stress states, which result from loading one body against another.

For Hertzian contact stress theory, the following assumptions can be made, see Deeg, (1992):

- (1) at the point of contact the shape of each of the contacting surfaces can be described by a homogenous quadratic polynomial in two variables,
- (2) both surfaces are ideally smooth,
- (3) contact stresses and deformation satisfy the differential equations for stress and strain of homogenous, isotropic and elastic bodies in equilibrium,
- (4) the stress disappears at great distance from the contact zone,
- (5) tangential stress components are zero at both surfaces within and outside the contact zone,
- (6) normal stress components are zero at both surfaces outside the contact zone,
- (7) the stress integrated over the contact zone equals the force pushing the two bodies together,
- (8) the distance between the two bodies is zero within but finite outside the contact zone,

(9) in the absence of an external force, the contact zone degenerates to a point.

The two cylindrical bodies in the DVC system that come into contact, which are of significant importance, are the guideshaft and gudgeon pin. The contacting surfaces have the only line contact that does not have an obvious arrangement in existing engines.

The maximum Hertzian contact pressure for two cylinders pressed together by a force is given by the equation, see Shigley (1989)

$$p_{\max} = \frac{2F}{\pi bl} \quad (3.1)$$

Where

p_{\max} = Maximum contact pressure,

F = Contact force,

b = Contact half width,

l = Width of guideshaft.

3. RESULTS AND DISCUSSION

3.1 Computer Simulation

From Chapter 3, it was seen that the measured maximum valve lift of the Vectra engine was 9mm and the valve duration was 130 degrees. To obtain a comparison between the valve lift profiles of the Vectra engine and the proposed DVC system, the DVC prototype was modeled using ADAMS, a virtual prototyping software, to attain valve lift characteristics.

Virtual prototyping technology has made significant advances in recent years and many companies are utilising the technology in the design of products such as automobiles, aircraft, railway, defense and industrial machinery. Virtual prototyping enables one to realistically simulate the full motion behavior of a mechanical system, to detect component interference, evaluate levels of vibration in the system, predict deflection of parts and determine loads and forces on components.

ADAMS is a widely used virtual prototyping software, and the DVC system was modeled using ADAMS. ADAMS provides the user with the tools to build a virtual prototype, to test the virtual prototype and to validate the performance of the virtual prototype against known measurements.

3.2 DVC Components

The design of the DVC components, the rocker arm and guideshaft are critical to the performance of the system and the design rationale of these components were as follows:

- (1) provide an actuating lever to interact with the top of the original valve bucket with minimal deviation of contact from the valve axis,
- (2) ensure the rocker arm did not interfere with any other part of the bucket,

- (3) provide a concave, circular arc surface concentric with the axis of the guideshaft for contact with the pin,
- (4) ensure the line contact pressure on the rocker arm does not exceed what is considered acceptable for conventional valve train components,
- (5) ensure internal stresses of the rocker arm do not exceed the fatigue limit of its material,
- (6) provide a base circle surface that results in close to zero valve lift as possible during interaction with the gudgeon pin,
- (7) provide a concave arc that results in valve acceleration no greater than the standard Holden Vectra valve train,
- (8) ensure the line contact pressure of the interacting gudgeon pin does not exceed that of conventional valve train components.

The DVC components were designed to allow minimum modification to the standard Vectra cylinder head.

The proposed components were constructed using SolidWorks, which is a 3D CAD modeling software and their shells were then imported into ADAMS. The components that make up the DVC system can be seen from Figures 4.1, 4.2, 4.3, 4.4, 4.5, 4.6 and 4.7. The components used are the same for the inlet and exhaust valves. The materials chosen were similar to conventional valve train materials and Table 4.1 details the material and the mass properties of the components.

Component	Material	Mass (kg)
Bucket	Steel	0.049
Valve	Steel	0.042
Rocker Arm	Steel	0.0267
Valve Crank	Steel	0.15013
Rockershaft	Steel	0.05661
Guideshaft	Steel	0.03269
Conrods	Aluminium	0.00714
Gudgeon Pin	Aluminium	0.00968

Table 4.1–Component mass property and material



Figure 4.1 – DVC valve as modeled using ADAMS

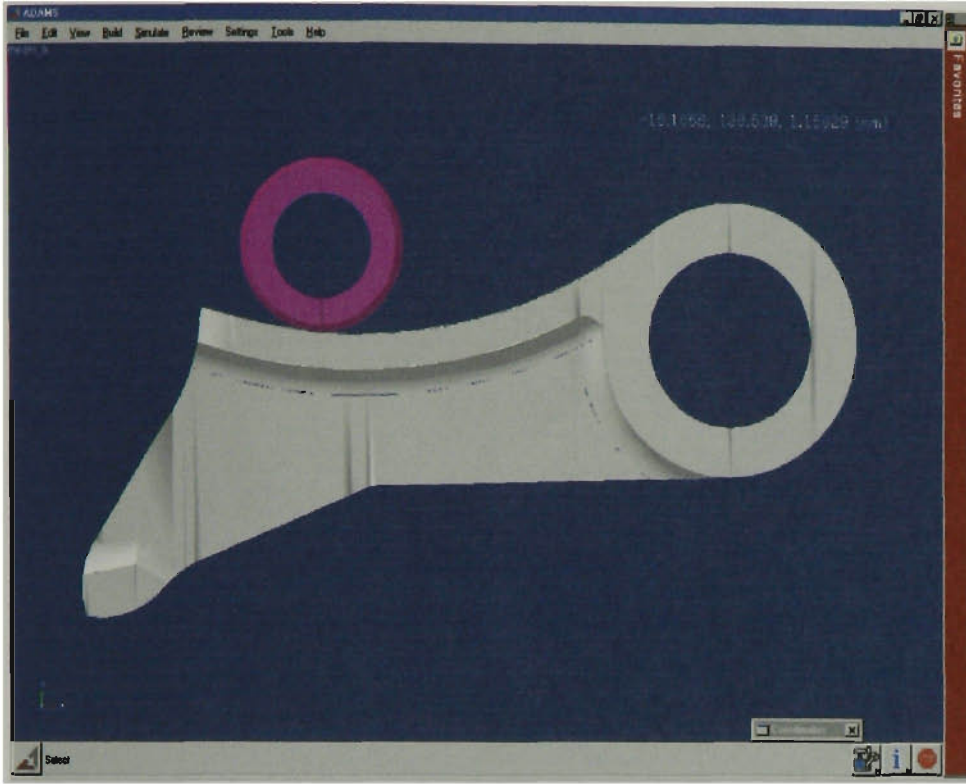


Figure 4.2 – Gudgeon pin (pink component) and rockerarm as modeled using ADAMS

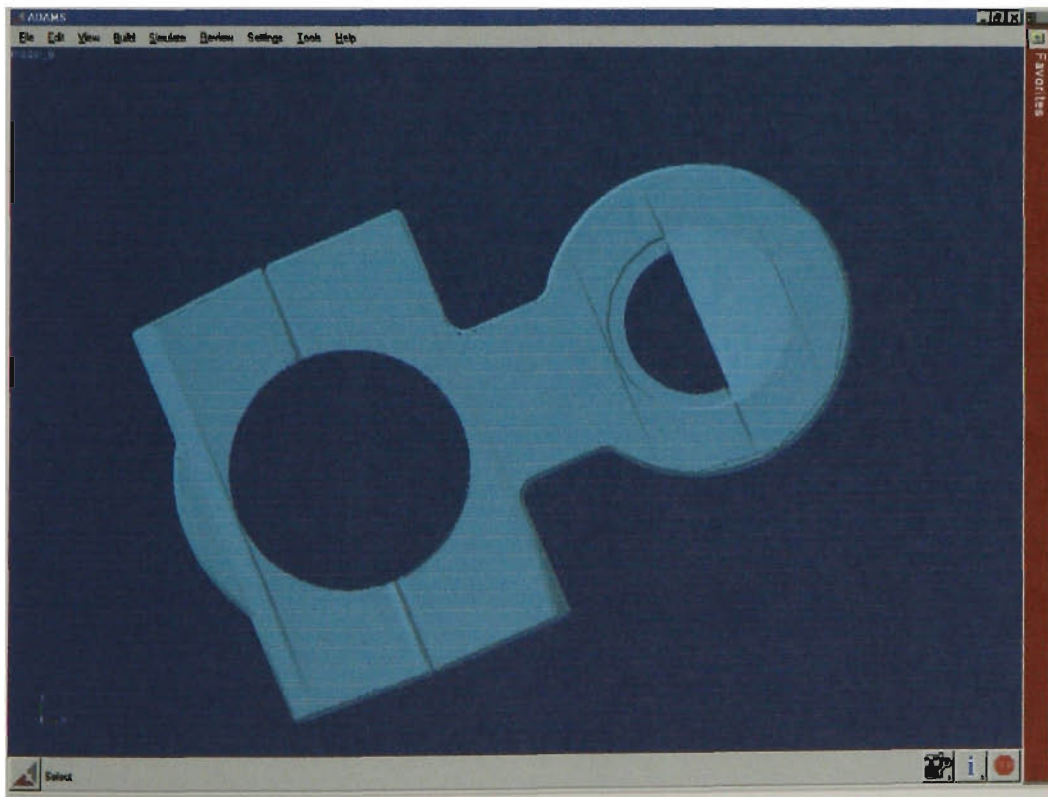


Figure 4.3 – Conrod as modeled using ADAMS

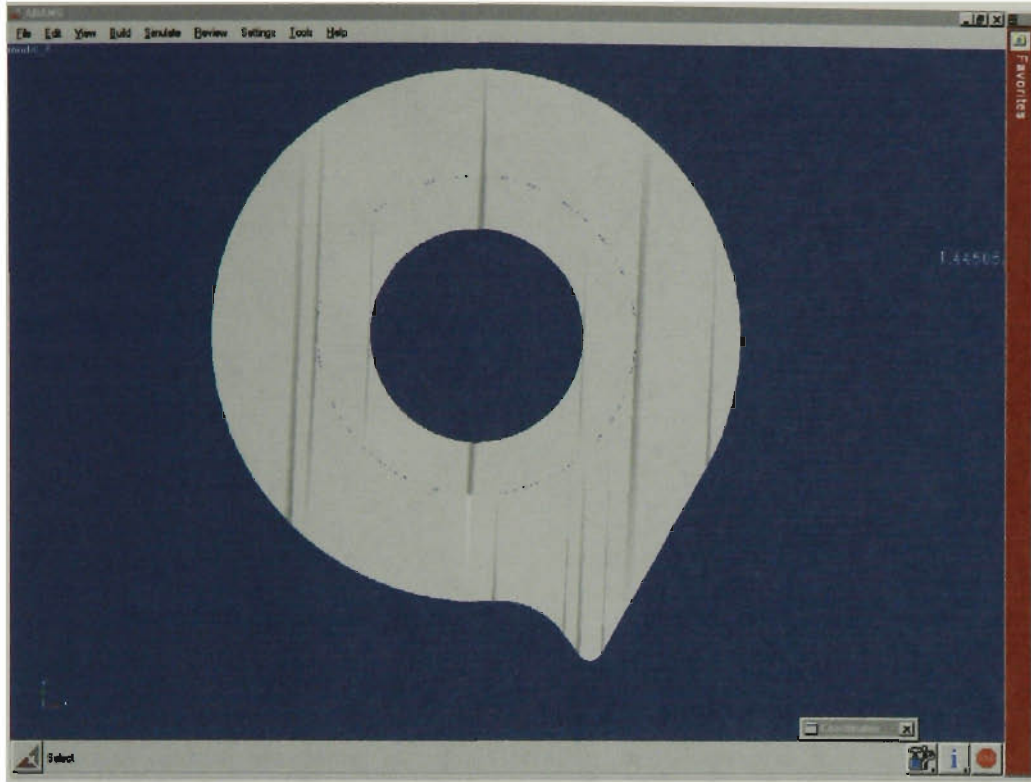


Figure 4.4 – Guideshaft as modeled using ADAMS

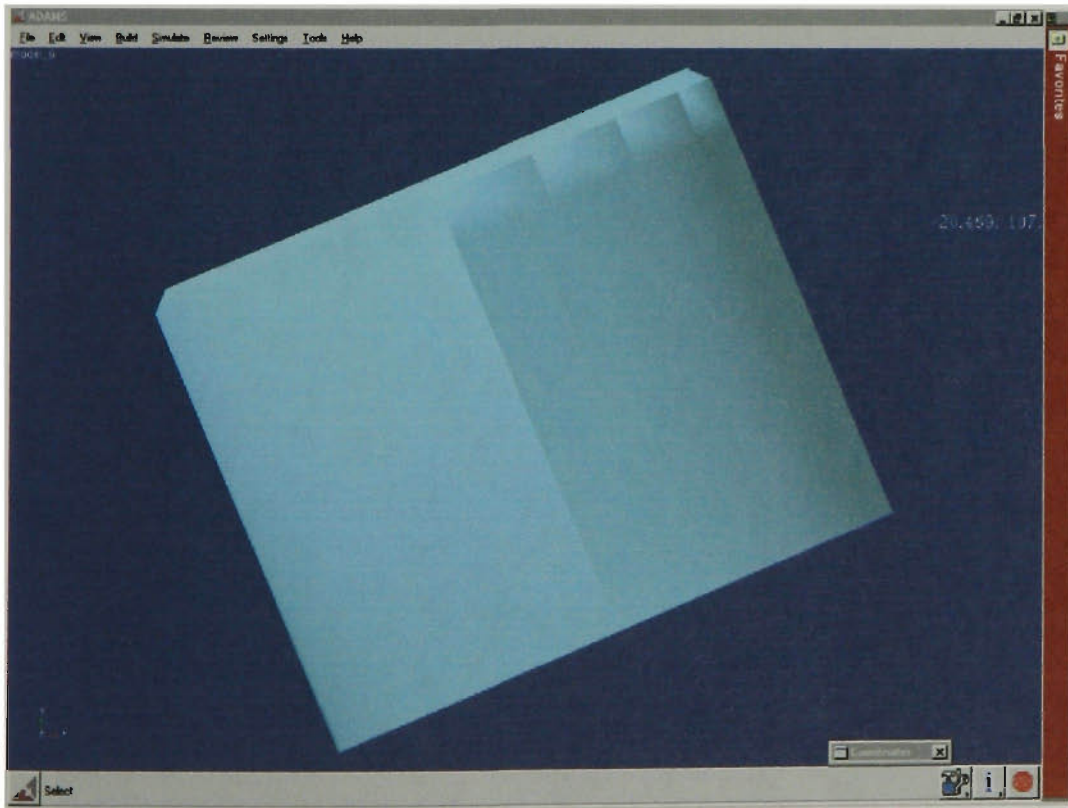


Figure 4.5 - Bucket as modeled using ADAMS

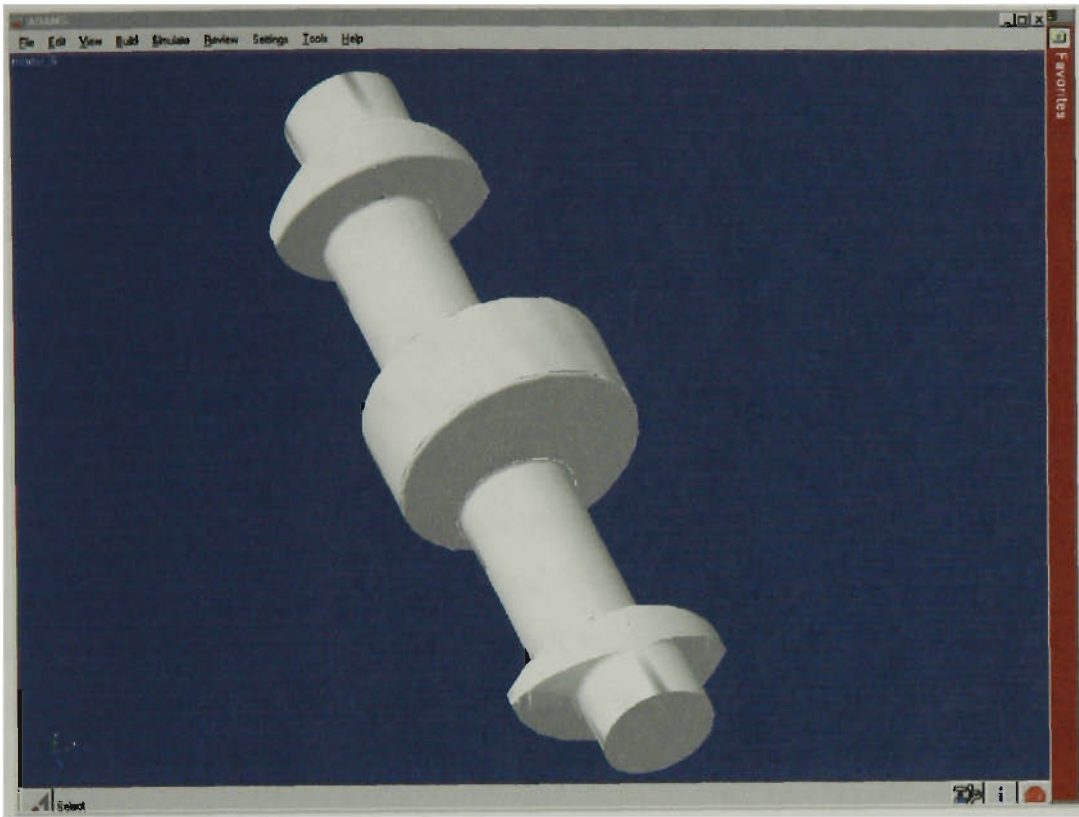


Figure 4.6 – Valve crank as modeled using ADAMS

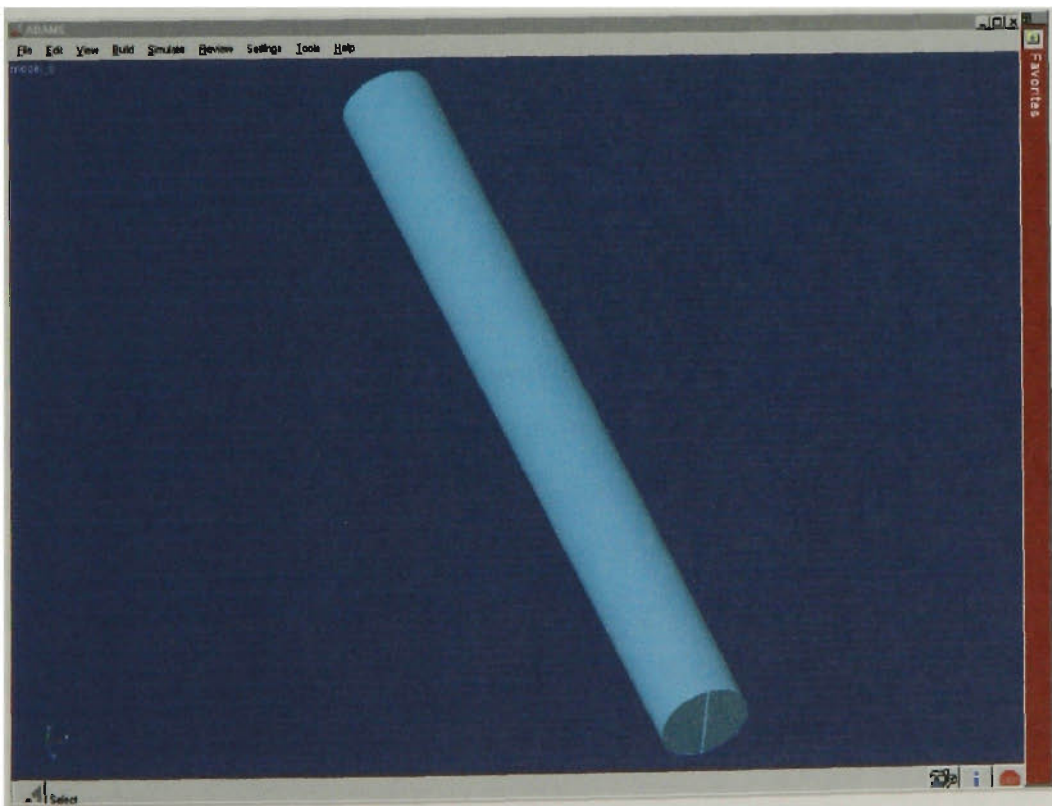


Figure 4.7 – Rockershaft as modeled using ADAMS

All the DVC components are rigid 3D bodies, and the extrusion tool was used to create the components. SolidWorks models begin with a 2D outline, which is then extruded in the third dimension to form a 3D model. The type of extrusion used determines the shape of the desired component.

The valve and the bucket were created by sketching a half cross section with one edge of the sketch formed by the central axis of symmetry. The torus extrusion was then selected and the cross section was extruded through 360 degrees around the central axis. The crankshaft, rocker and conrods required the linear extrusion tool and the edges of the geometry were chamfered, filleted, holes and bosses were added and the solids were hollowed. For the guideshaft, three rigid bodies were joined to create that component. First of all the shape of the guideshaft profile was created and the rockershaft was attached to the profile. The guideshaft can be seen in Figure 4.4.

Once the parts were created, they were imported into ADAMS. The material and mass properties of the components were defined and the components were then arranged in their correct co-ordinate positions.

4.2.1 Constraints

In order to correctly simulate the model, once the parts were created and positioned correctly, they had to be constrained, that is, constraints are used to specify part attachments and movement. How the parts will be attached to one another and how they move relative to each other has to be defined. A description of all the constraints used can be seen in Appendix B. Figure 4.8 shows the bucket and valve, the bucket pushes the valve open, once the rocker arm pushes on the bucket. The same figure also shows the constraints between the bucket and the valve. A translational joint was used between the bucket and ground, so that once the rocker arm pushes on the bucket, it will translate along a vector aligned with respect to the valve. However, during a simulation run the bucket separated from the valve and the valve did not return to its original position.

Therefore a fixed joint was introduced to prevent the bucket and the valve from separating from one another during simulation. Also a coil spring is used so that the valve will be able to close, once it opens.

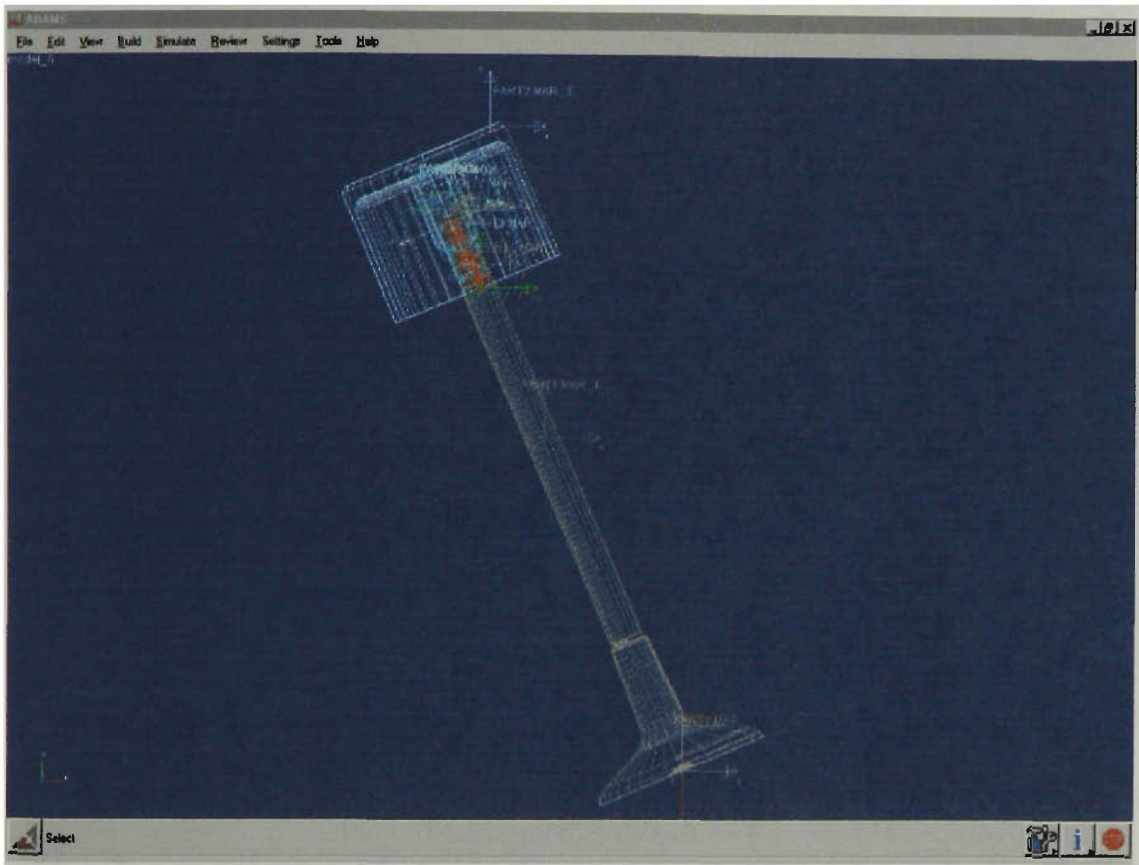


Figure 4.8 – Bucket and valve as constrained using ADAMS.

The rocker arm pushes the bucket, which in turn opens the valve, however, the rocker arm can only push the bucket due to the gudgeon pin moving backwards and forwards between the rocker arm and guideshaft profile. The gudgeon pin moves towards the end of the rocker arm, which is towards the rocker shaft, this in turn allows the bucket to be pushed by the rocker arm. Figures 4.9, 4.10, 4.11, 4.12, 4.13, 4.14, 4.15, 4.16, 4.17 and 4.18 illustrate how the rocker arm, gudgeon pin, guideshaft, rockershaft and conrods were assembled together.

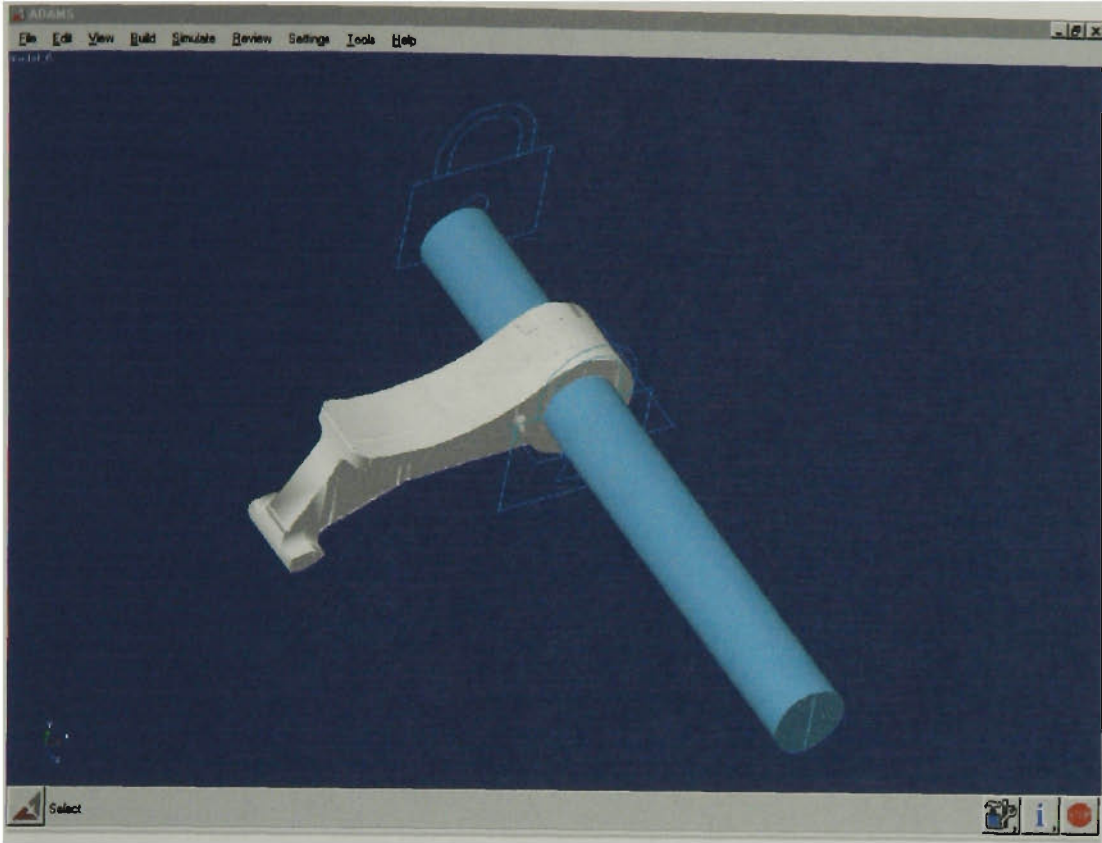


Figure 4.9 – 3D illustration of rockershaft and rocker arm

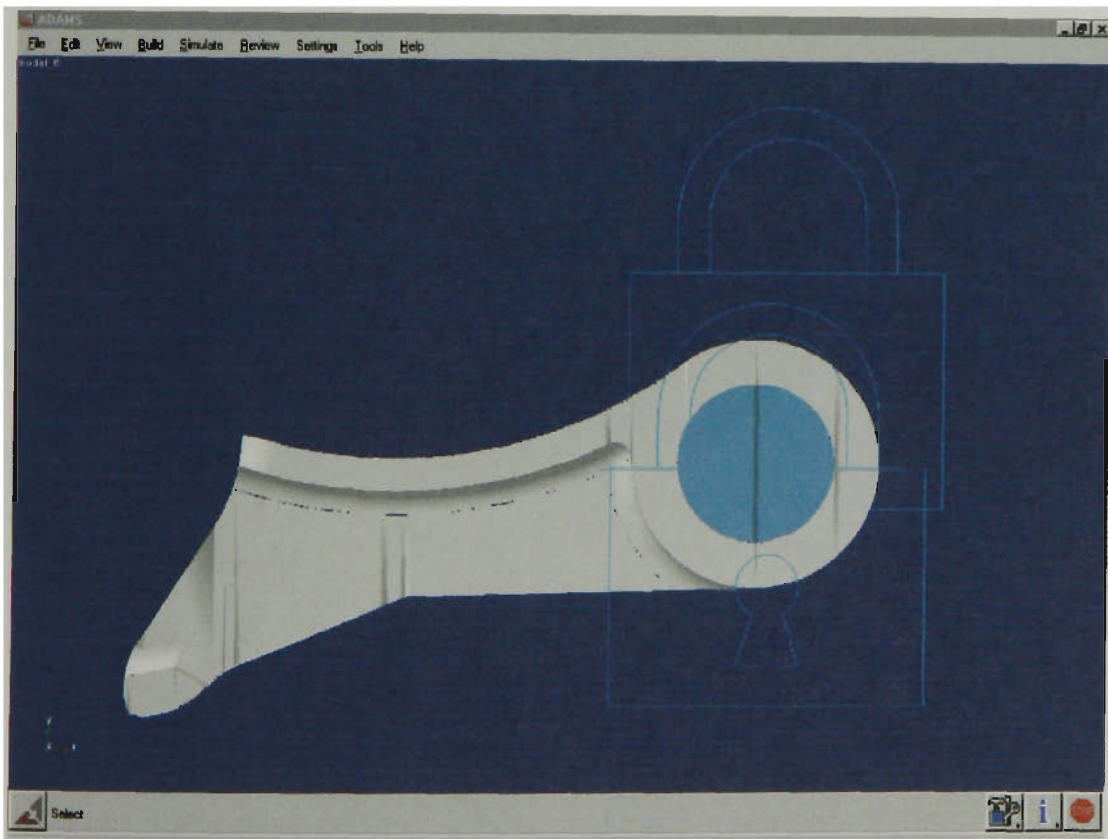


Figure 4.10 – 2D illustration of rockershaft and rocker arm

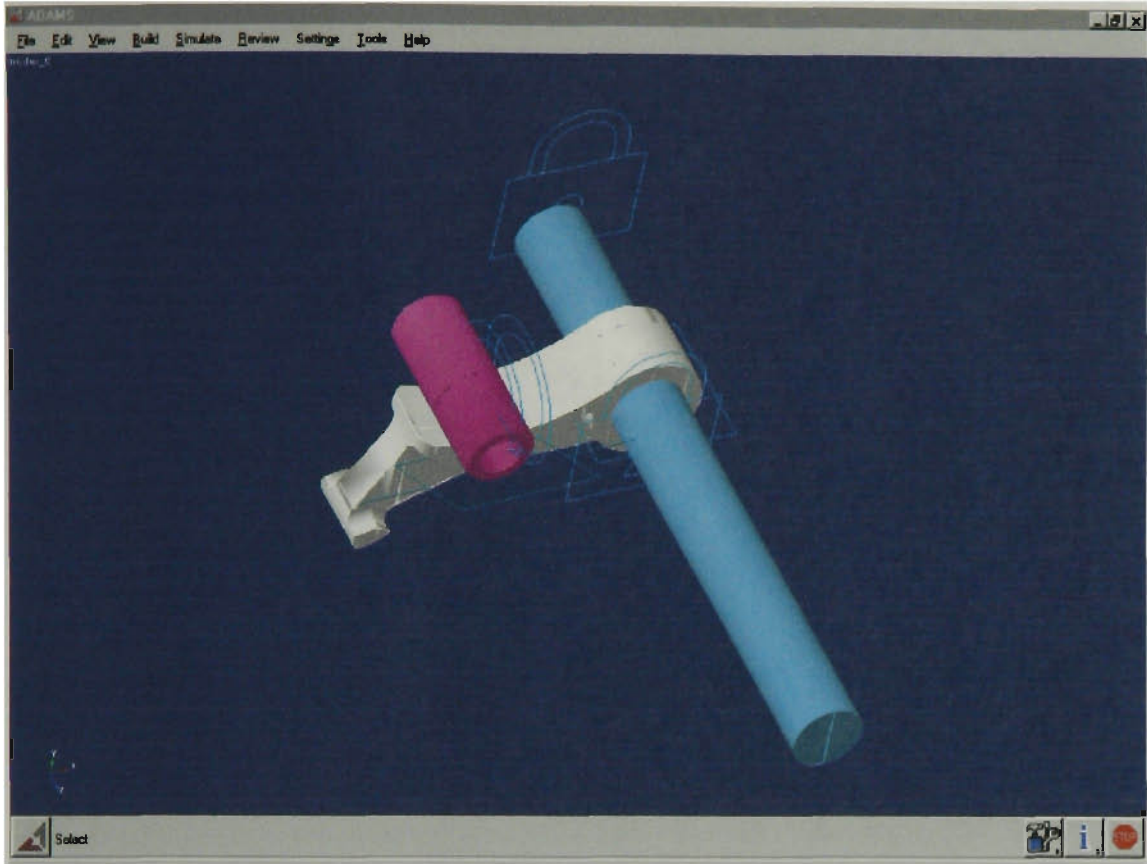


Figure 4.11 – 3D illustration of rockershaft, rocker arm and gudgeon pin

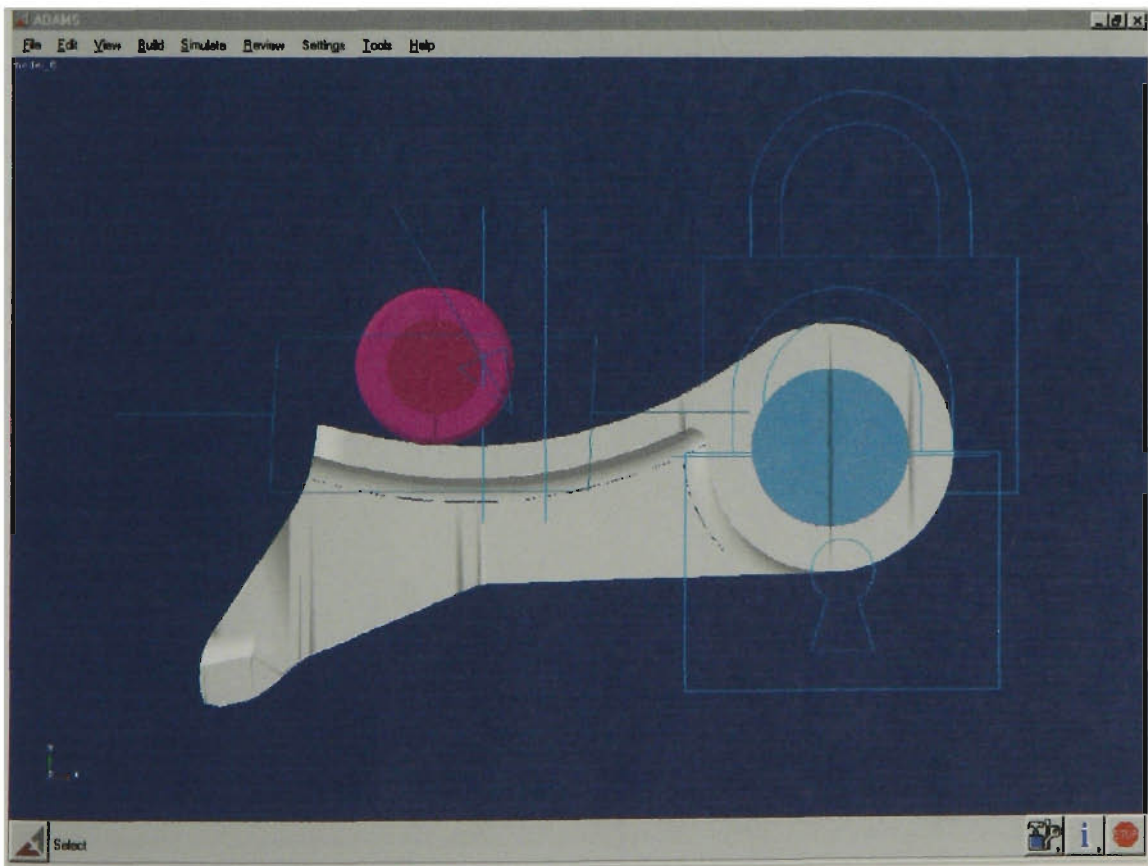


Figure 4.12 – 2D illustration of rockershaft, rocker arm and gudgeon pin

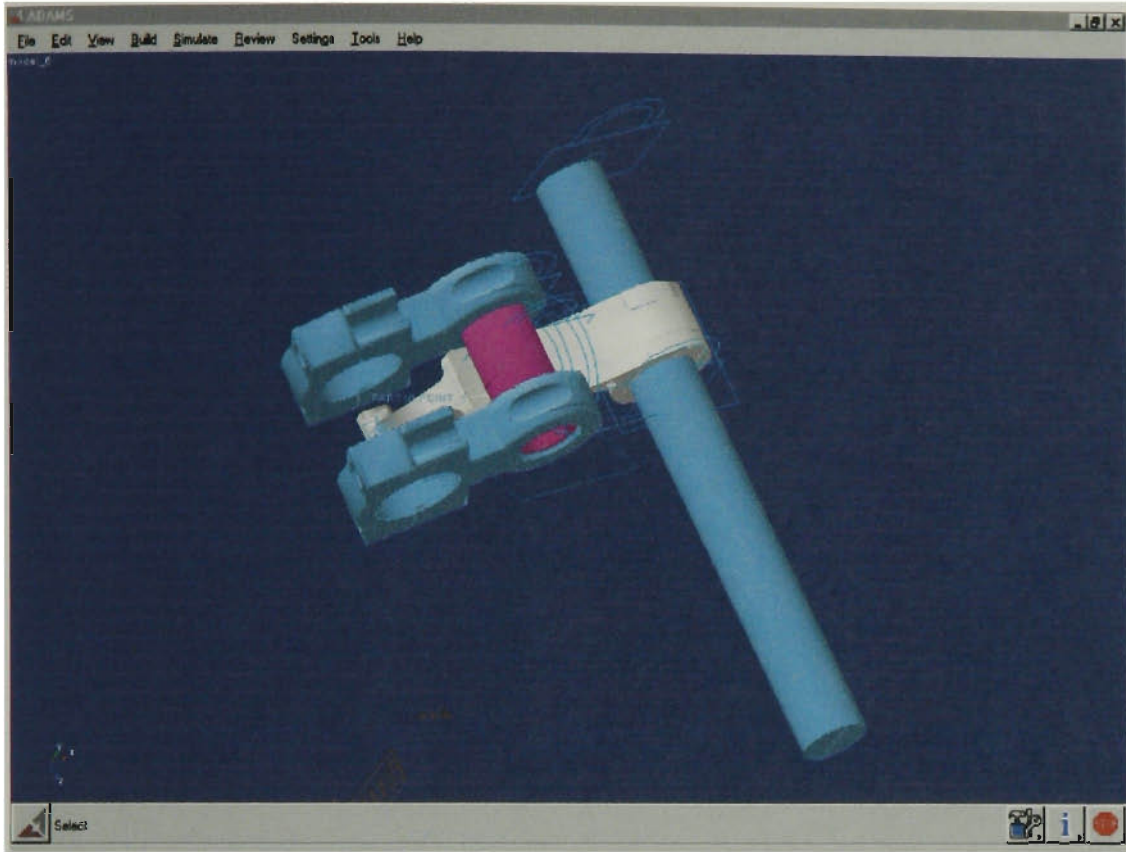


Figure 4.13 – 3D illustration of rockershaft, rocker arm, gudgeon pin and conrods

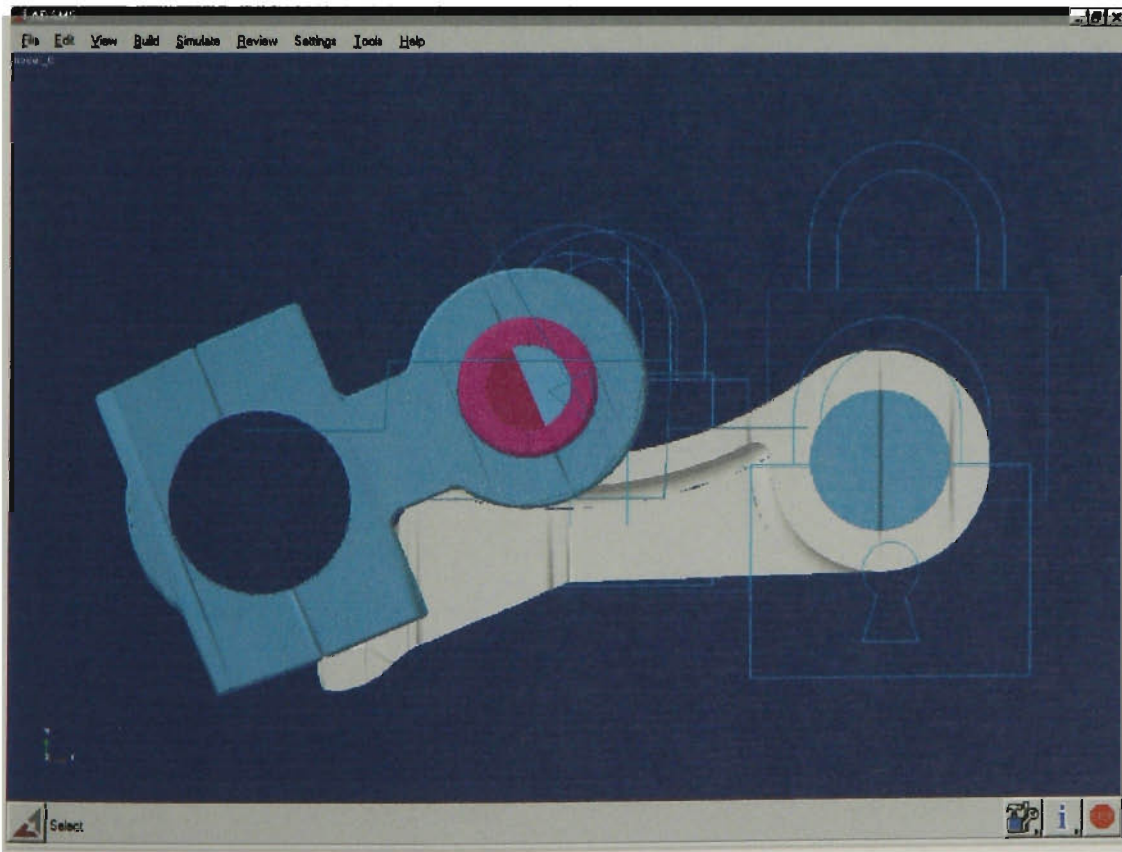


Figure 4.14 – 2D illustration of rockershaft, rocker arm, gudgeon pin and conrods

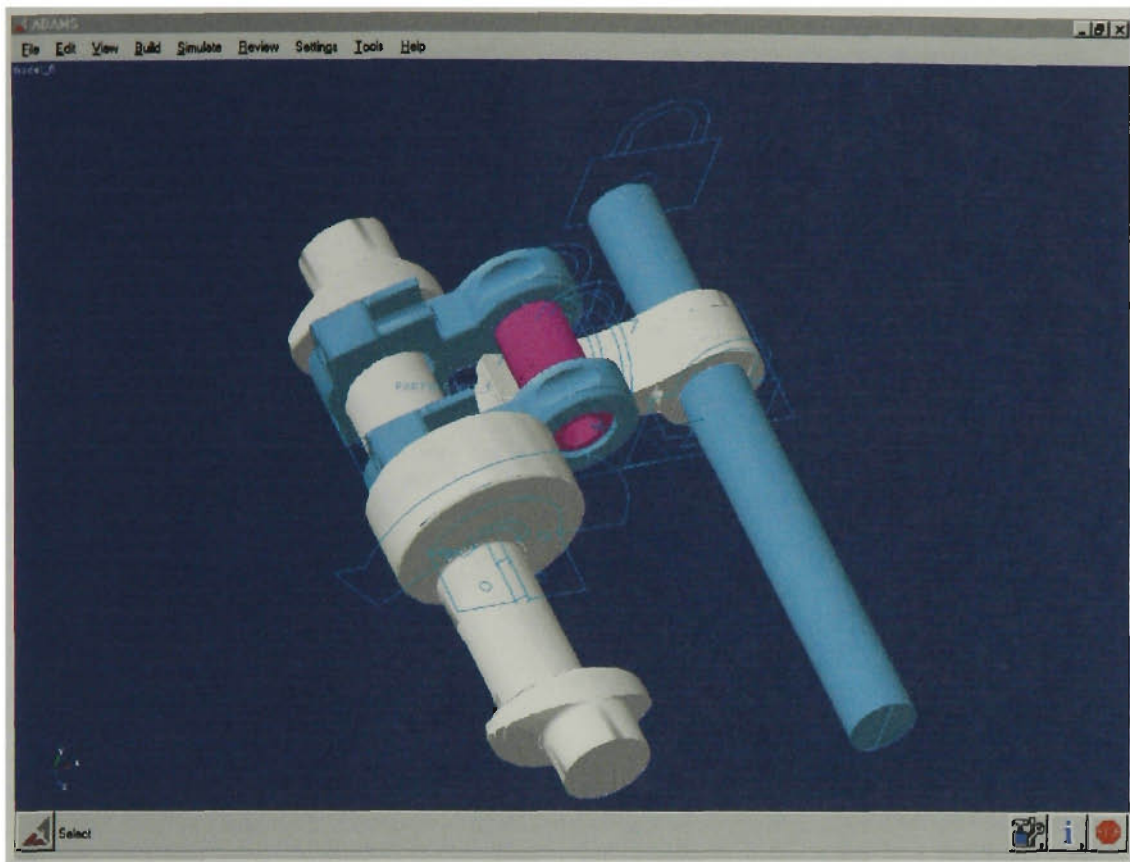


Figure 4.15 – 3D illustration of rockershaft, rocker arm, gudgeon pin, conrods and valve crank

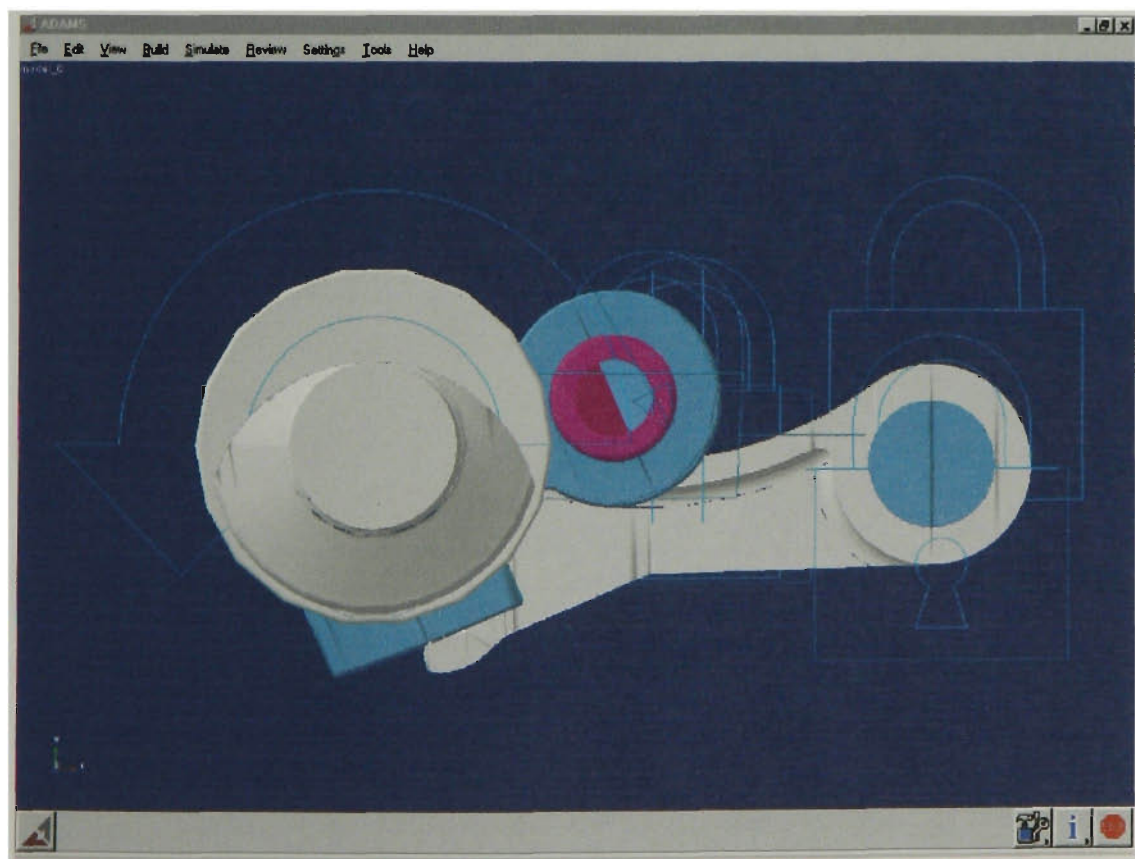


Figure 4.16 – 2D illustration of rockershaft, rocker arm, gudgeon pin, conrods and valve crank

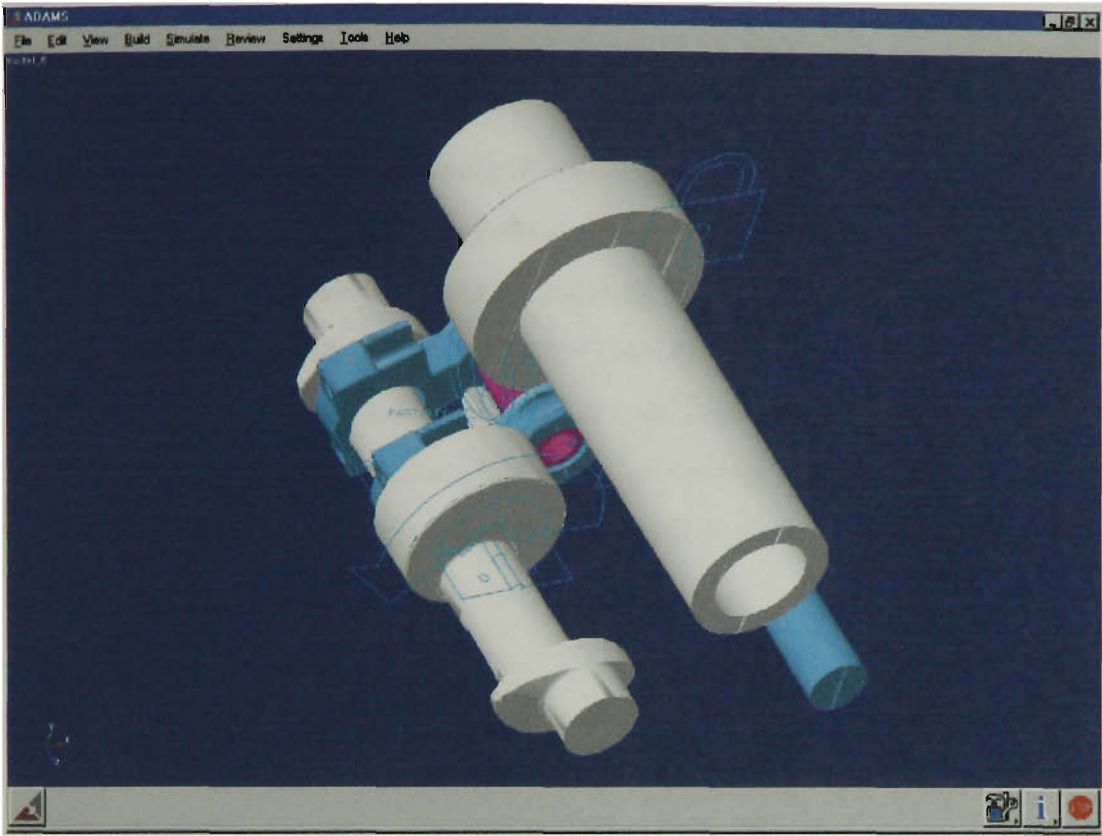


Figure 4.17 – 3D illustration of rockershaft, rocker arm, gudgeon pin, conrods, valve crank and guideshaft

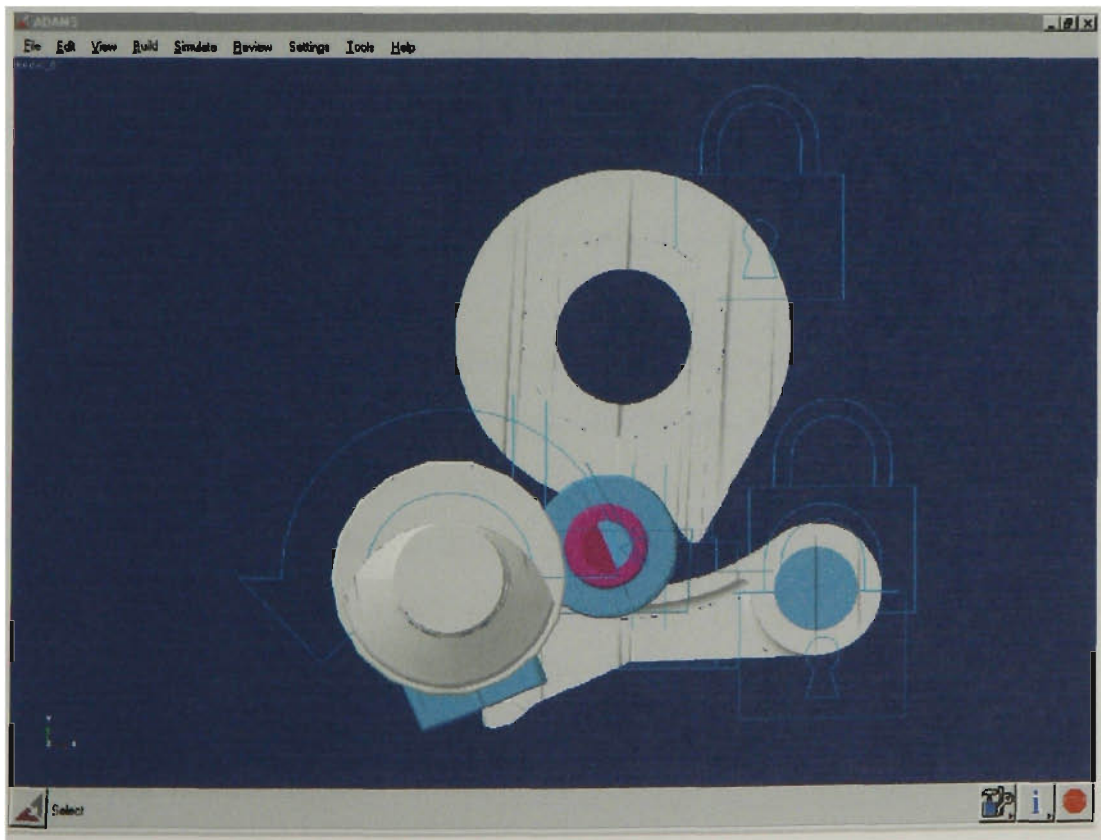


Figure 4.18 – 2D illustration of rockershaft, rocker arm, gudgeon pin, conrods, valve crank and guideshaft

In order for the rocker arm to come into contact with the bucket, so that the bucket can push open the valve, a contact force needs to be applied between the rocker arm and bucket. Before a contact force can be applied, the surfaces of the rocker arm and bucket where the contact will occur must be specified. Originally the whole of the rocker arm and the bucket was specified, however this proved to be a problem as the rocker arm was constrained from pushing onto the valve. The problem was solved by specifying only the point of contact rather than the whole component. Therefore the tip of the rocker arm and top of the bucket were specified as the contact surfaces, and a simulated contact force was applied. Also, a revolute joint was specified between the rocker shaft and ground, so that the rocker arm was able to pivot down onto the bucket.

A problem arose when the contact surfaces of the gudgeon pin and the guideshaft were specified, in that the gudgeon pin could not move along the guideshaft profile, namely along the activating curve of the guideshaft. This was due to the fact that when a contact surface is chosen, the number of points along the contact surface for the contact force to function properly must be introduced. In this instance, too many points were allocated along the activating curve of the guideshaft profile and this restricted the gudgeon pin's movement. A smaller number of points were designated along the curve and the gudgeon pin was then able to move between the guideshaft profile and the rocker arm. Contact forces were then applied between the gudgeon pin and rocker arm and between gudgeon pin and guideshaft.

The gudgeon pin is moved along the rocker arm and guideshaft profile by the valve crank, which is connected to the gudgeon pin by the conrods. As the valve crank rotates, the pin is pushed backwards and forwards, with the amount of the valve lift determined by the guideshaft position. By changing the degree of rotation of the guideshaft, the valve lift opening can be made either larger or smaller. In order for the valve crank to rotate, a revolute joint was specified between the valve crank and ground. Rotational motion was applied to the revolute joint, so that the speed of the valve crank was controlled.

Previously a fixed joint was introduced between the conrods big ends and the valve crank. It was found that this prevented the conrods from rotating about the valve crank, so instead of applying a fixed joint, a revolute joint was used so that the conrods could rotate about the valve crank. The gudgeon pin was fixed to the conrods little ends, and as the valve crank rotated, the gudgeon pin was able to move backwards and forwards, with the sandwiching contact forces preventing the gudgeon pin from leaving the rocker arm or guideshaft.

3.3 Dynamic Valve Control

The system is operated by the rotation of the valve crank. As the valve crank rotates, the gudgeon pin, which is connected to the valve crank by the conrod's, moves forwards and backwards along the guideshaft profile. Figure 4.19 illustrates the gudgeon pin as it moves forwards along the guideshaft and rocker arm.

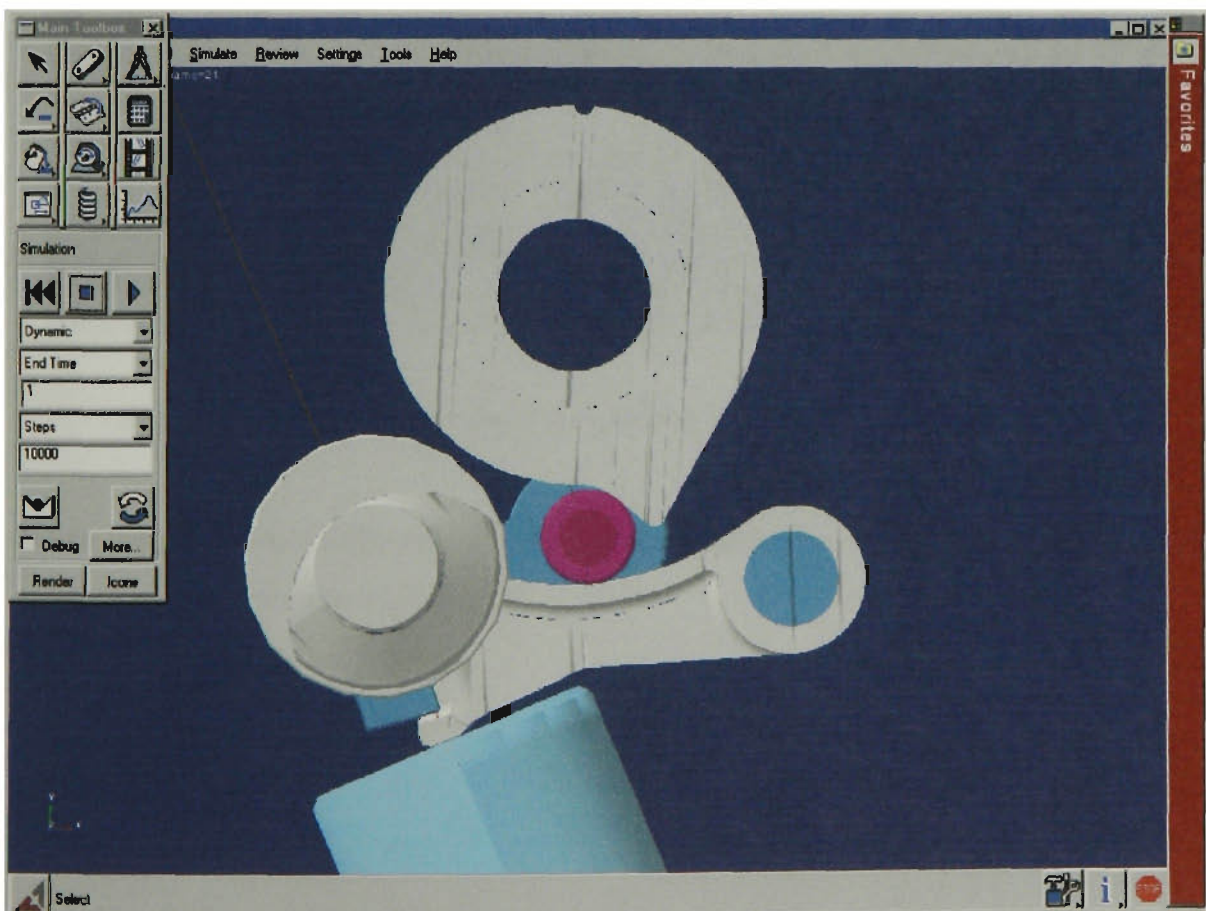


Figure 4.19 – Gudgeon pin approaching actuating curve

It should be noted that in Figures 4.19 to 4.21, one of the conrods was made invisible, so that the movement of the gudgeon pin along the rocker arm and guideshaft could be seen clearly. Once the pin reaches the activating curve of the guideshaft, it pushes the rocker arm down against the bucket, which in turn opens the valve, as illustrated in Figure 4.20.

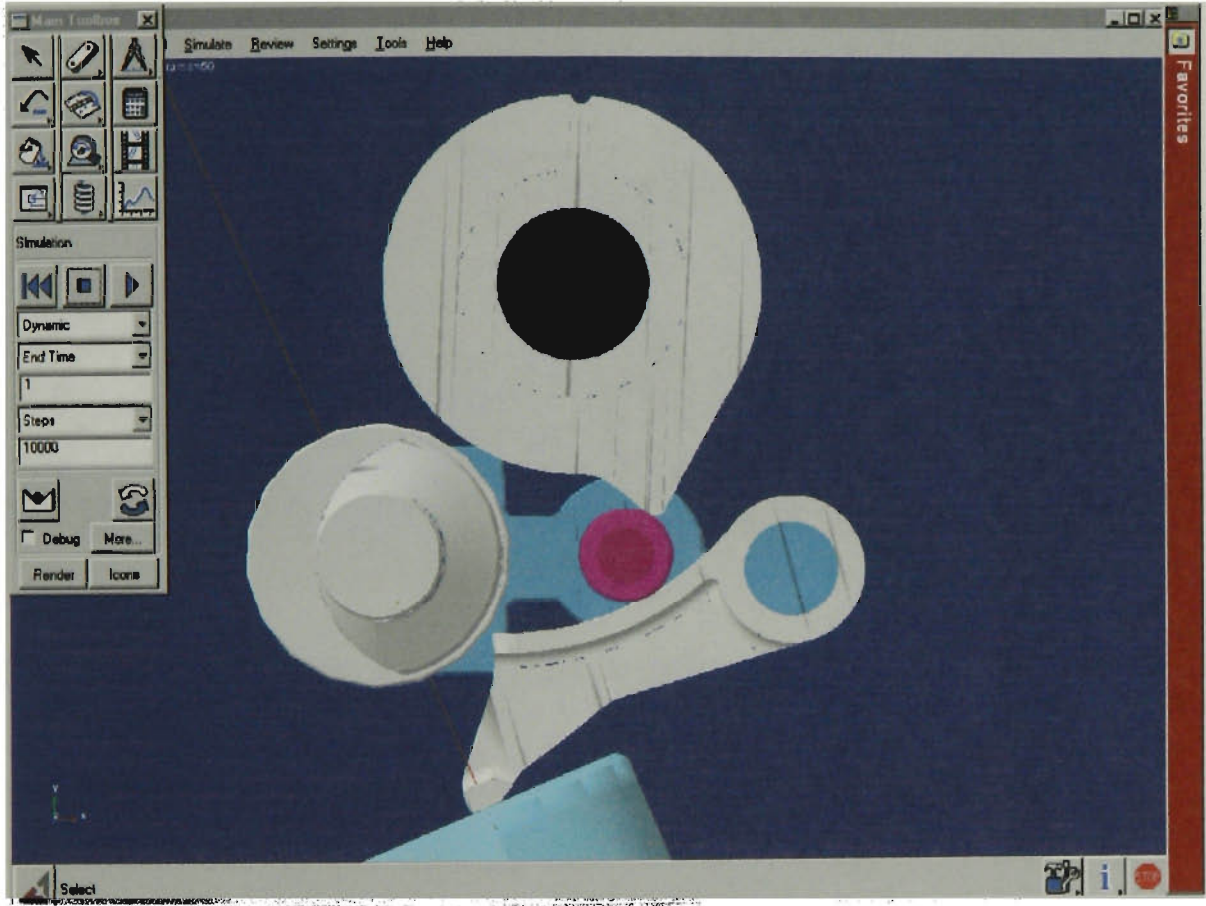


Figure 4.20 – Gudgeon pin at the activating curve of the guideshaft

When the pin moves backwards along the guideshaft and rocker arm, the valve begins to close, as illustrated in Figure 4.21.

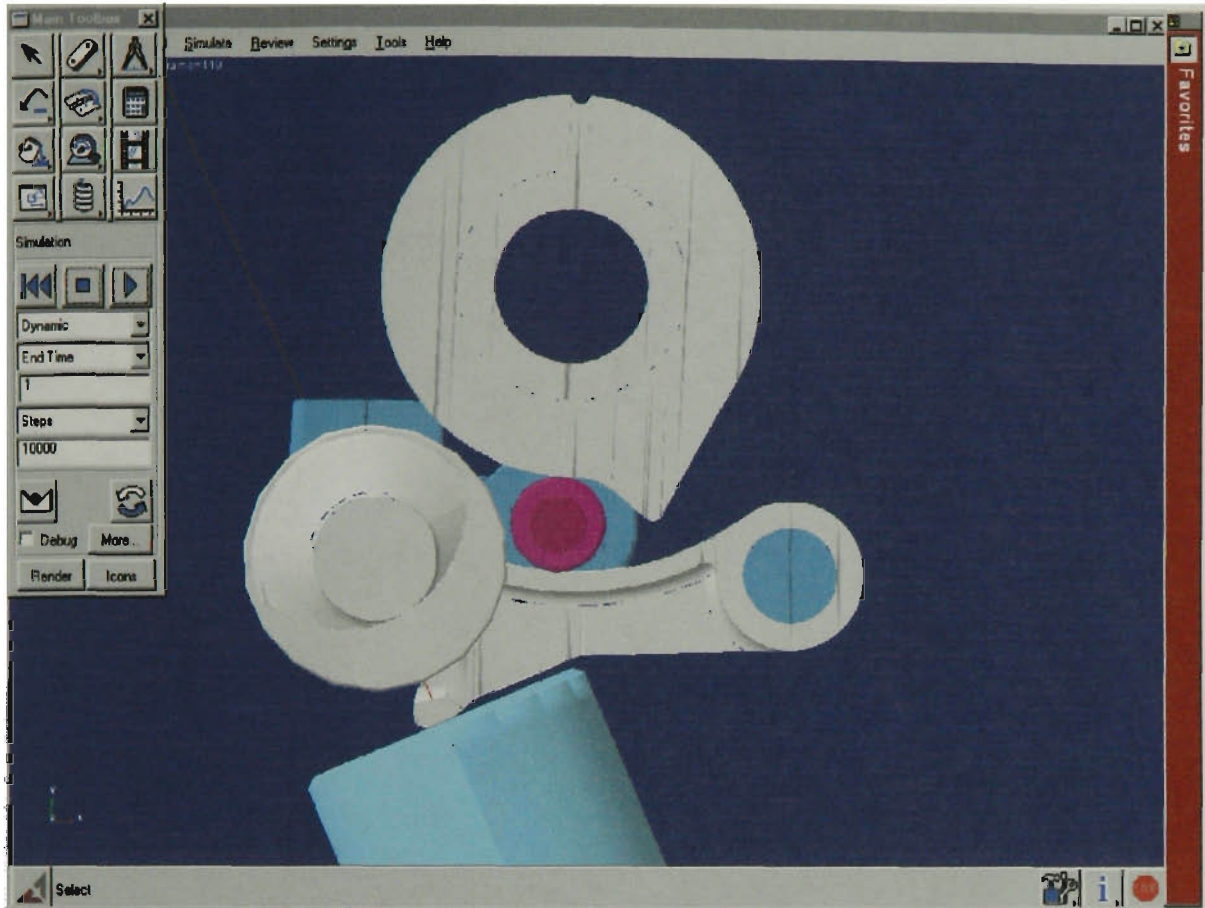


Figure 4.21 – Valve closing as gudgeon pin moves backwards along the guideshaft

Variable lift is achieved by the guideshaft, which is controlled by a hydraulic mechanism, connected to the engine management system. The guideshaft profile moves backwards and forwards according to engine speed and load, varying the interaction of the gudgeon pin as it moves backwards and forwards along the rocker arm. The degree of valve lift is dependent on the amount the guideshaft is rotated. At idle, the pin only touches the initial portion of the actuation curve of the guideshaft, this effectively opens the valve by a small amount. This small opening of the valve substitutes for the throttle, a device in the engine that regulates the flow of air into the cylinders.

The DVC system will have a continuously variable lift, this means that the valves will be able to open to lifts of say, 5mm, 6mm or 7mm, with stepless variation and does not just open fully to its maximum lift.

Figure 4.22 shows the DVC system when the valve is closed which is when the

guideshaft is positioned at seven degrees or at start location, while Figure 4.23 illustrates the DVC system when the valve is fully opened, when the guideshaft is at 357 degrees (three degrees clockwise from start location)

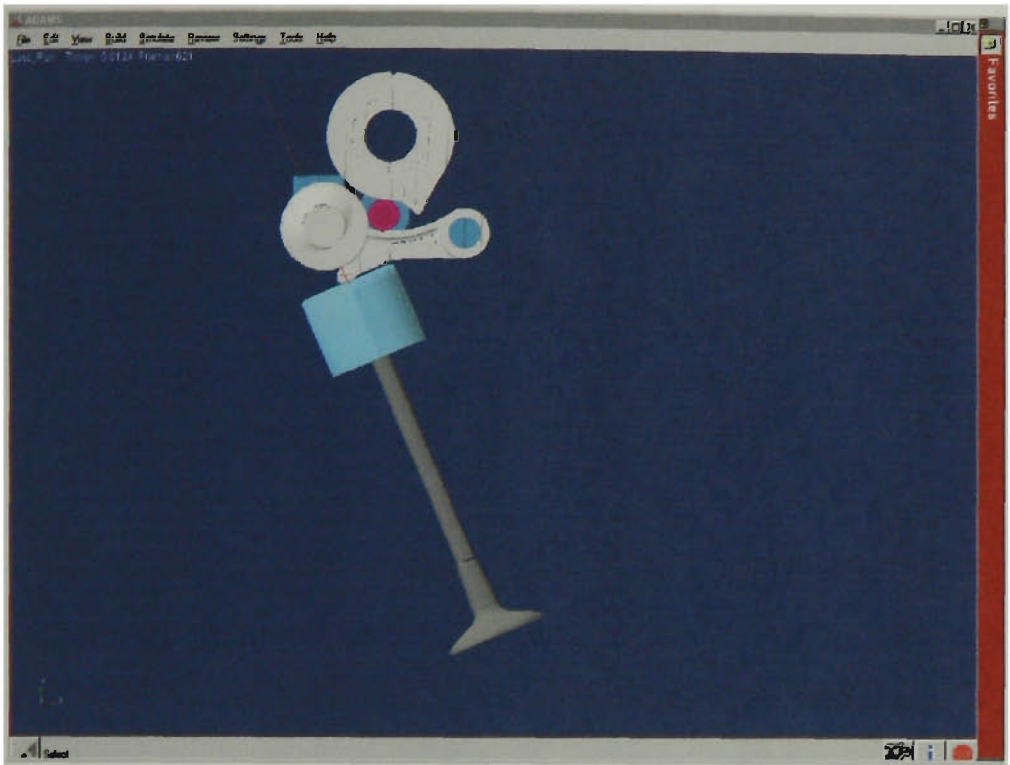


Figure 4.22 –DVC system when the valve is closed

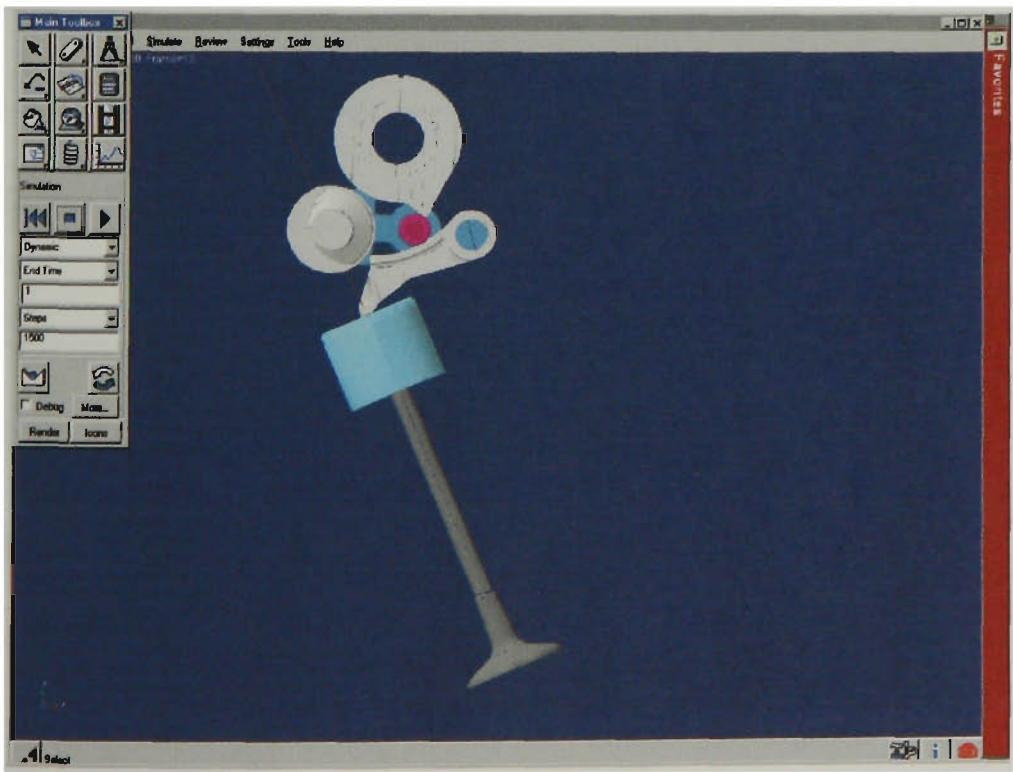


Figure 4.23 – DVC system when the valve is fully opened

4.3 Simulation Results

Once the DVC model was complete, computer simulations were performed under various operating conditions. The purpose was to determine the valve lifts, velocities, acceleration and constraint forces generated in the DVC model. Each simulation was for 1 second, with 50000 steps. The steps represent the total number of times output information is provided over the entire simulation.

The engine speeds for the DVC simulation were 60 rpm, 3000 rpm, and 6000 rpm. The valve crank is a substitute for the camshaft and the camshaft rotates at half the speed of the engine. The camshaft speeds are shown in Table 4.2.

Due to the fact there is rotational motion applied to the valve crank for it to drive the model, these speeds were converted to degrees/sec using the equation below,

$$\omega = \text{RPM} / 60 * 360 \quad (4.1)$$

Engine Speed (rpm)	Camshaft Speed (rpm)	Converted ADAMS Speed (deg/sec)
60	30	180
3000	1500	9000
6000	3000	18000

Table 4.2 - Converted engine and camshaft speeds

4.3.1 DVC Valve Profile

The rotational location of the guideshaft determines the valve lift. The guideshaft, which is connected to the engine management system via a hydraulic mechanism, rotates according to the engine speed and load much in the same manner as that developed by Steinberg et al. (1998). The DVC system would use a hydraulic hub connected to the guideshaft and the ECU would control the valves that supply oil to the hydraulic hub. However, the DVC design would be simpler because it wouldn't rotate like those connected to a continuously spinning camshaft. Using ADAMS, the guideshaft was rotated to fixed positions in increments of 1 degree between minimum lift and maximum lift.

As the guideshaft rotates clockwise, the valve lift increases and the valve lift decreases when the guideshaft rotates anti - clockwise. The guideshaft can rotate from minimum lift to maximum lift in a span of 10 degrees. The valve lifts of the DVC system are shown in Figures 4.24, 4.25, 4.26, 4.27, 4.28, 4.29, 4.30, 4.31, 4.32, 4.33 and 4.34.

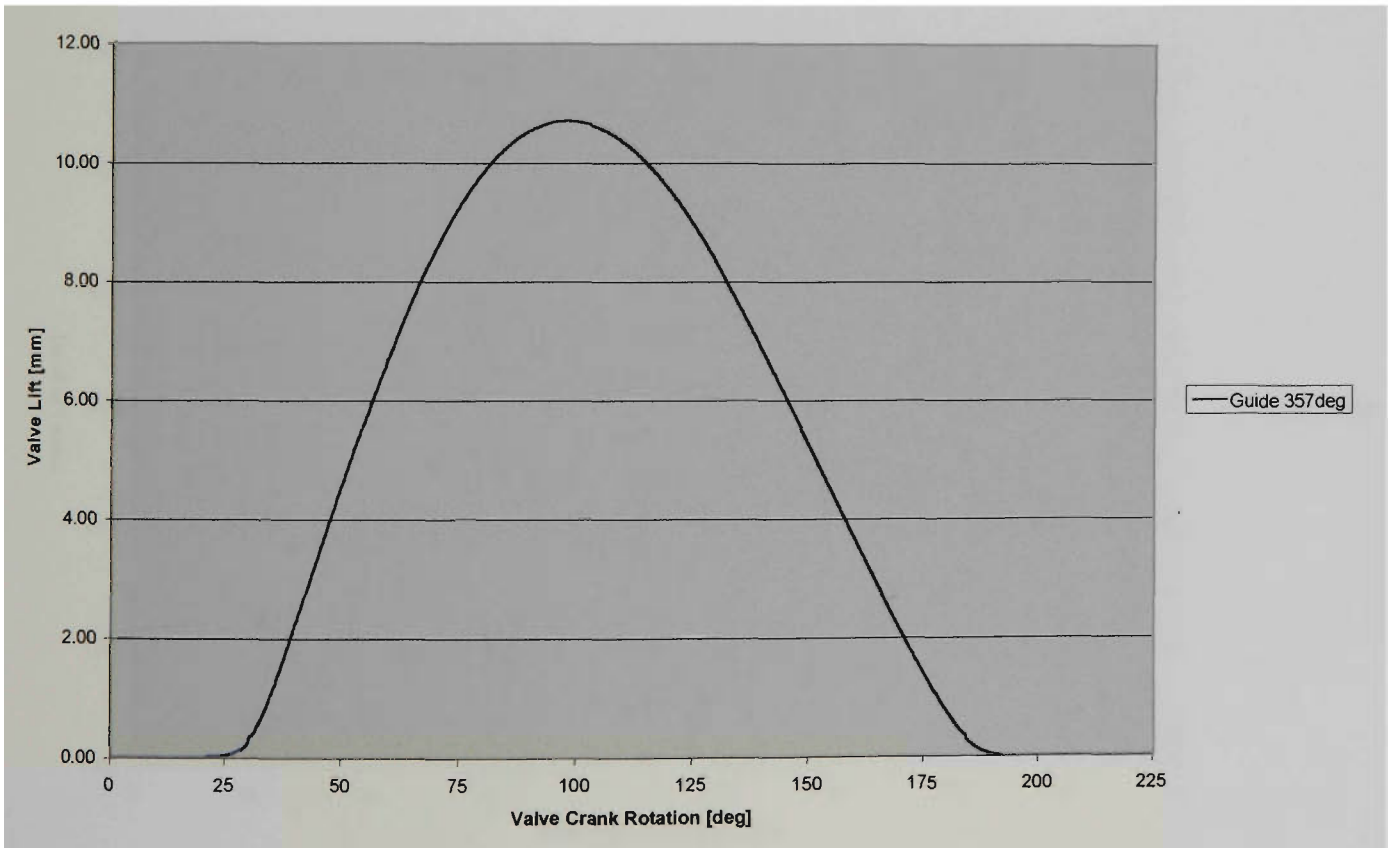
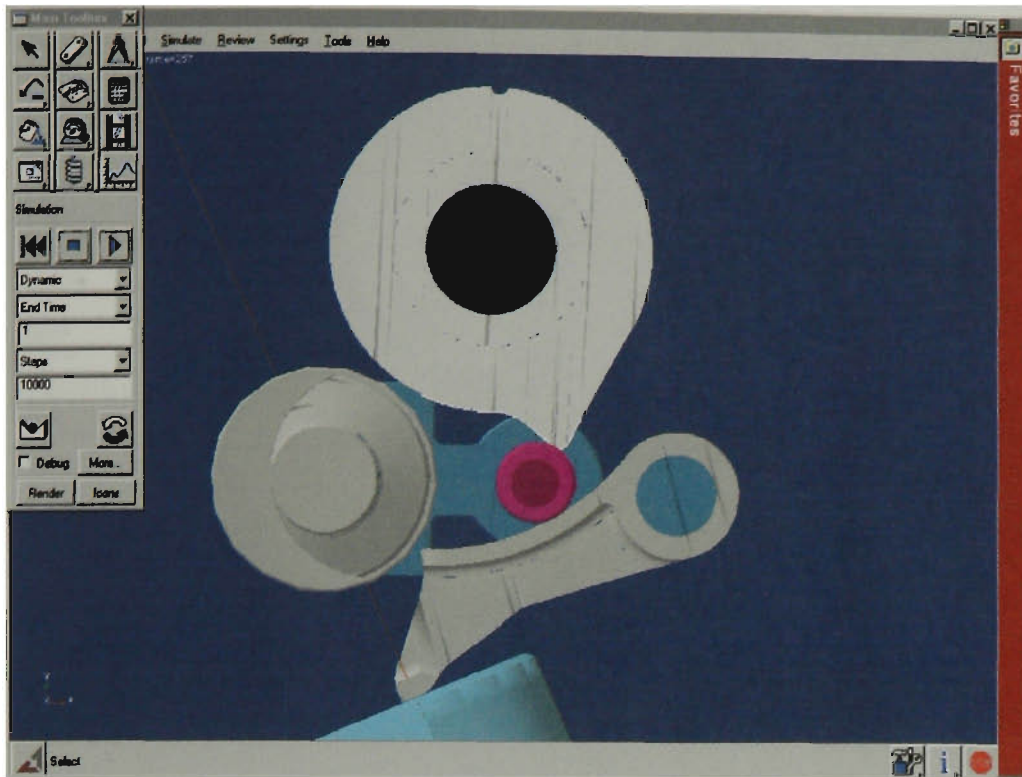


Figure 4.24 – Valve profile of DVC system at 357 degrees

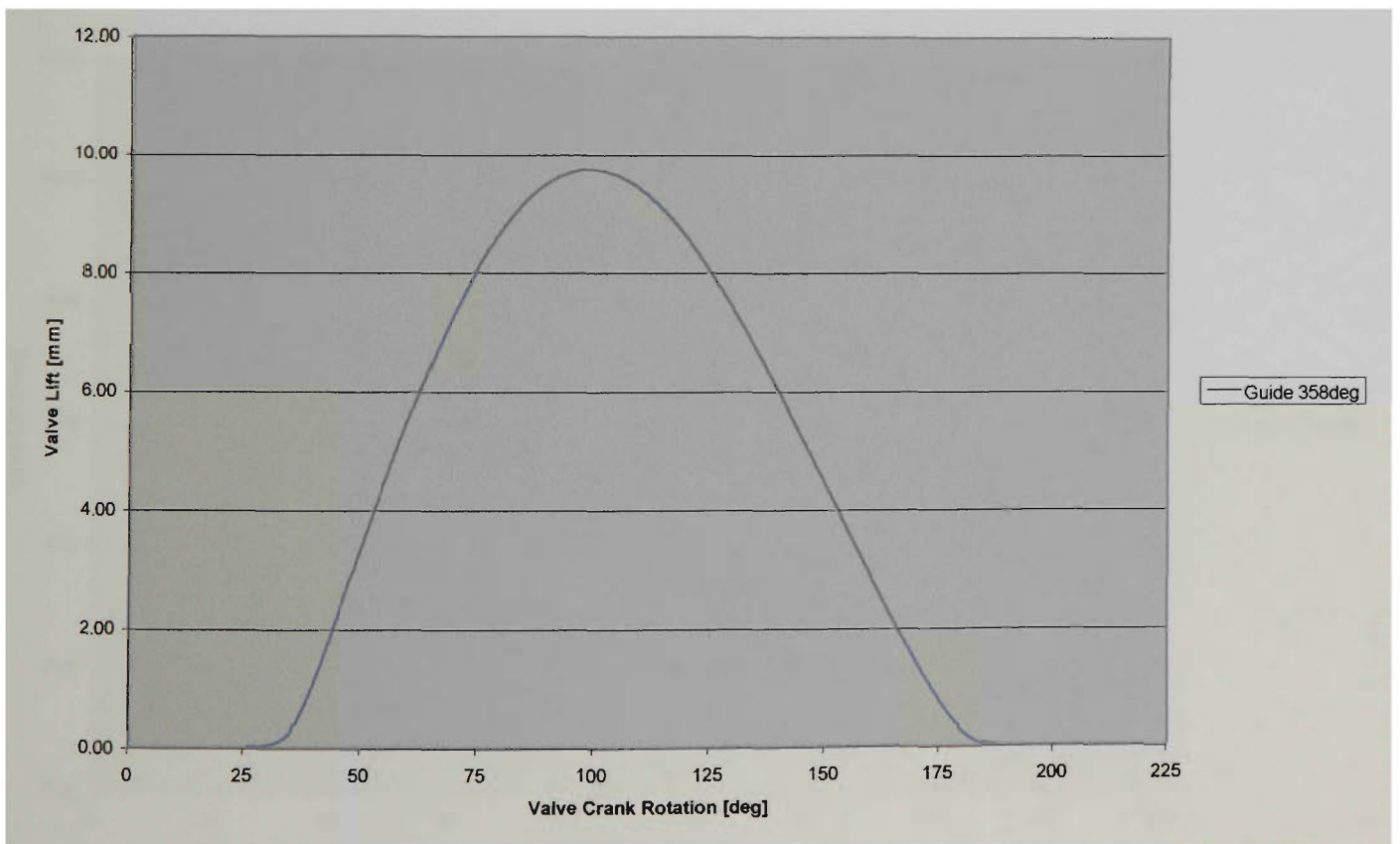
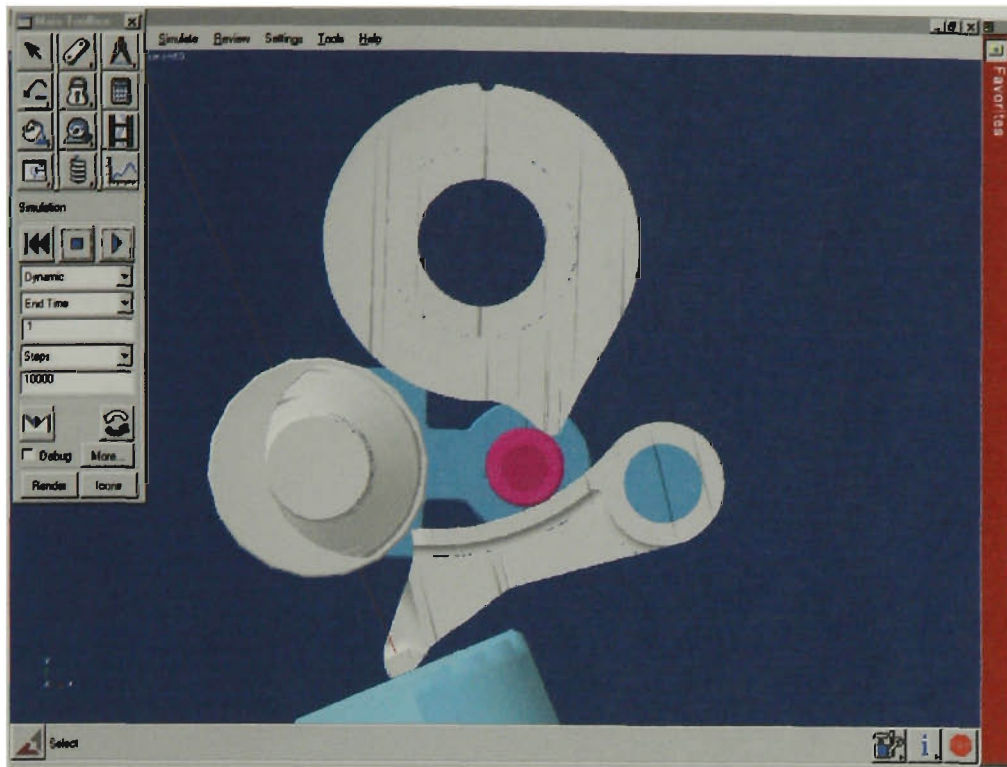


Figure 4.25 – Valve profile of DVC system at 358 degrees

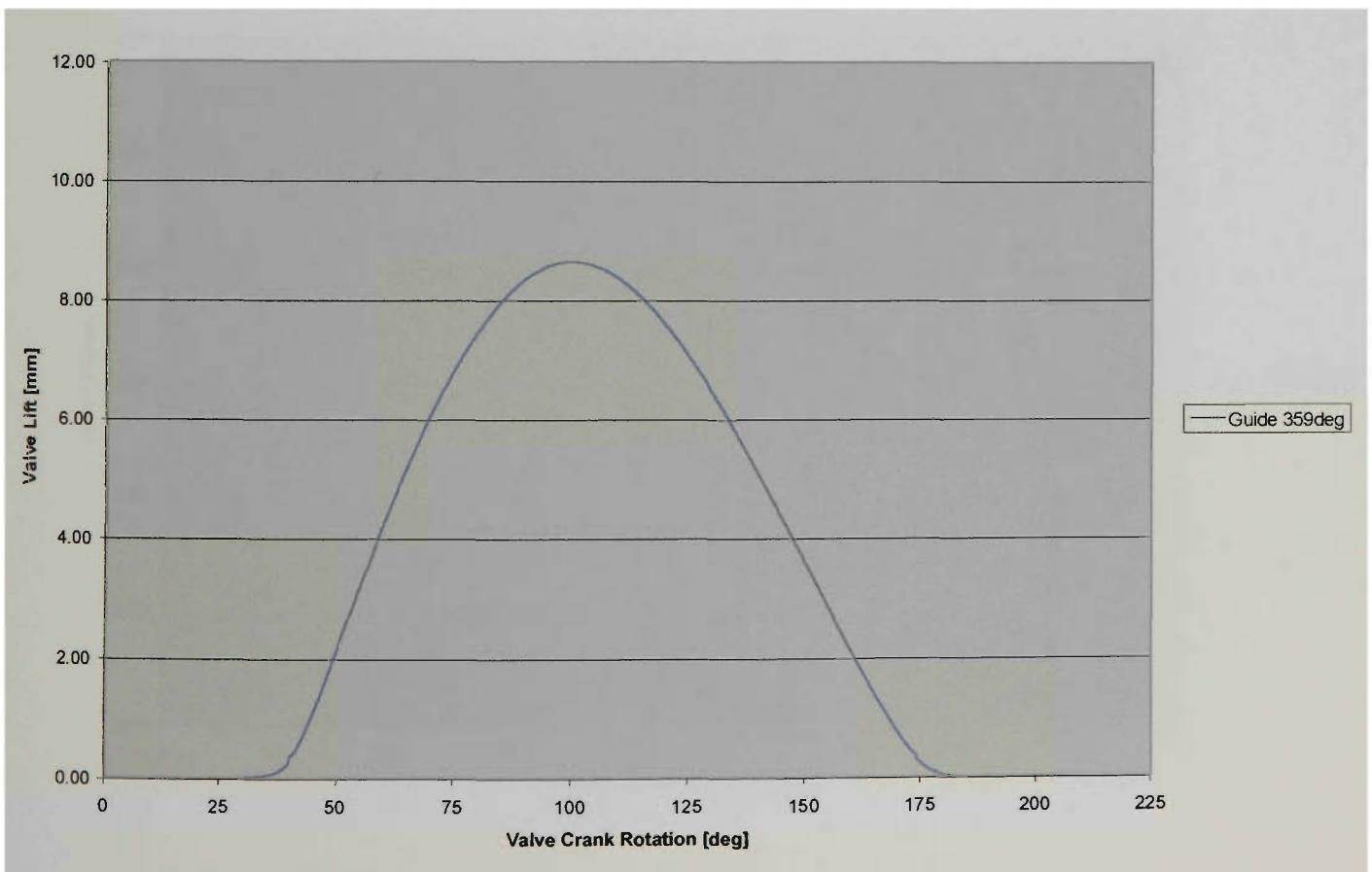
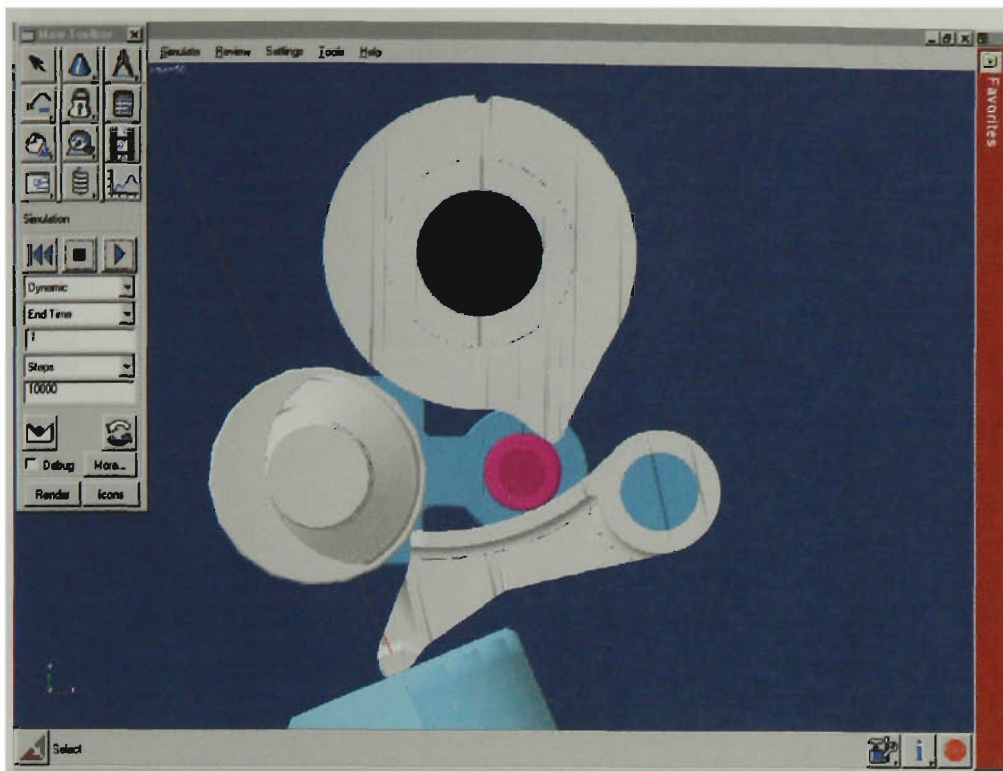


Figure 4.26 – Valve lift and duration at 359 degrees.

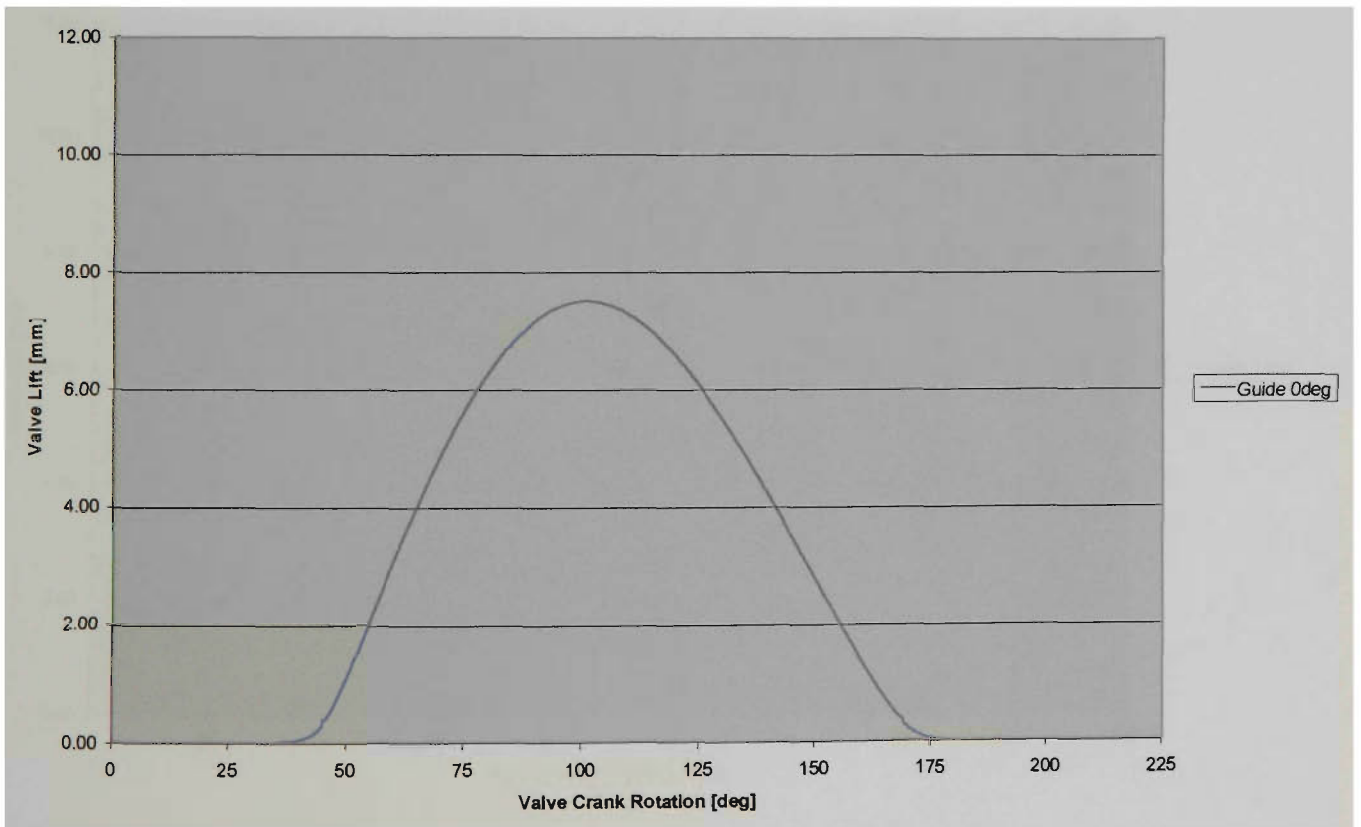
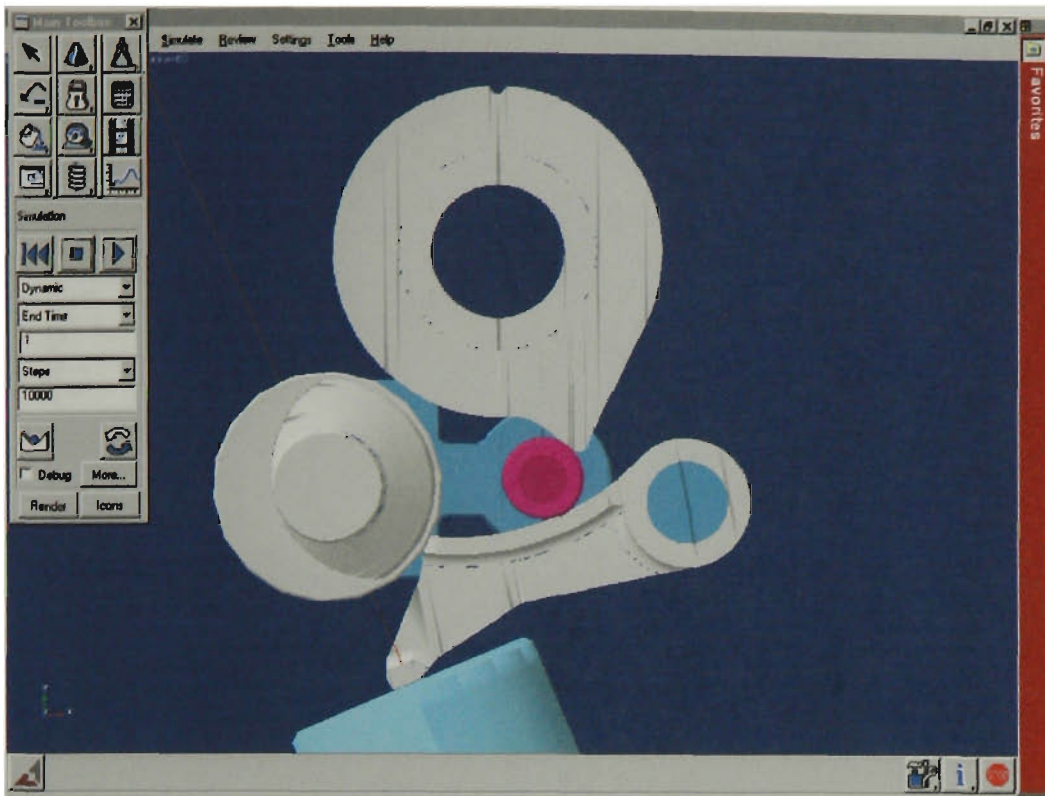


Figure 4.27 – Valve lift and duration at 0 degrees.

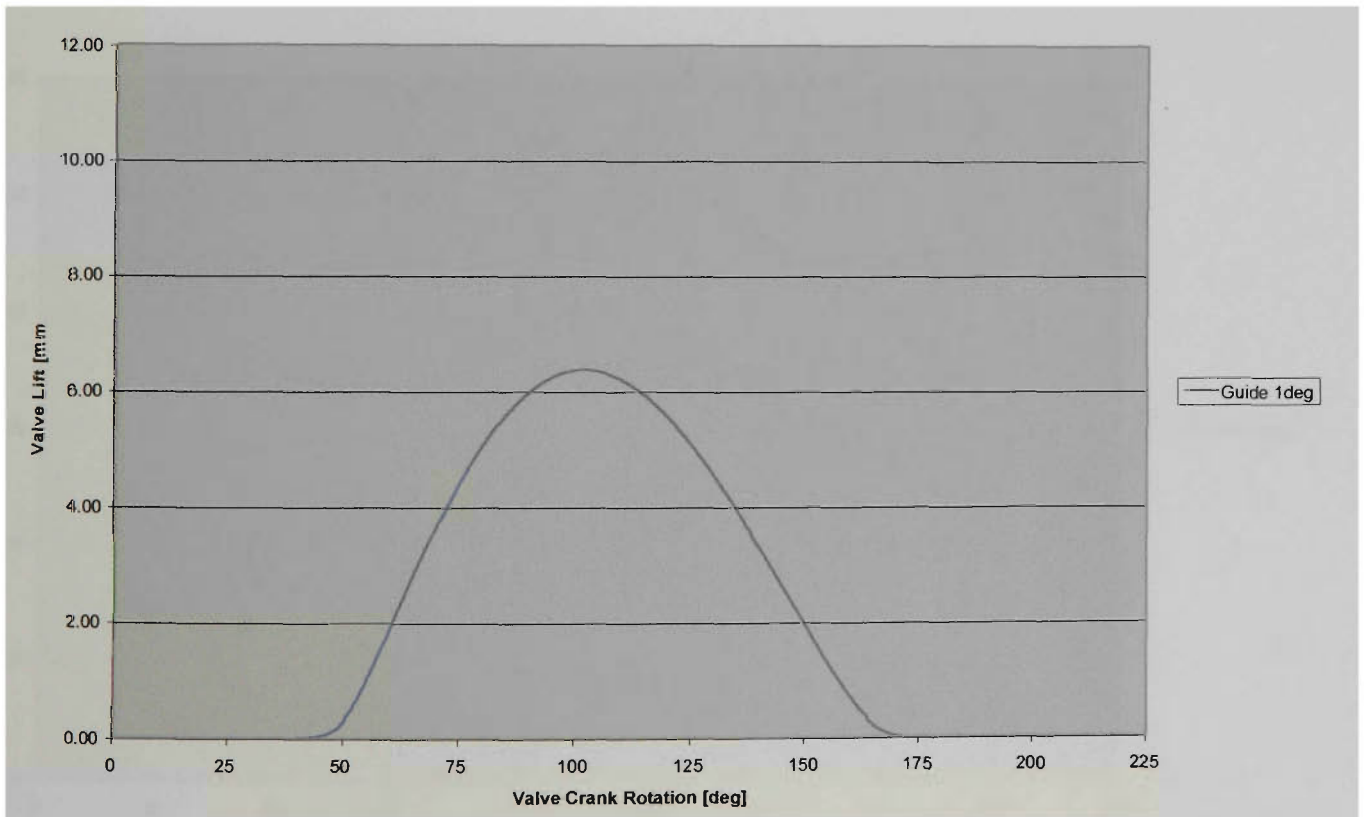
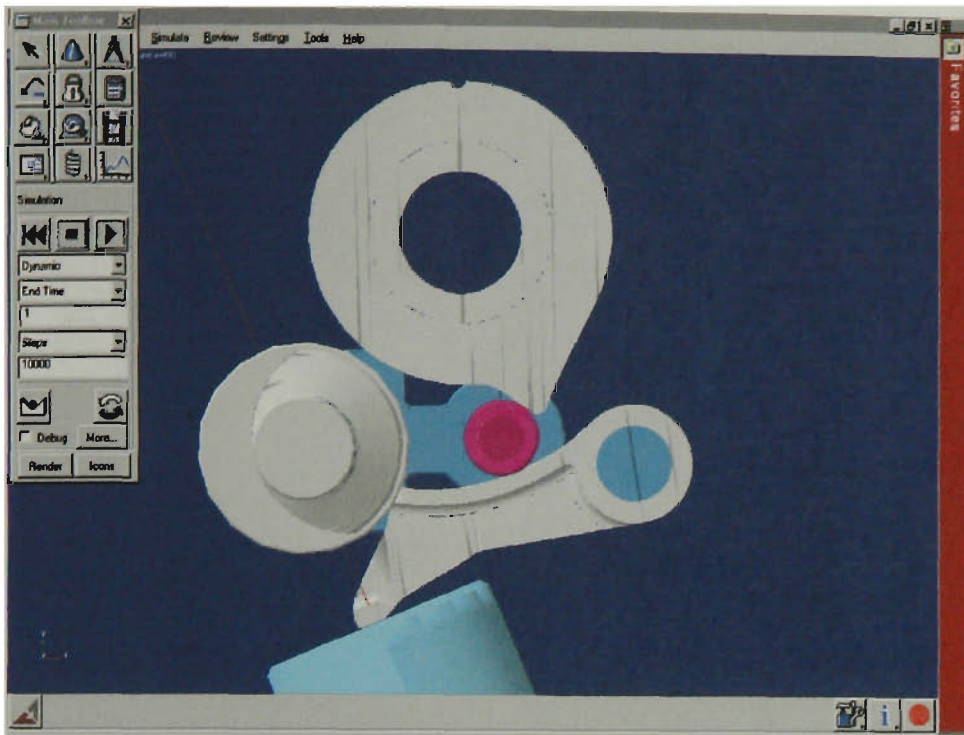


Figure 4.28 – Valve profile of DVC system at 1 degree

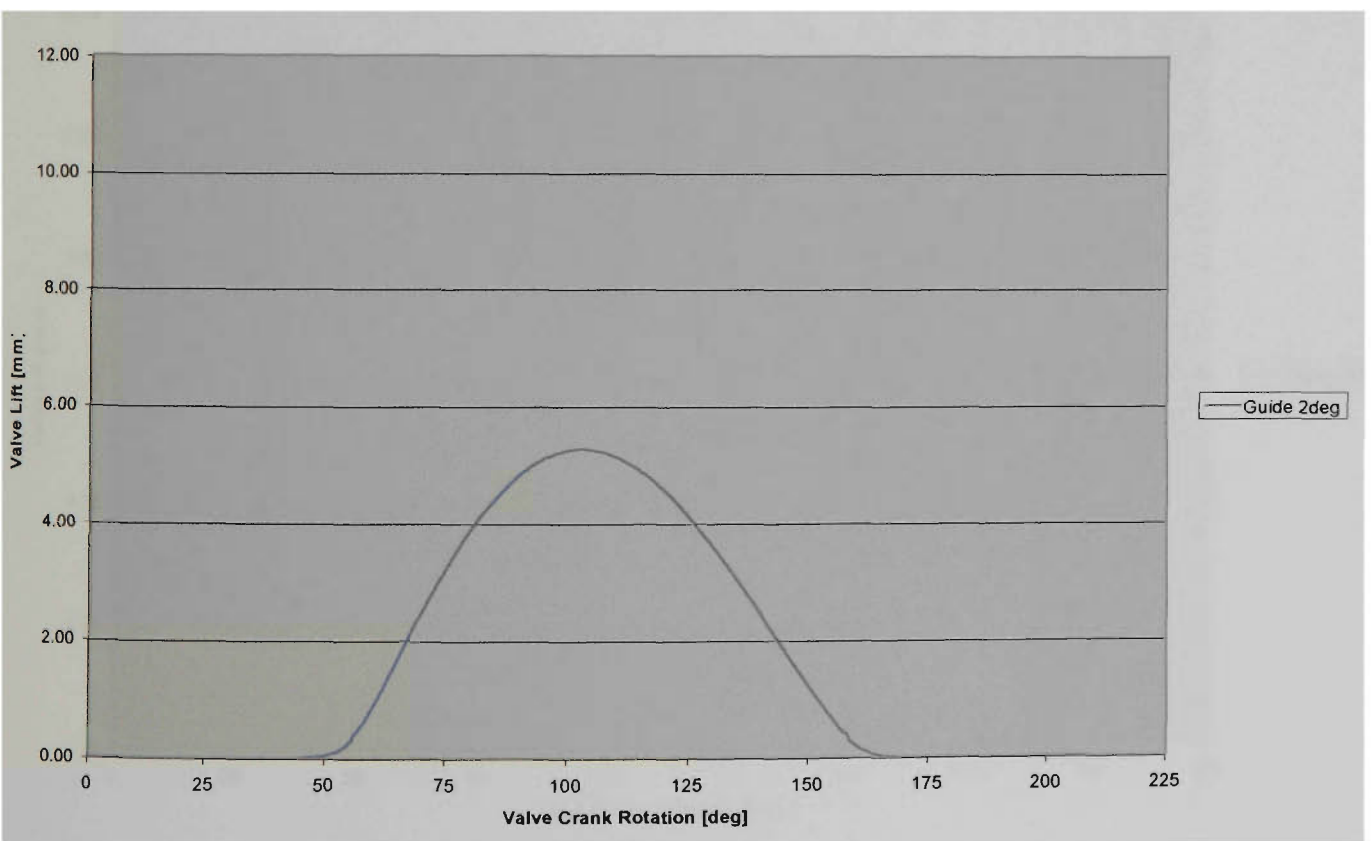
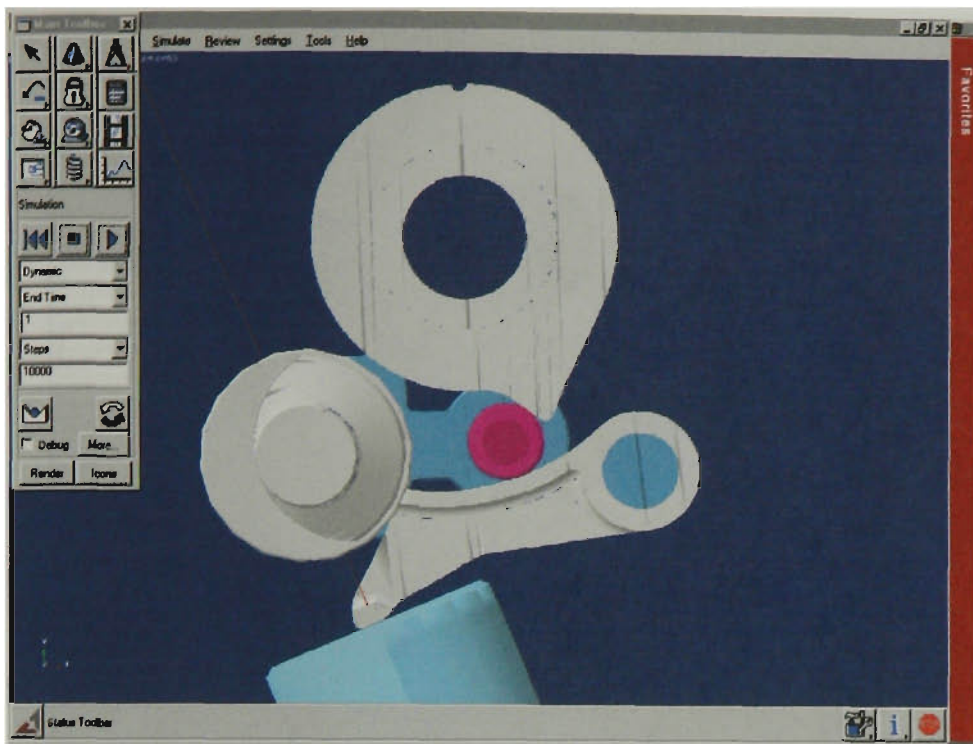


Figure 4.29 – Valve profile of the DVC system at 2 degrees.

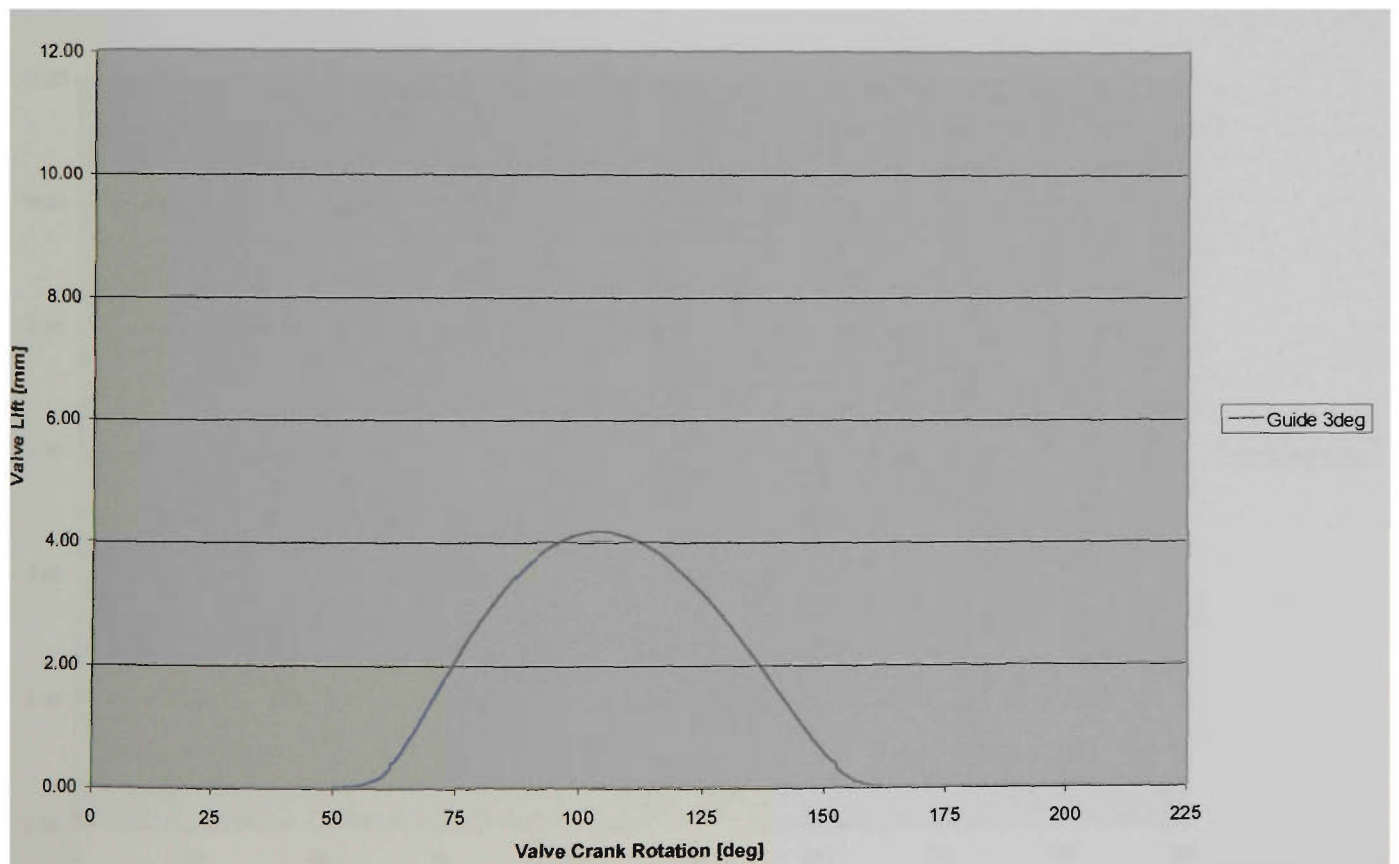
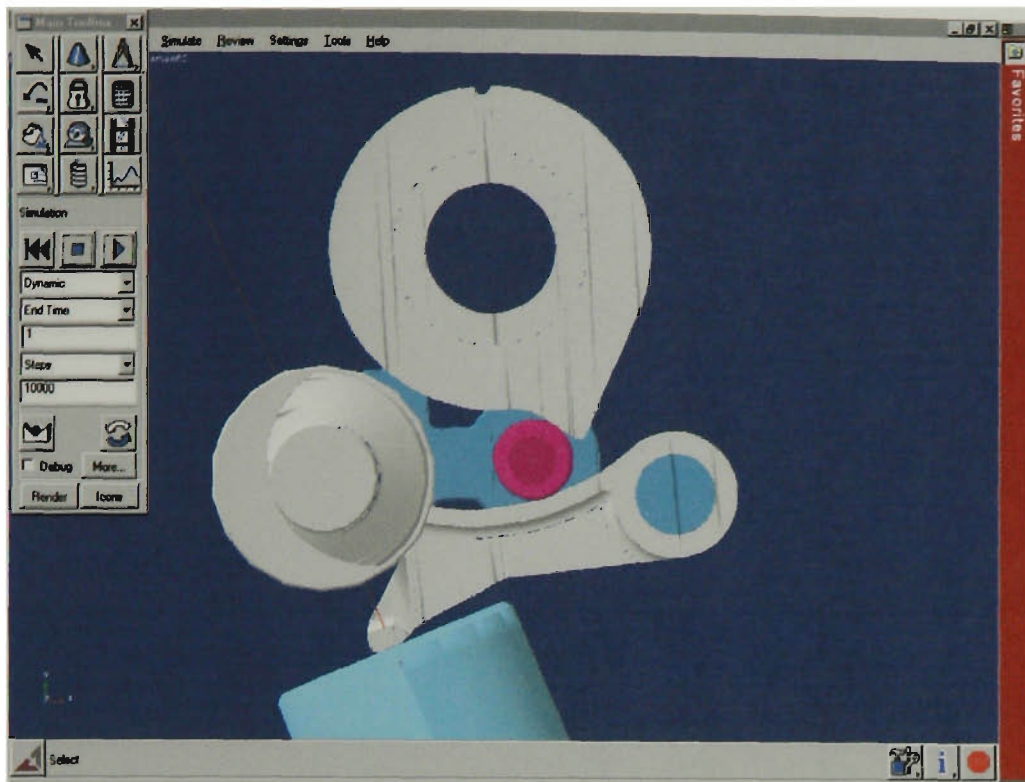


Figure 4.30 – Valve profile of DVC system at 3 degrees.

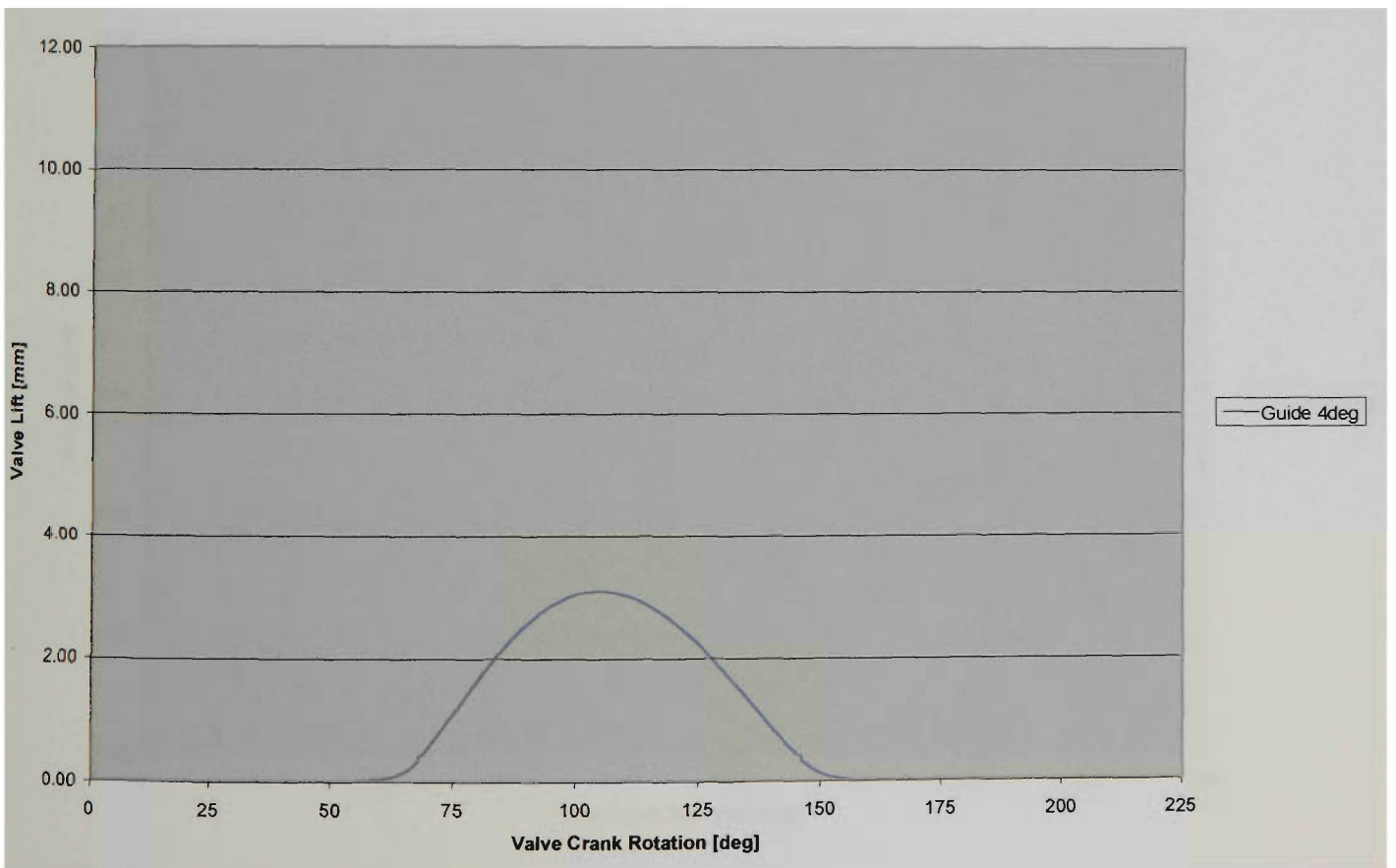
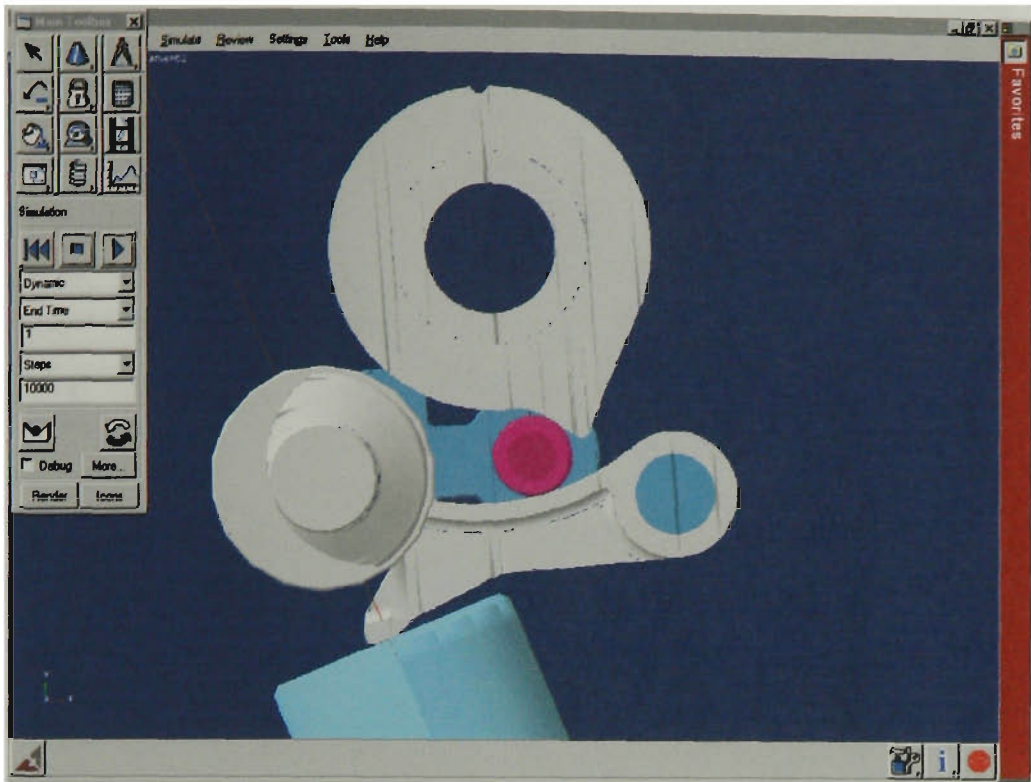


Figure 4.31 – Valve profile of DVC system at 4 degrees.

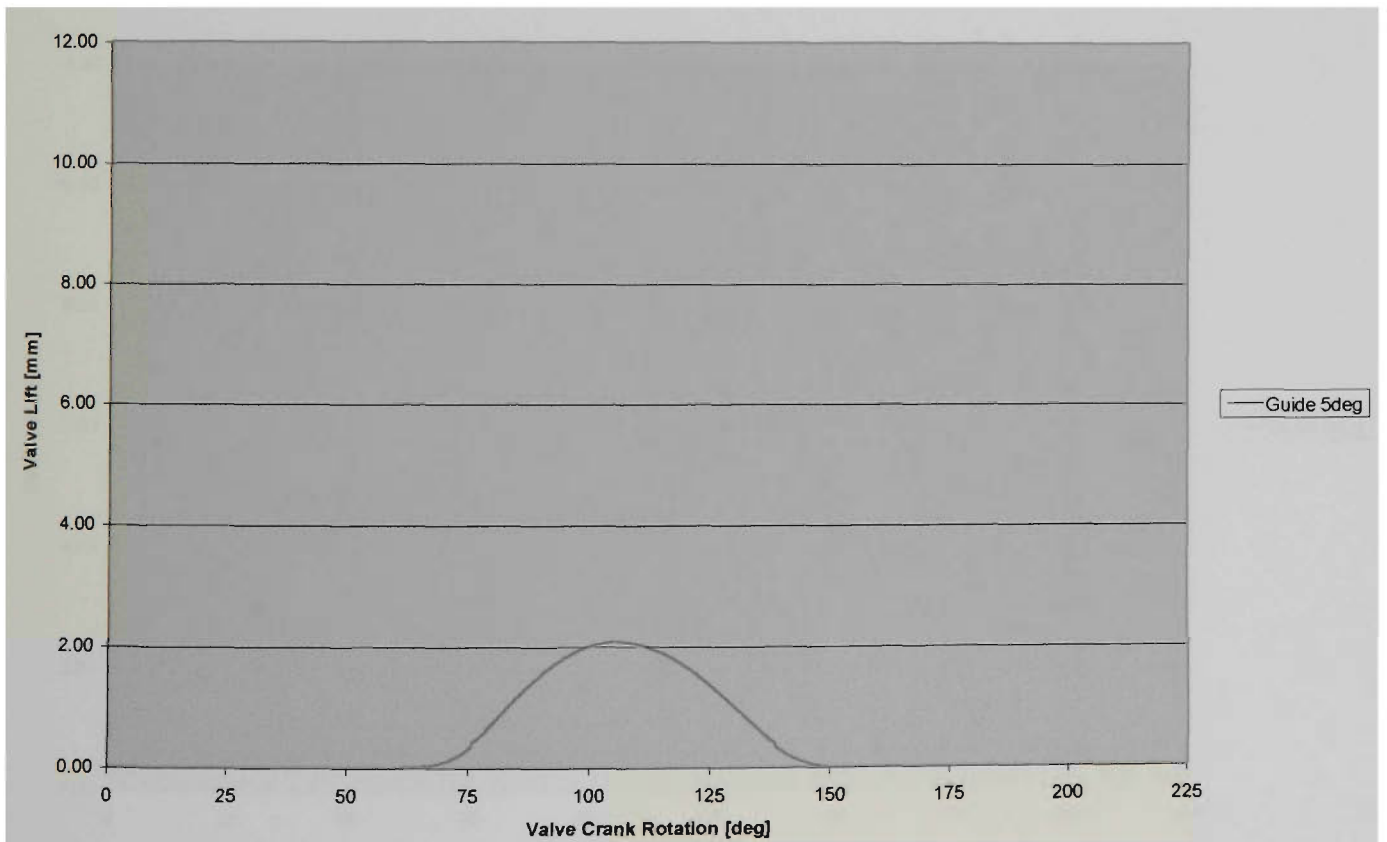
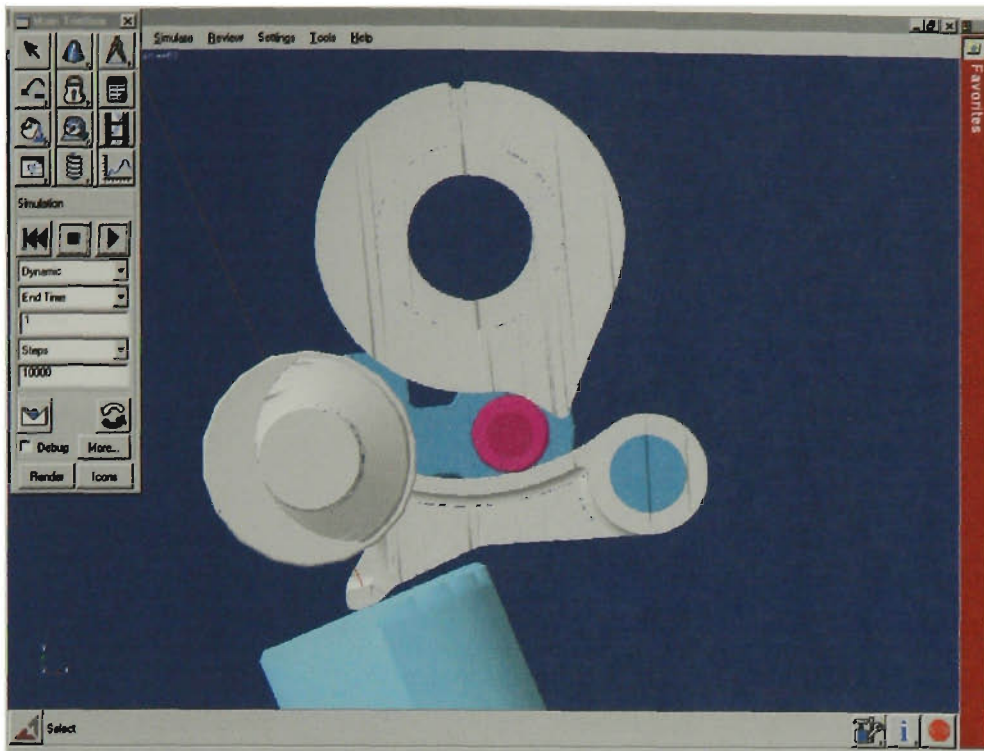


Figure 4.32 – Valve profile of DVC system at 5 degrees.

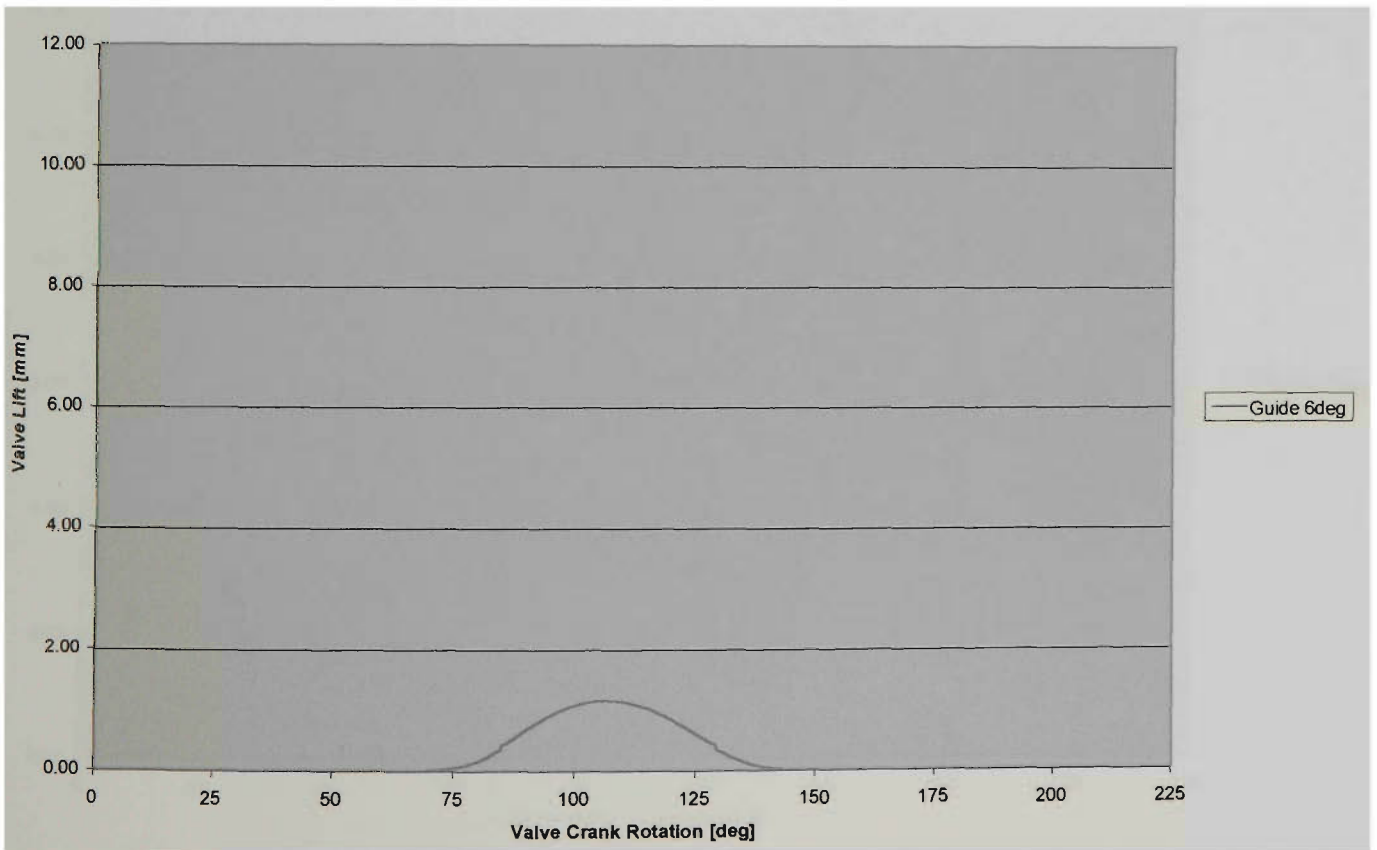
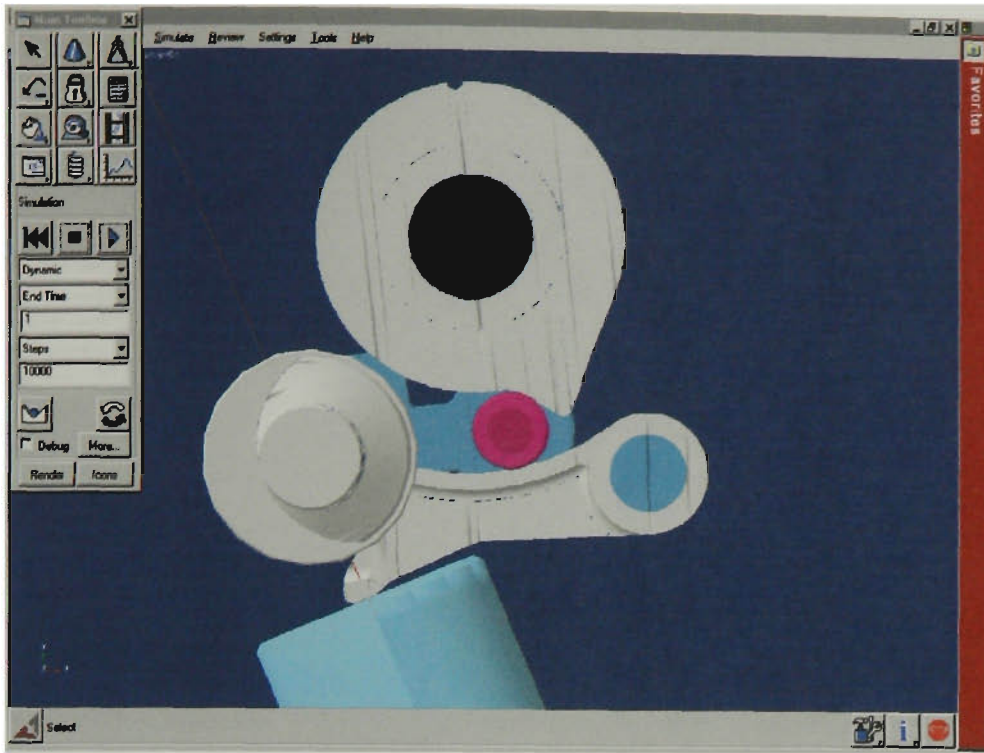


Figure 4.33 – Valve profile of DVC system at 6 degrees.

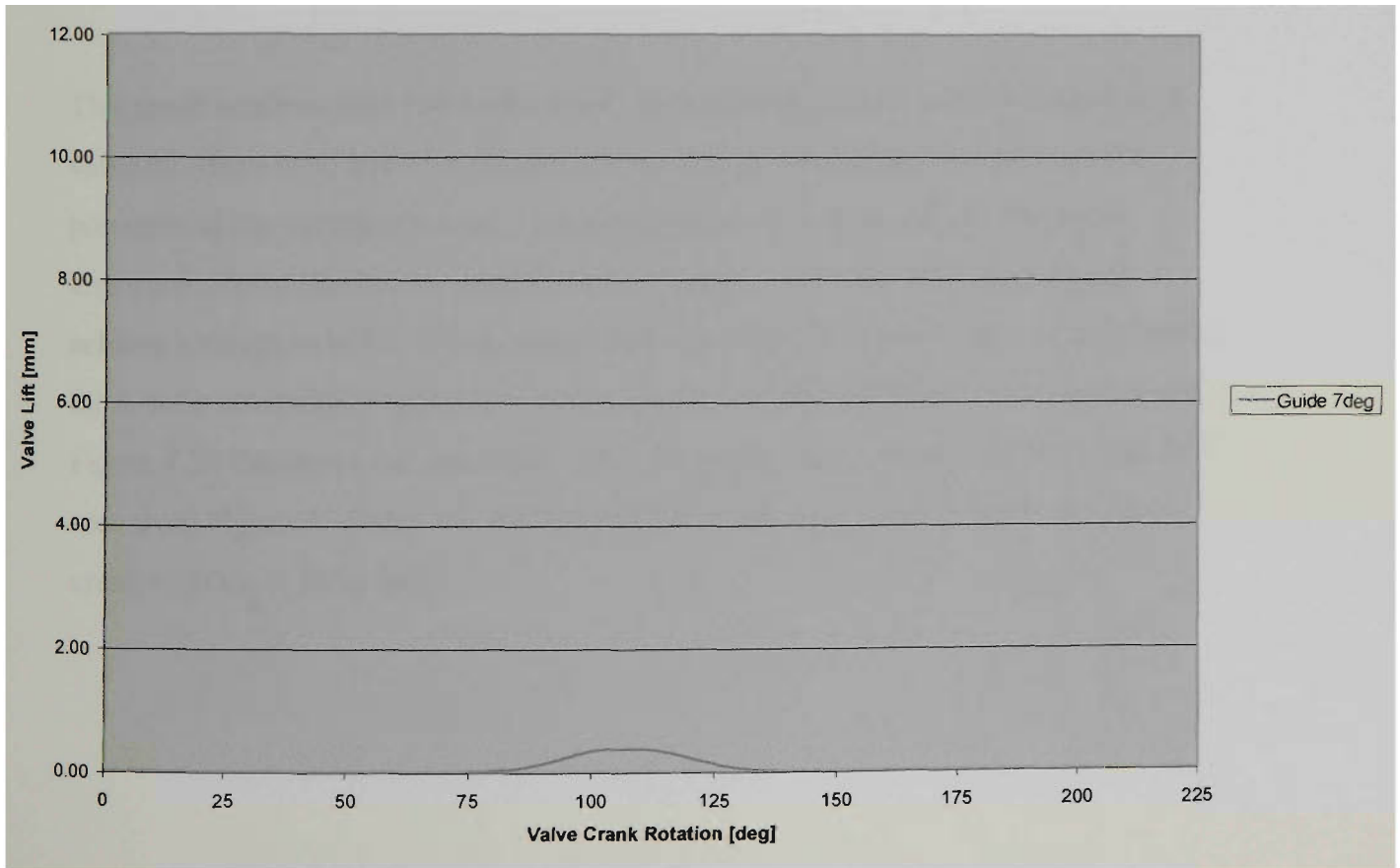
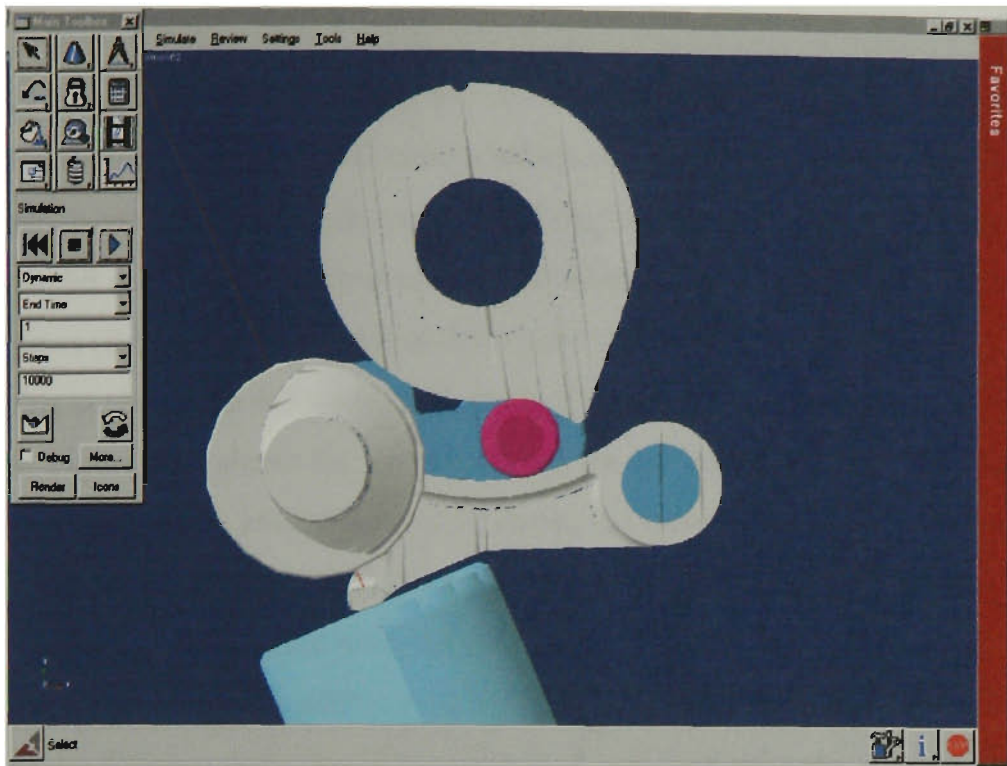


Figure 4.34 – Valve profile of DVC system at 7 degrees.

Figures 4.24 to 4.34, show the valve lifts from maximum lift in Figure 4.24 to almost zero lift in Figure 4.34. The DVC system moves the valve from a maximum lift of 10.70 mm to virtually zero lift in a span of 10 degrees rotation of the guideshaft. Maximum lift of 10.70 millimetres is achieved when the guideshaft is positioned at 357 degrees (three degrees clockwise from start location), with the valve lift decreasing at about one millimetre with every 1 degree rotation of the guideshaft. For example, Figure 4.25 shows the valve lift when the guideshaft is at 358 degrees, with the lift being 9.73 mm, while Figure 4.26 shows the valve lift at 8.63 mm, when the guideshaft is positioned at 359 degrees. As the guideshaft begins to rotate anti-clockwise from the maximum valve lift position of 357 degrees, the valve lift gradually decreases. The positions of the guideshaft as seen from Figures 4.24 to 4.34, illustrate the different positions of the guideshaft and their subsequent effect on the valve lift. Minimum lift is achieved when the guideshaft is at 7 degrees, as seen in Figure 4.34, the valve lift is 0.36 mm which is virtually zero.

This result confirms that due to the DVC system being able to achieve almost zero valve lift, there is no need for the throttle, as the valves themselves can limit the pressures in the cylinders and as a consequence, limit engine output. The most important aspect that can be seen from the figures, is that the DVC system can achieve a variation in lift, which means that any valve lift between zero to maximum lift is quite attainable. Figure 4.35 illustrates the variable lift of the DVC system and Figure 4.36 illustrates the maximum valve lift versus valve crank rotation. It can be seen from Figure 4.36 that the relationship between maximum valve lift and valve crank rotation is fairly linear.

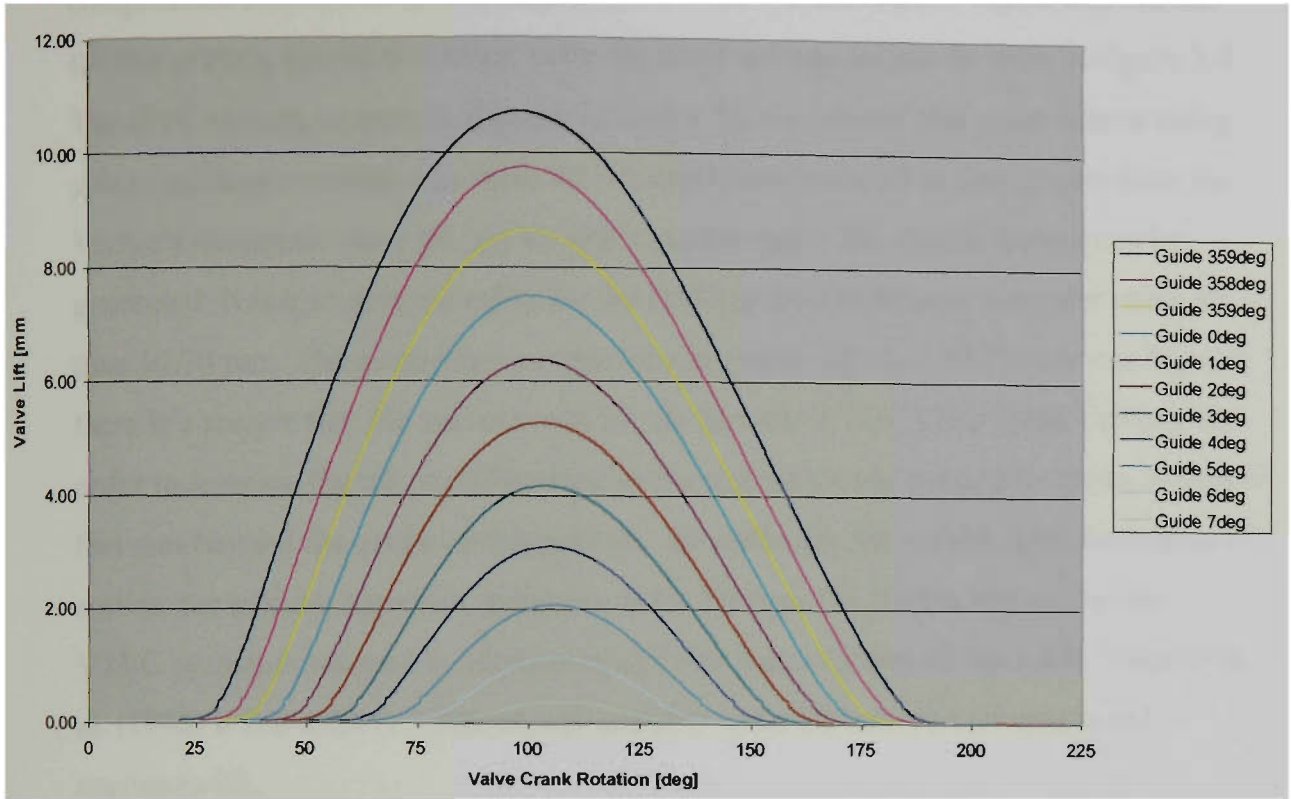


Figure 4.35 – Variable lift of DVC system

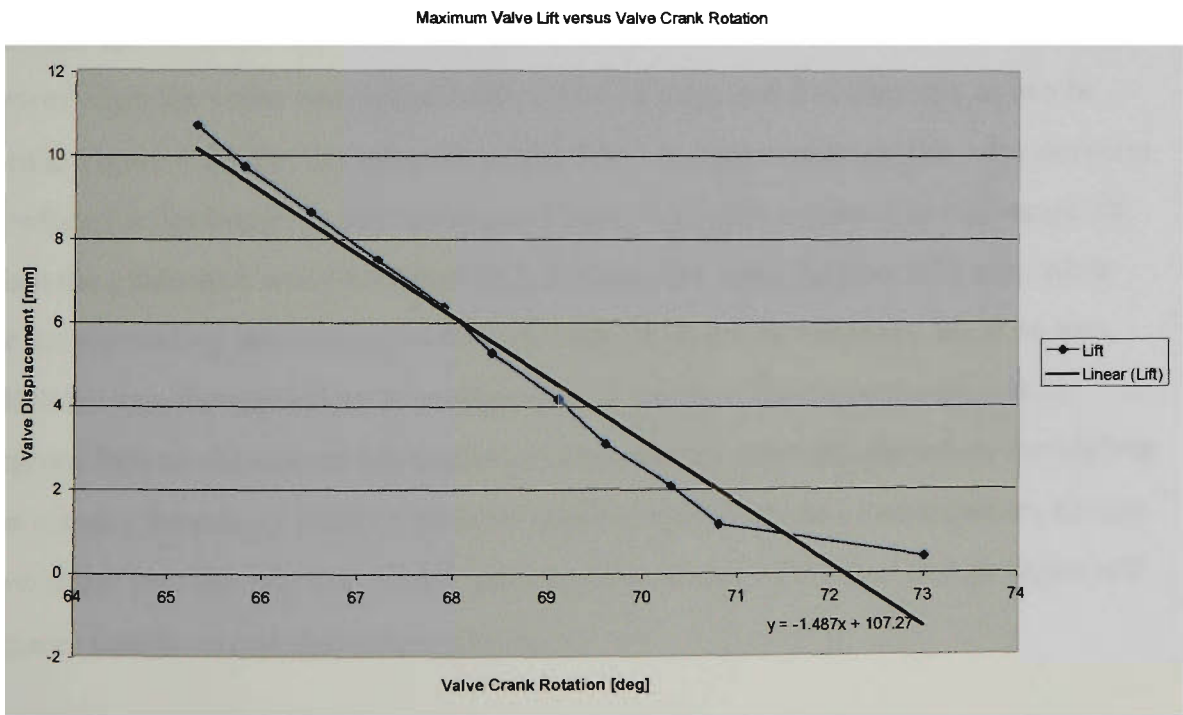


Figure 4.36 – Plot of maximum valve lift versus valve crank rotation

The valve timing in conventional engines is fixed at a certain lift, which is basically a compromise only suited to one engine speed. The Vectra engine, which was utilised for this project, has its maximum valve lift fixed at 9mm, as can be seen in Figure 3.4. The DVC system, as seen in Figures 4.24 to 4.34 also shows that apart from it being able to achieve a variation in valve lift, its maximum valve lift is also greater than the Vectra's maximum valve lift. By having a greater valve lift, greater power can be generated. It is also quite possible for the DVC system to achieve a greater valve lift than 10.70 mm. The reason for not pursuing a greater lift than 10.70 mm was because there is a danger that the valves could hit the pistons at TDC (Top Dead Centre). In order to increase the lift, modifications to the pistons would need to be made, however that was beyond the scope of this project. Nevertheless the results show that the DVC system can achieve a greater maximum valve lift than the Vectra and unlike the VTEC system developed by Hosaka et al. (1991) and further advanced by Matsuki et al. (1996) it can achieve continuously variable valve lift between minimum and maximum lift.

Another notable outcome of the simulation results was that the DVC system's valve duration can be larger than the Vectra's. The maximum valve duration for the DVC system when the valve was opened fully at 10.70 mm, was 140 degrees, as can be seen in Figure 4.24. As the valve lift of the DVC system decreases, the valve duration is reduced accordingly, as can be seen in Figure 4.35. For instance, at mid-range lift, when the guideshaft was positioned at 2 degrees, the valve lift was 5.25 mm, while the corresponding valve duration was 90 degrees. While at minimum lift, 0.36 mm, which is when the guideshaft is positioned at 7 degrees, the valve duration is 35 degrees. Due to the system being able to achieve zero valve lift, the valves themselves can act as a throttle by limiting pressure into the cylinders. As a consequence, air can flow faster into the cylinder, which improves the mixing of the fuel and air better and reduces emissions and fuel consumption.

An engine fitted with the DVC system would have a 'drive by wire' "throttle" in which the accelerator position is input to the Engine Control Unit (ECU) as a voltage. The ECU would determine how much to throttle the engine by taking the accelerator

voltage into account. An engine would be throttled by modulating the amount of inlet valve lift and duration. For example if the engine is meant to be idling, the guideshaft would oscillate back and forth in response to the engine speed. If the engine speed begins to decrease below the idle set point, the guideshaft would rotate a little to increase the valve lift and duration until the speed increases. When the engine accelerates, the ECU would respond by rotating the guideshaft sufficiently to respond to the driver's desired amount of power. While cold starts would be taken care of by the engine temperature input to the ECU.

From the Figures, it can be seen that valve lift and duration are coupled in the DVC system. It is proposed that light loads would be accomplished by reduced valve lift and contracted duration resulting in a delayed inlet valve opening if the DVC system is used in isolation. However, the system will employ a phase shifting drive to the valve crank so that inlet valve opening timing can be optimised. The performance implications of using valve lift variation for load regulation can be demonstrated by reference to the performance of BMW's Valvetronic series of engines now available in Australia. Valvetronic has almost identical valve motion characteristics to the DVC system. Edgar (2001) stated that the Valvetronic does not utilise a throttle to control engine load, much like the DVC system, the valve lift can be reduced so close to zero lift that the engine is throttled by the inlet valves. By pressing on the throttle pedal the engine management system increases the amount of inlet valve lift to allow more airflow and therefore more power. The same can be achieved with the DVC system.

The DVC system will also use a low reduction worm gear drive to control the rotation of the guideshaft. Wear of critical components such as the guideshaft profile, gudgeon pin and rocker arm would result in valve lift scatter. The scatter would have most effect at very low load such as idle. This could be compensated for to a considerable degree by the engine management system. Also by adherence to conventional specifications for materials, contact pressures and lubrication, the DVC system would have similar wear characteristics as conventional valve trains.

Figure 4.37 illustrates a comparison between the valve profile of the DVC system and the existing Vectra engine.

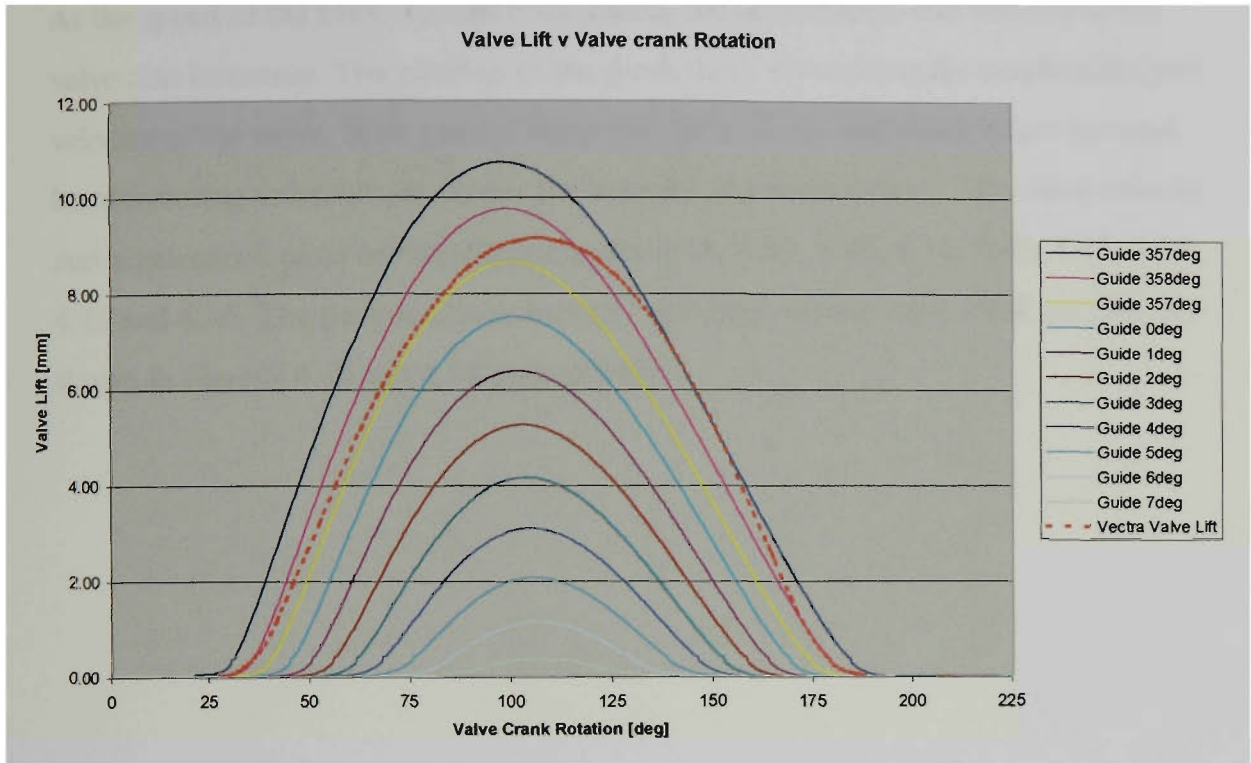
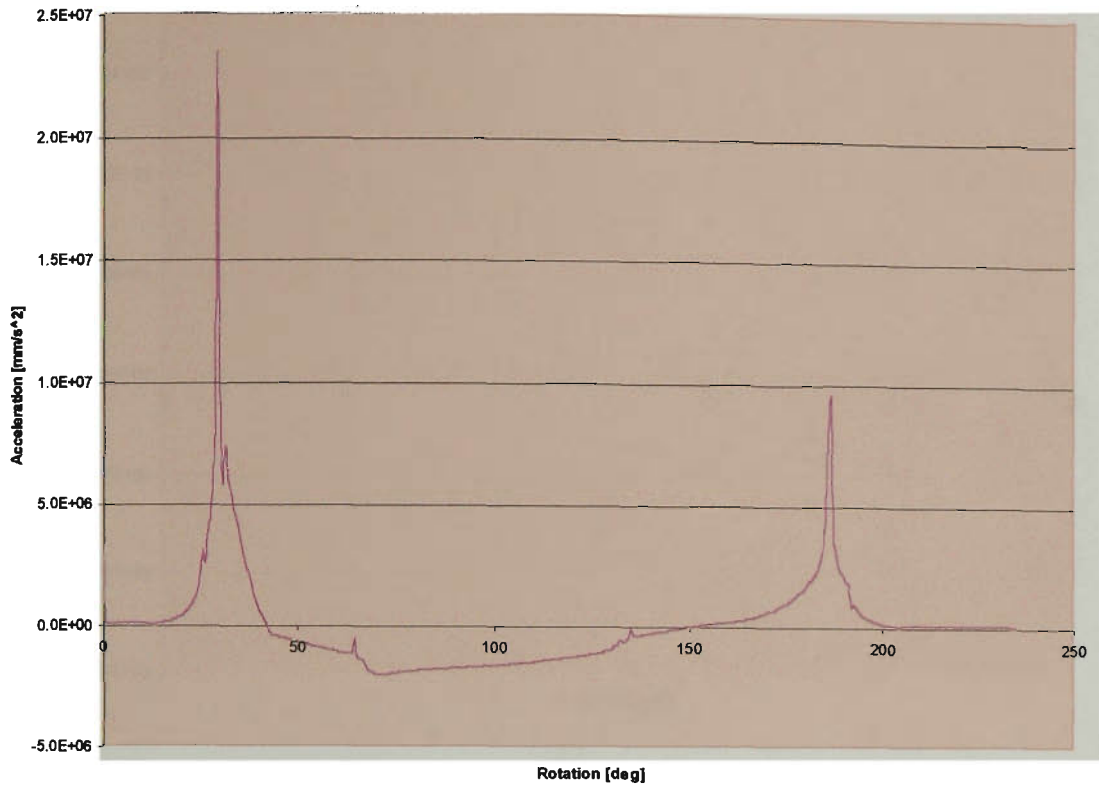


Figure 4.37 – Comparison of valve lifts between the DVC system and the Vectra cylinder head.

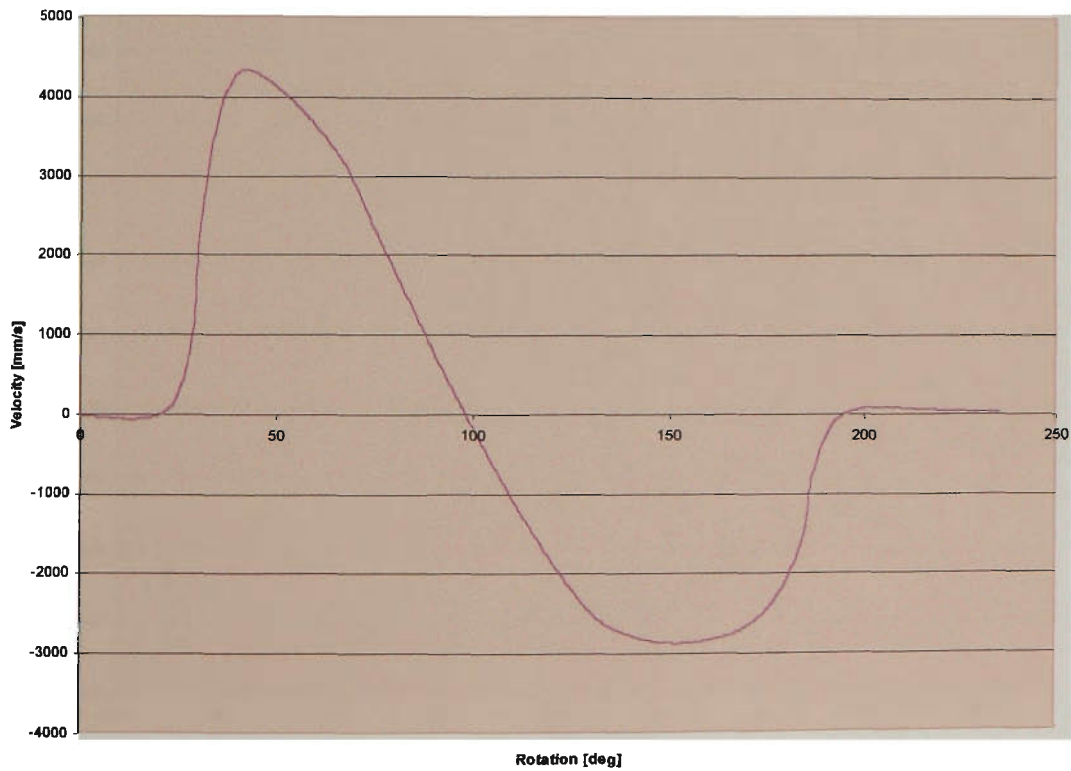
It can be seen from Figure 4.37 that not only does the DVC system have a greater maximum lift than the Vectra, but also, its valves are able to stay open for a longer period than the Vectra's valves. This increased valve duration produces greater power at higher rpm.

4.3.2 Valve Velocity and Acceleration Results

As the speed of the DVC system is increased, the acceleration and velocity of the valve also increases. The position of the guideshaft, also affects the acceleration and velocity of the valve. With greater valve lift, the velocity and acceleration increase, but decreasing valve lift, decreases the velocity and acceleration. The valve velocity and acceleration plots are shown in Figures 4.38, 4.39, 4.40, 4.41, 4.42, 4.43, 4.44, 4.45 and 4.46. The peak accelerations and velocities versus valve crank rotation are shown in Figures 4.47 and 4.48 respectively.

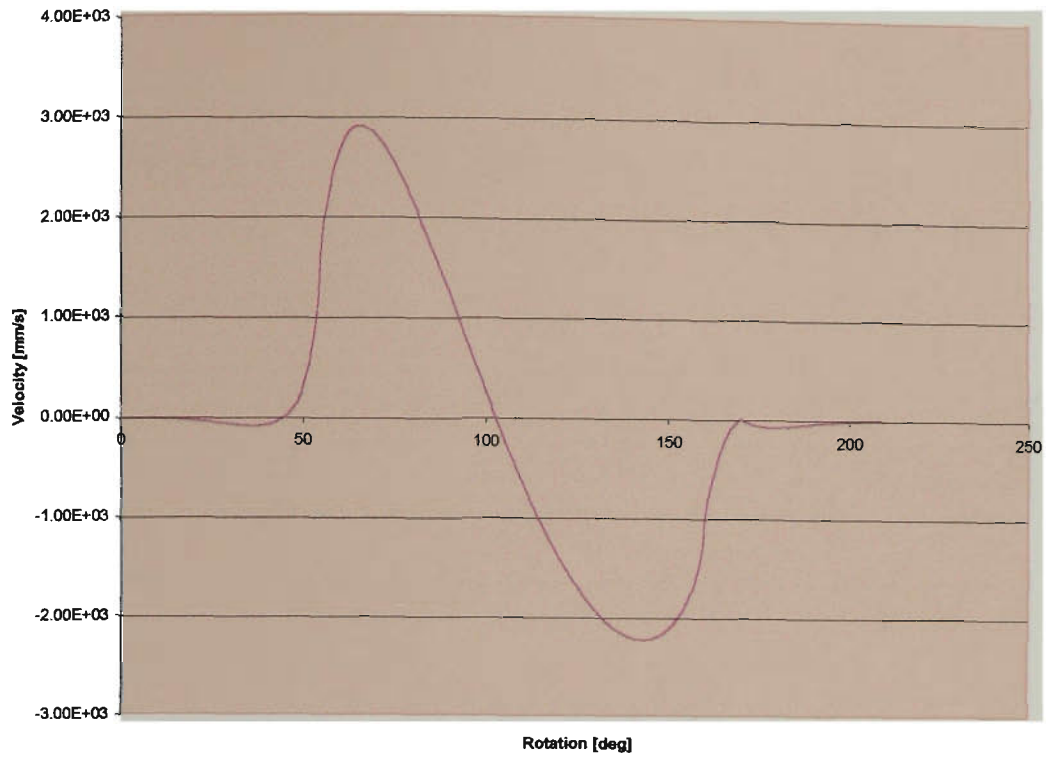


(a)

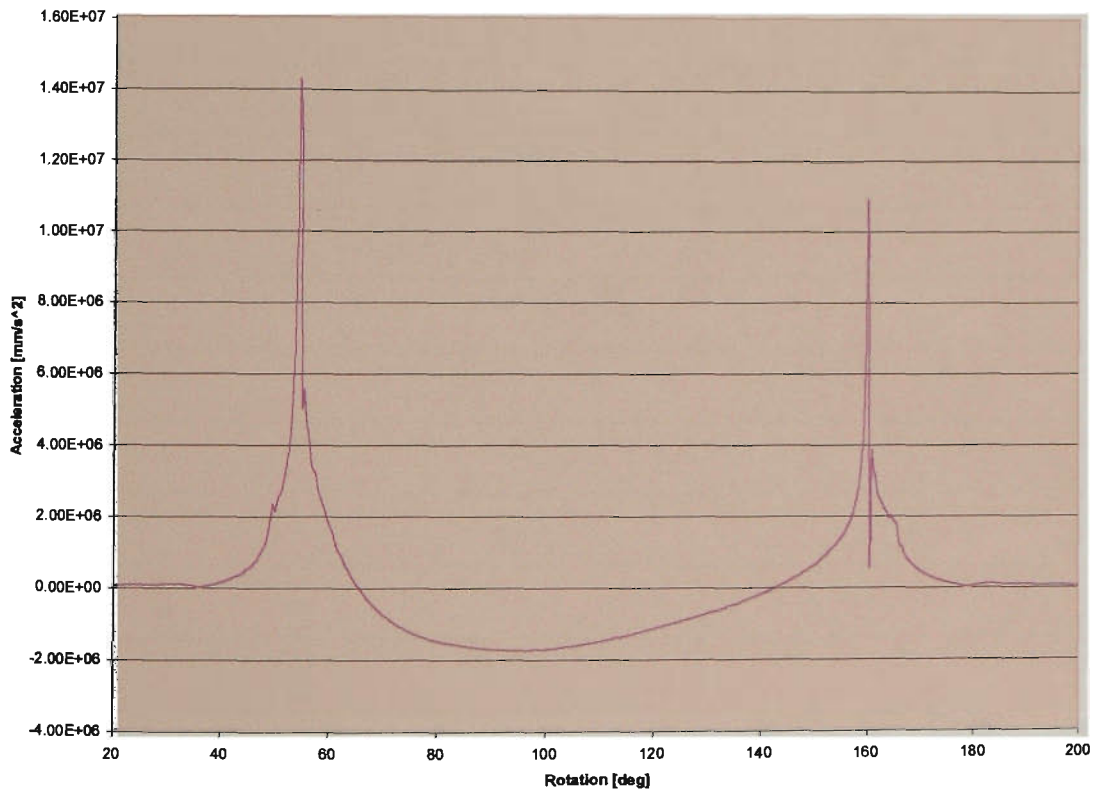


(b)

Figure 4.38 – Plot of (a) velocity and (b) acceleration at 18000 degrees/sec with guideshaft positioned at 357 degrees.

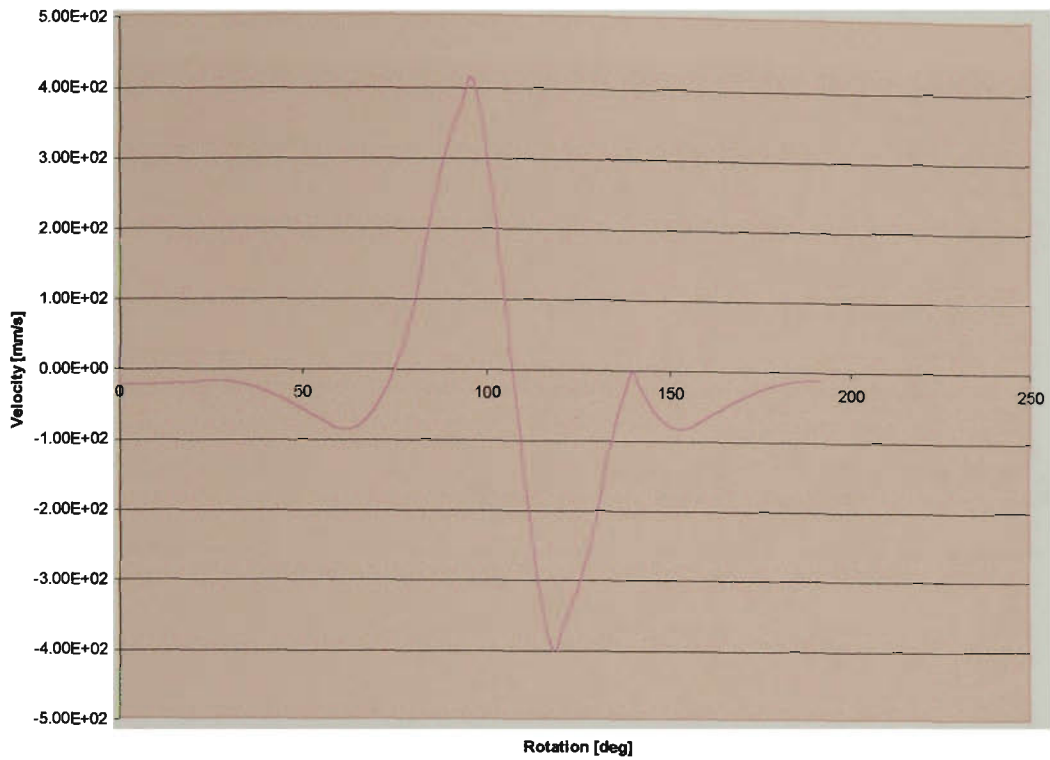


(a)

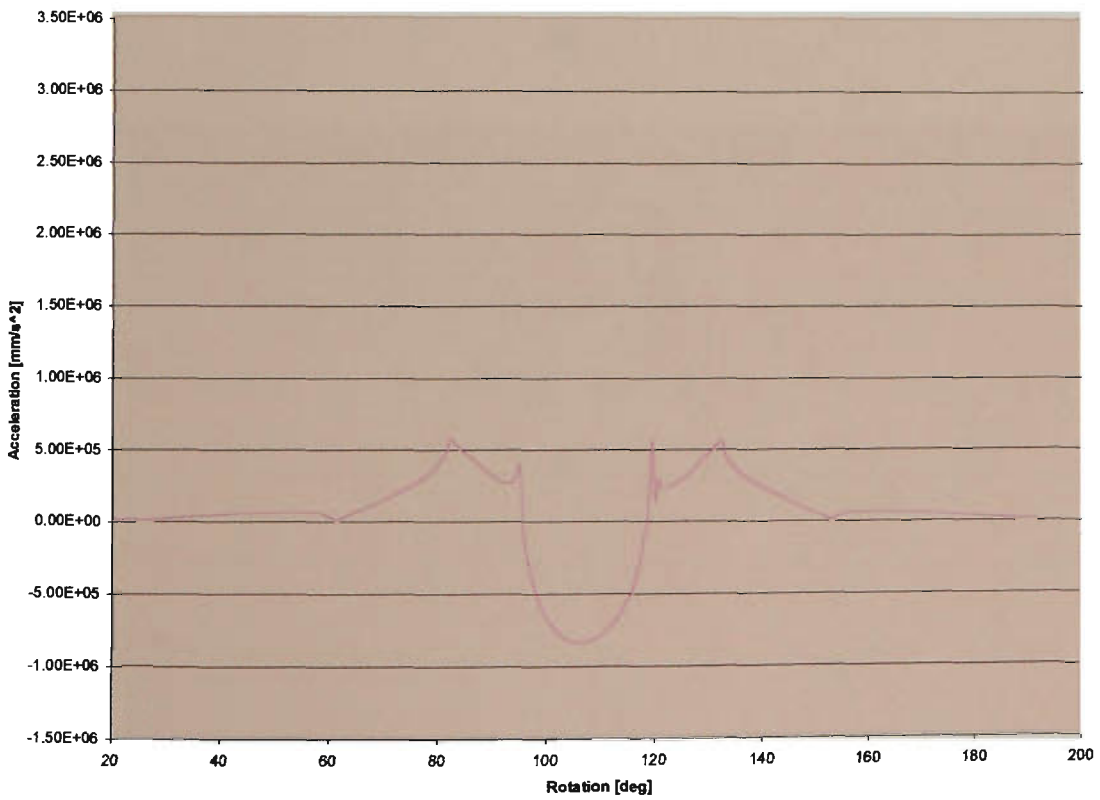


(b)

Figure 4.39 – Plot of (a) velocity and (b) acceleration at 18000 deg/sec with guideshaft positioned at 2 degrees.

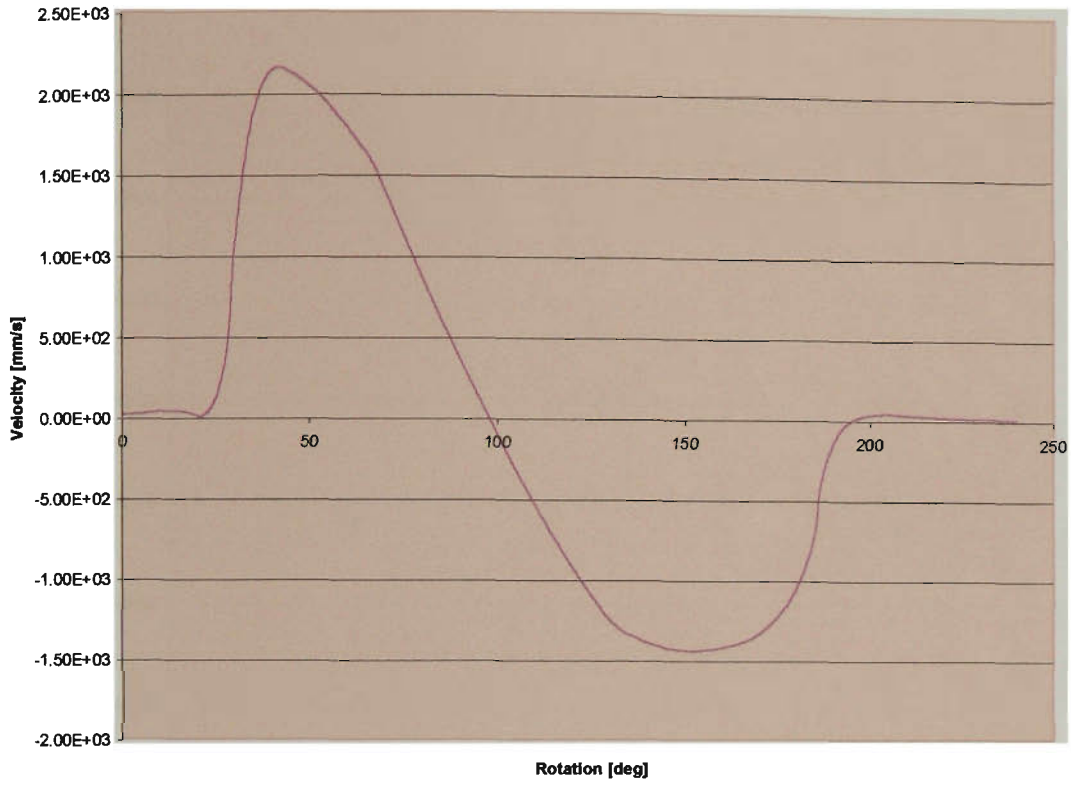


(a)

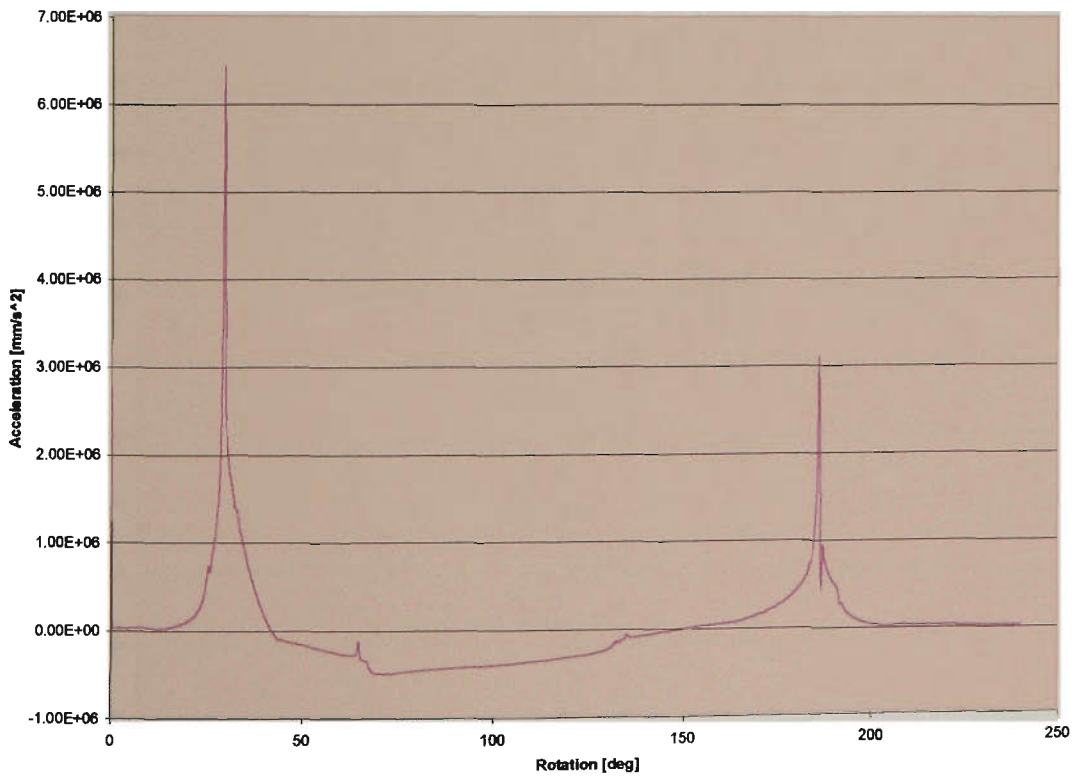


(b)

Figure 4.40 – Plot of (a) velocity and (b) acceleration at 18000 deg/sec, with guideshaft position at 7 degrees.

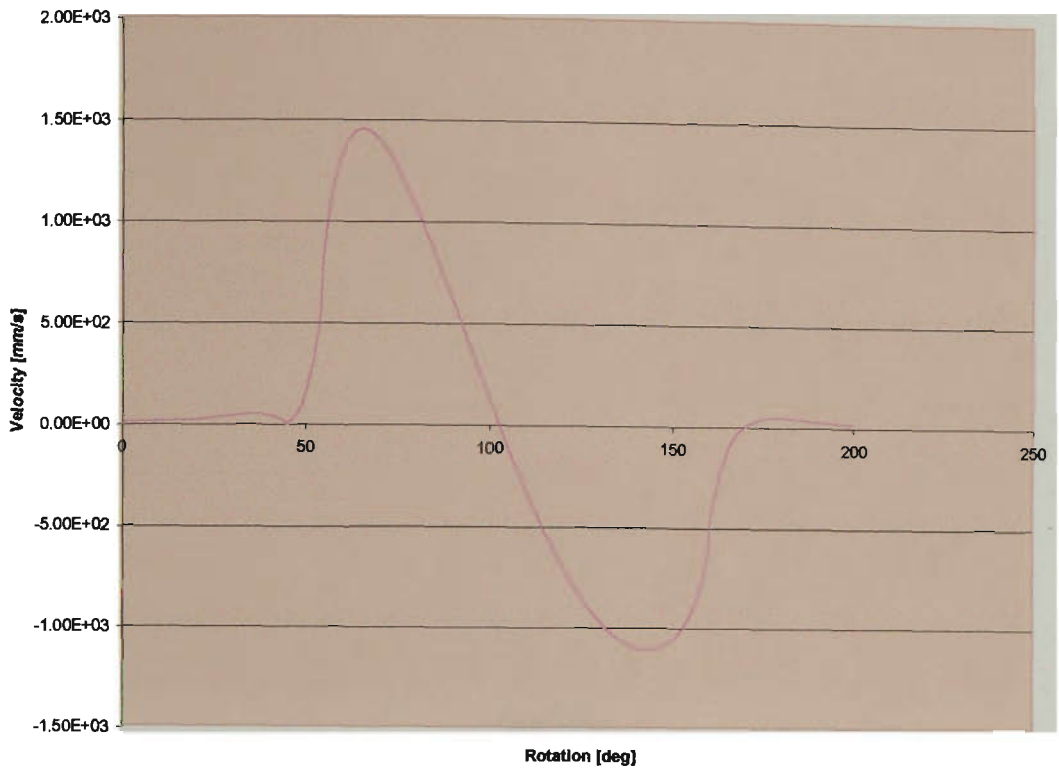


(a)

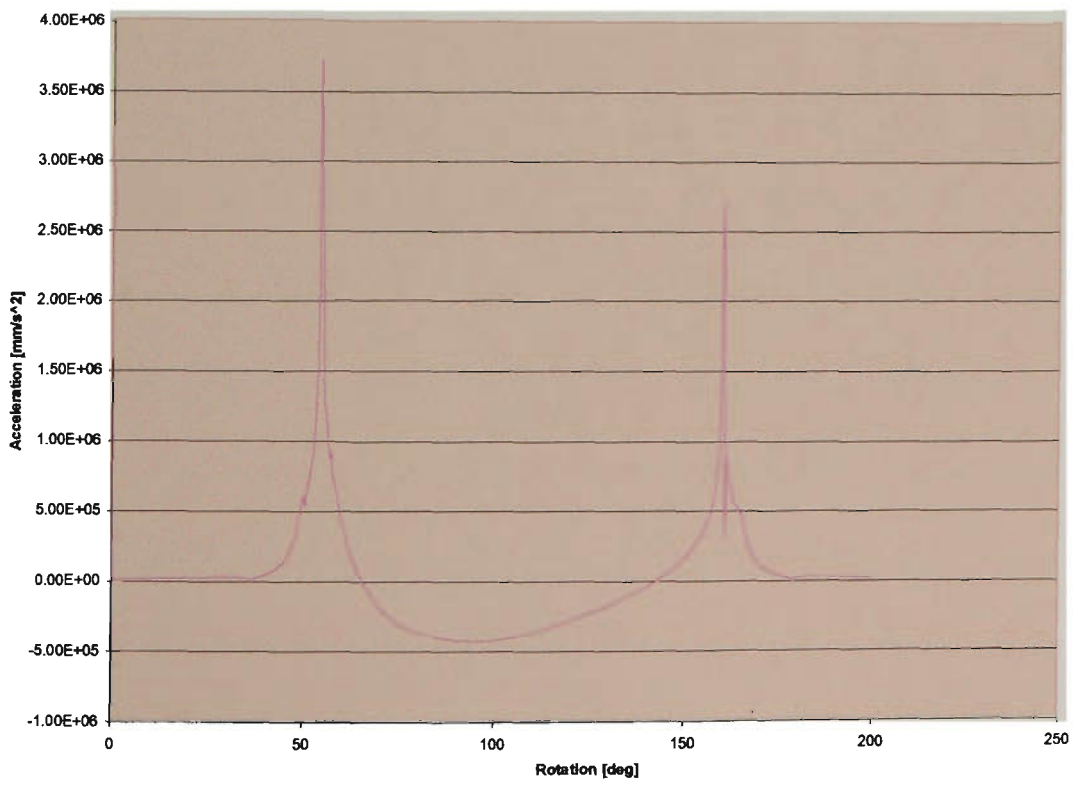


(b)

Figure 4.41 – Plot of (a) velocity and (b) acceleration at 9000 degrees/sec, with guideshaft position at 357 degrees.

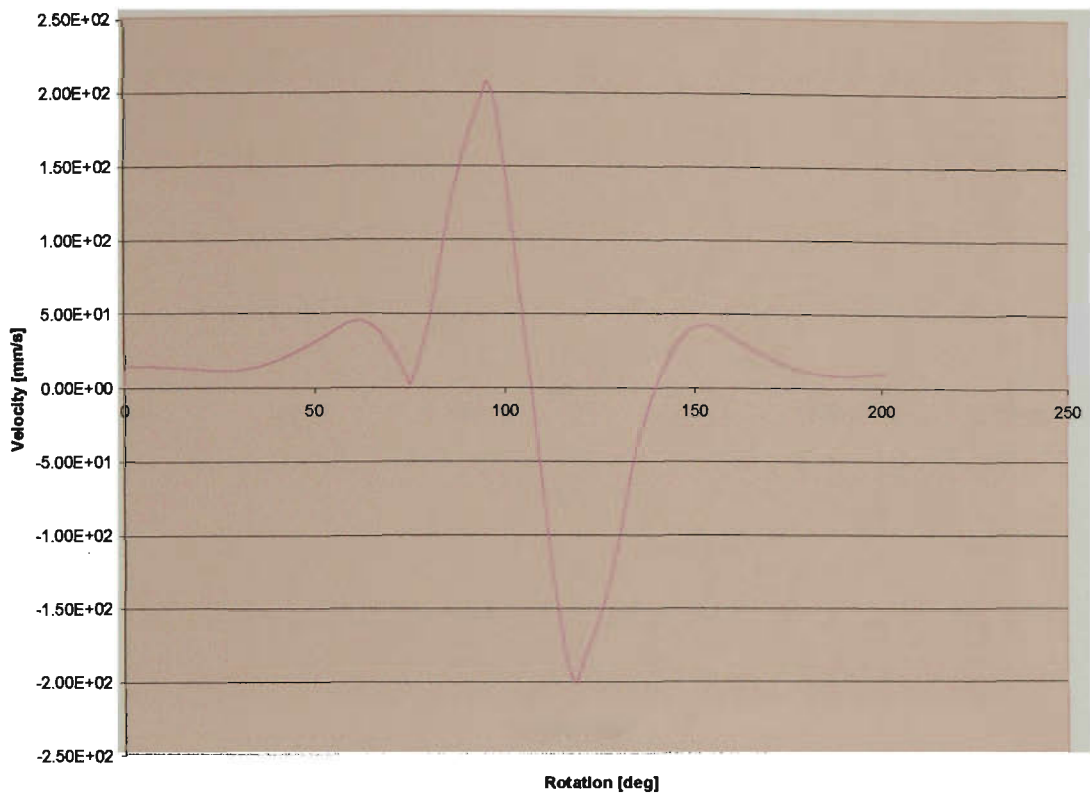


(a)

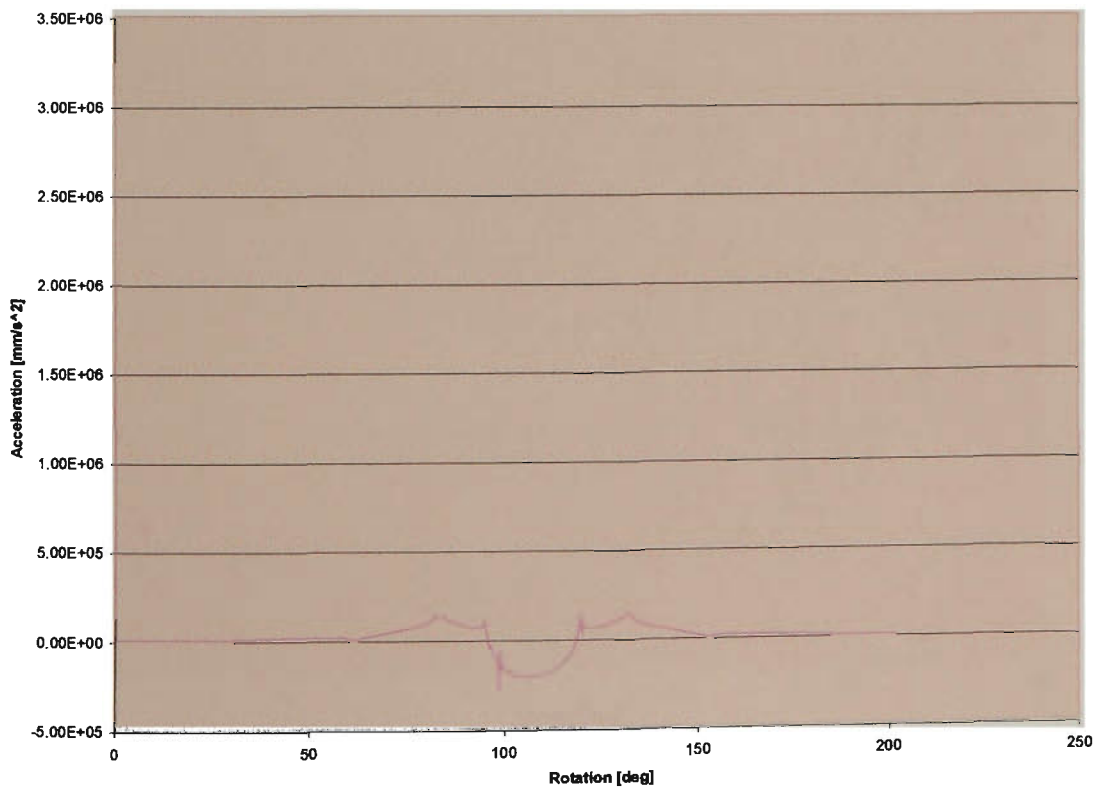


(b)

Figure 4.42 – Plot of (a) velocity and (a) acceleration at 9000 degrees/sec, with guideshaft positioned at 2 degrees.

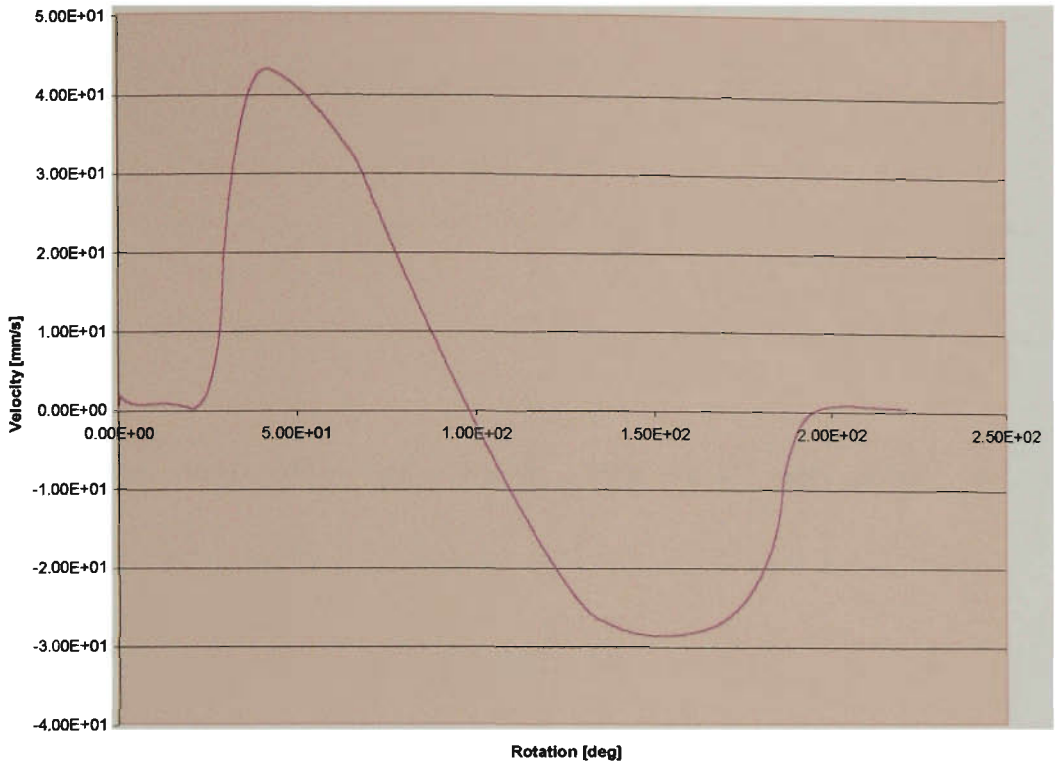


(a)

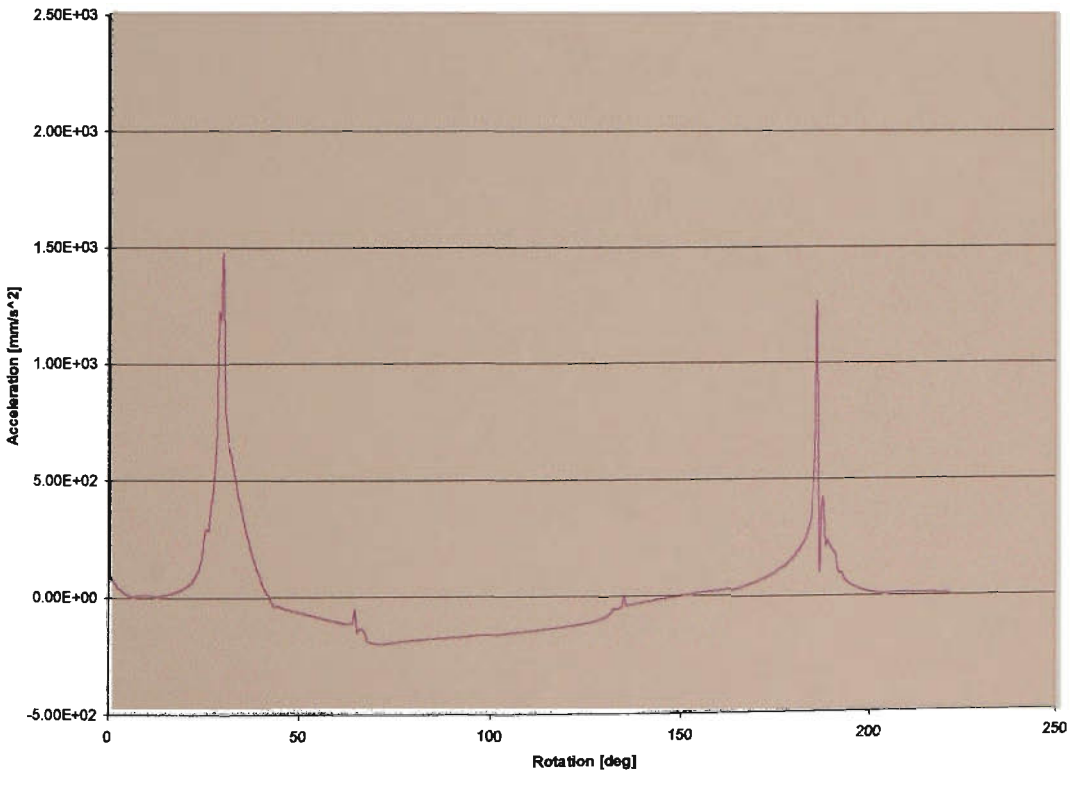


(b)

Figure 4.43 – Plot of (a) velocity and (b) acceleration at 9000 degrees/sec, with guideshaft positioned at 7 degrees.

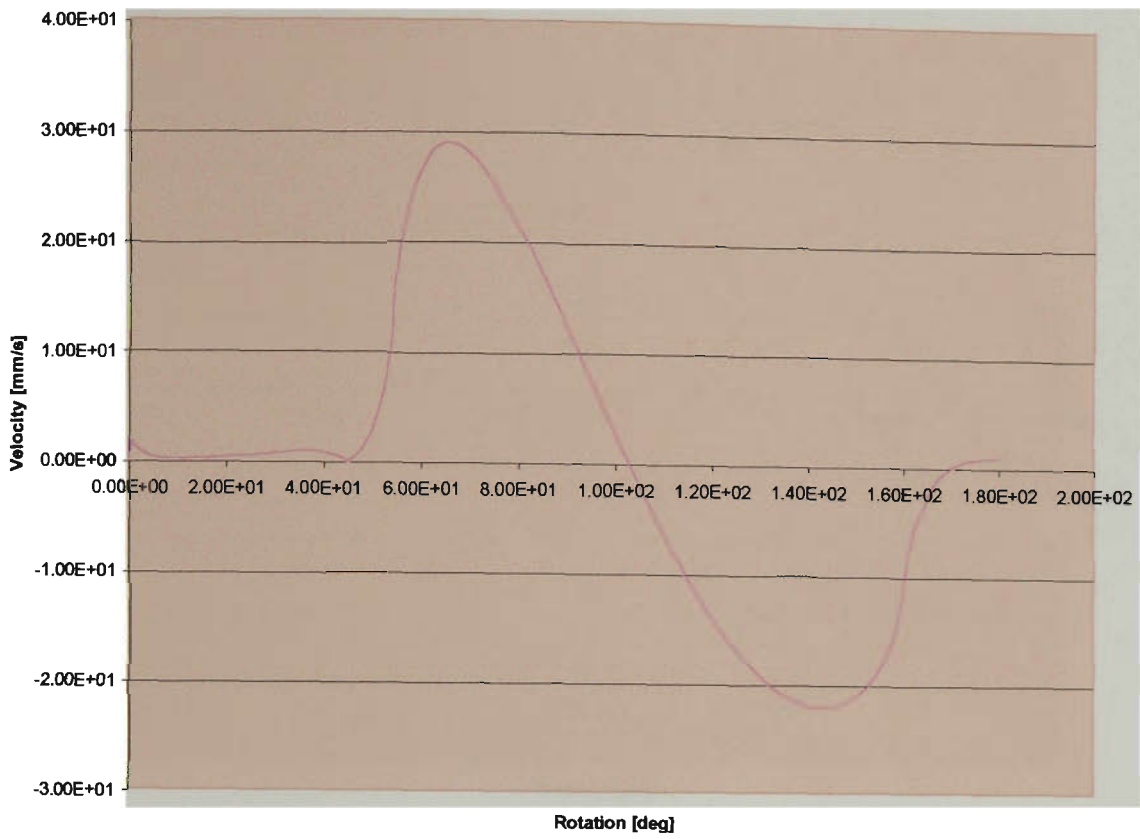


(a)

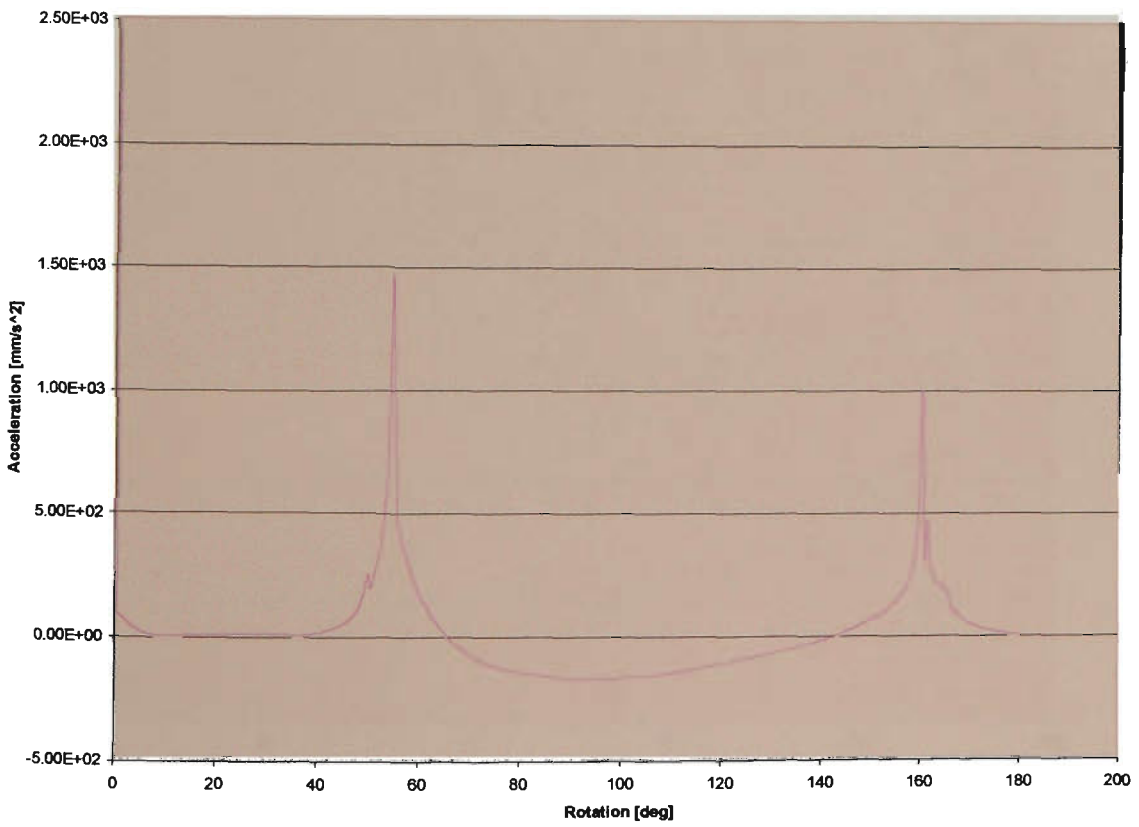


(b)

Figure 4.44 – Plot of (a) velocity and (b) acceleration at 180 degrees/sec, with guideshaft positioned at 357 degrees.

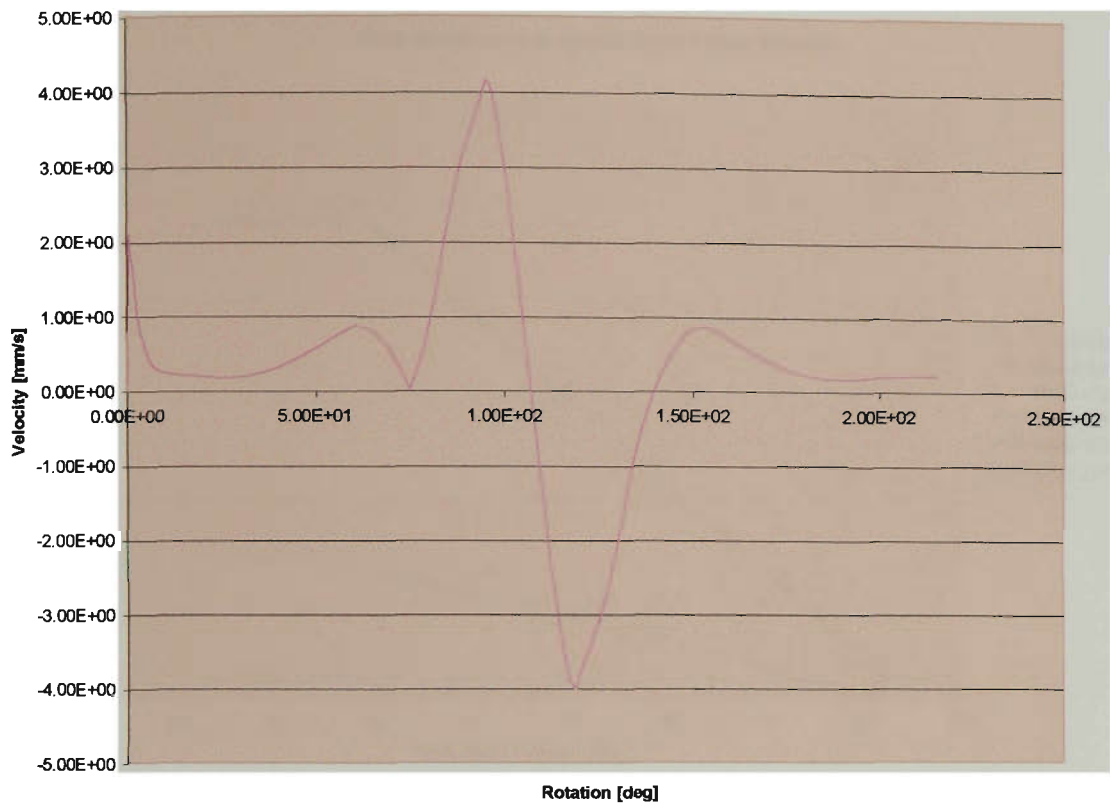


(a)

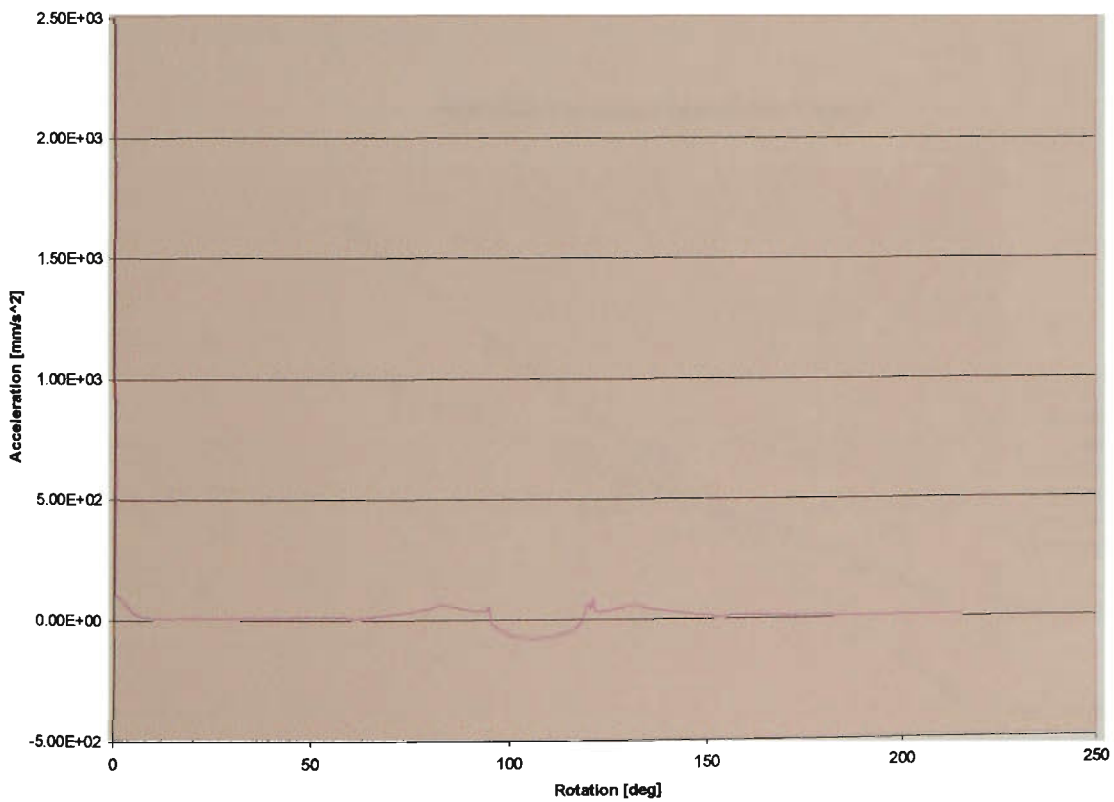


(b)

Figure 4.45 – Plot of (a) velocity and (b) acceleration at 180 degrees/sec, with guideshaft positioned at 2 degrees.



(a)



(b)

Figure 4.46 – Plot of (a) velocity and (b) acceleration at 180 degrees/sec, with guideshaft positioned at 7 degrees.

Peak Accelerations versus Valve Crank Position

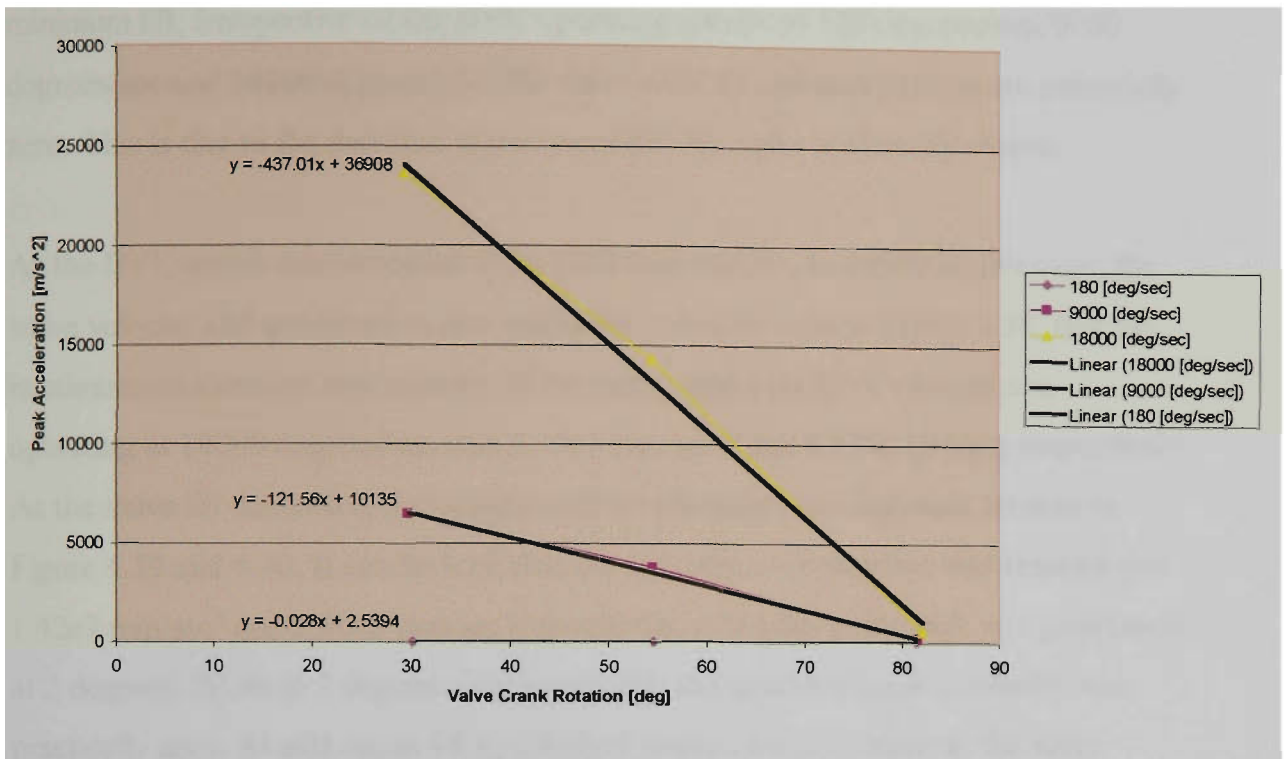


Figure 4.47 – Plot of peak acceleration versus valve crank rotation

Peak Velocities versus Valve Crank Rotation

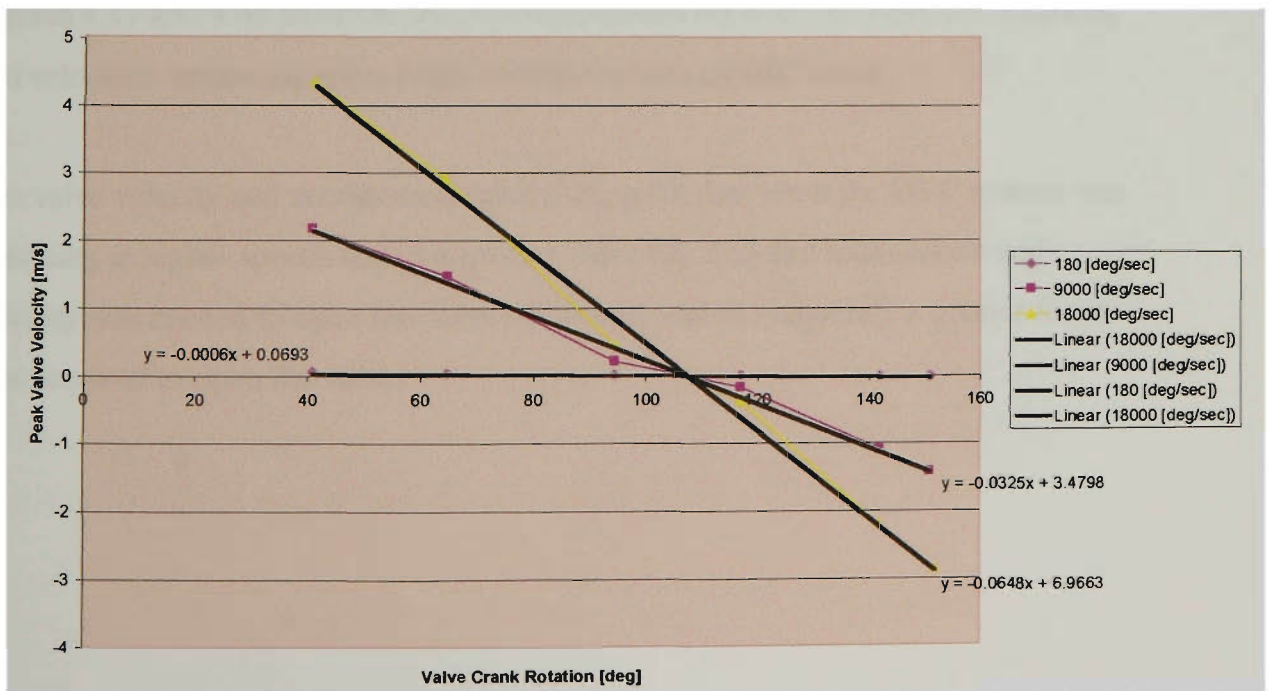


Figure 4.48 – Plot of peak velocity versus valve crank rotation

It can be seen from Figures 4.38 to 4.46, that both the valve velocity and acceleration result was greatly influenced by the speed of the system and its valve lift position. At minimum lift, irrespective of the DVC operating speeds of 180 degrees/sec, 9000 degrees/sec and 18000 degrees/sec, the valve velocity and acceleration are practically zero. This is due to the fact that at minimum lift, the valve is virtually closed.

As the DVC speed was increased from 9000 degrees/sec, to 18000 degrees/sec, the valve velocity and acceleration also increases. It can be seen in Figure 4.38, that the maximum acceleration and velocity of the valve, when the DVC system was operating at 18000 degrees/sec was $2.35e7$ mm/sec² and $4.33e3$ mm/sec respectively. As the valve lift decreases, the velocity and acceleration also decrease, as seen in Figure 4.39 and 4.40. It can be seen that the maximum acceleration and velocity was $1.42e7$ mm/sec² and $2.90e3$ mm/sec respectively, when the guideshaft was positioned at 2 degrees. While at 7 degrees (minimum lift), the acceleration and velocity was practically zero. At mid-range lift (guideshaft positioned at 2 degrees) the valve velocity and acceleration speed was half the velocity and acceleration speed when at maximum lift (guideshaft positioned at 357 degrees).

Figures 4.47 and 4.48 illustrate that the relationship between the peak accelerations and velocities versus the valve crank rotation are essentially linear.

The valve velocity and acceleration results illustrate that when the DVC system was operating at higher speeds and at a greater valve lift, a higher acceleration and velocity was needed to open the valve off its seat and consequently a greater force was required to open the valve.

4.5 Force and Stress Analysis of Components

The DVC system modeled using ADAMS software demonstrated the feasibility of the system and its valve timing sequencing. However the component forces generated at operational speeds need to be evaluated, hence the stress analysis of the most important DVC component, the rocker arm, can be carried out to assess whether it can withstand the forces acting on it.

The kinematic and dynamic predictions from the ADAMS simulation of the DVC system allowed the assessment of the loads on the system components. With the DVC system operating at its highest speed of 18000 deg/sec, or 6000 rpm, the “worst case” loads on the rocker arm (which is the part under the greatest bending load) were estimated.

The two most significant aspects of the DVC component loading investigated are the Hertzian contact pressures between the gudgeon pin and the guideshaft and localised stresses on the rocker arm due to bending. The line contact force between the gudgeon pin and guideshaft must not exceed a level that would create excessive Hertzian contact pressures. The second aspect was to ensure that the repetitive loading of the rocker arm does not create localised stresses that exceeded the fatigue limit of the proposed materials.

The hand calculation of the Hertzian contact pressures was based on the line contact between the gudgeon pin and guideshaft obtained from the ADAMS simulation. The loads acting on the rocker arm were obtained and then processed using a finite element package, called Cosmos/DesignStar. The stress estimations determined whether the rocker arm could withstand the stress placed on it.

The contact forces obtained from ADAMS and the stress estimations from Cosmos/DesignStar were evaluated.

4.5.1 Forces Acting on DVC Components

The maximum contact forces between the moving parts of the DVC system were obtained from ADAMS simulation. The contact force results can be seen in Figures 4.49, 4.50, 4.51, 4.52, 4.53, 4.54, 4.55, 4.56, 4.57, 4.58, 4.59 and 4.60. The peak forces versus valve crank rotation results can be seen in Figures 4.61, 4.62, 4.63 and 4.64.

When the valve is closed, the force acting between the components, which is the point where the valve is to be pushed down, is only the spring force, hence the reason why in the Figures, the contact force begins at 300 N. The spring rate was based on the measured spring rate from the standard Vectra engine cylinder head. The reason that the plot does not begin at zero is because the DVC system as modeled using ADAMS does not include a valve seat. In an automotive engine the valve seat would absorb that force, and as a result for our purposes the strength of the spring was not important. The reason the DVC system does not include a valve seat is because the model would be too complicated for ADAMS to compute. As a result the valve train of the DVC system as modeled using ADAMS was pre-stressed.

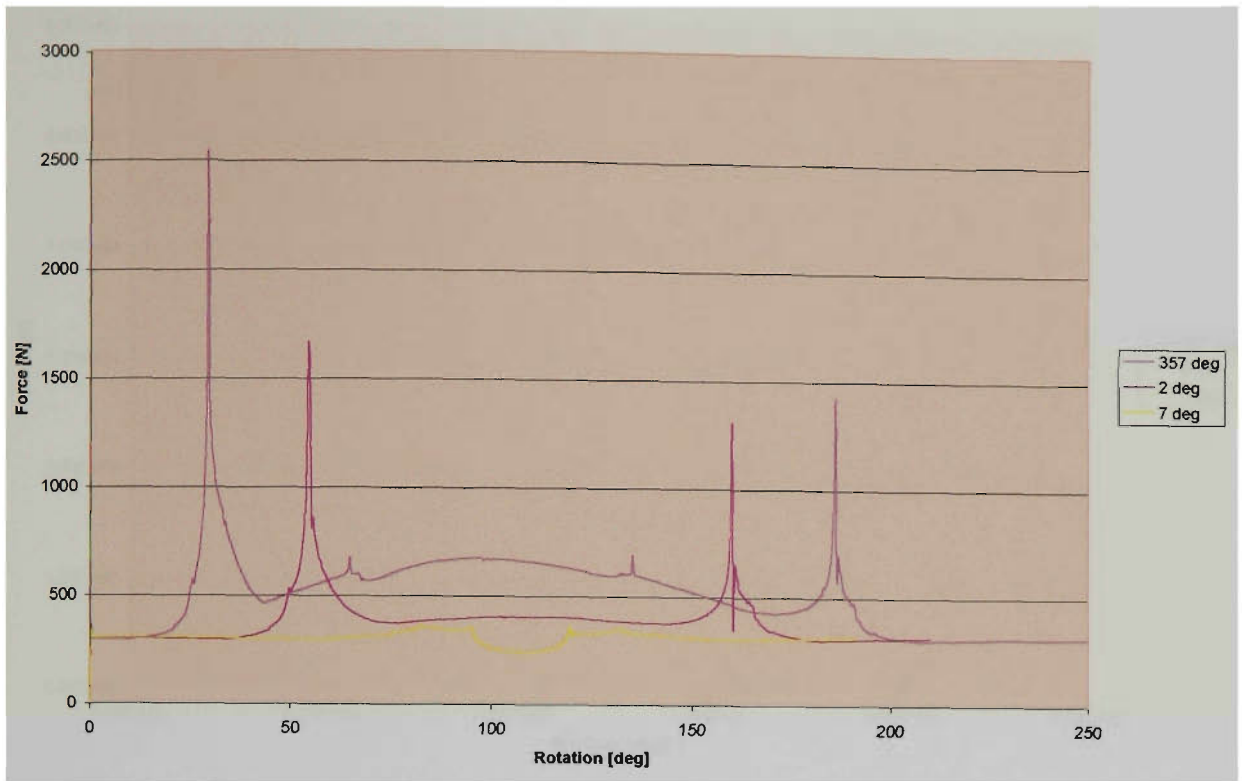


Figure 4.49 – Rocker Arm to Bucket Force at 18000 degrees/sec

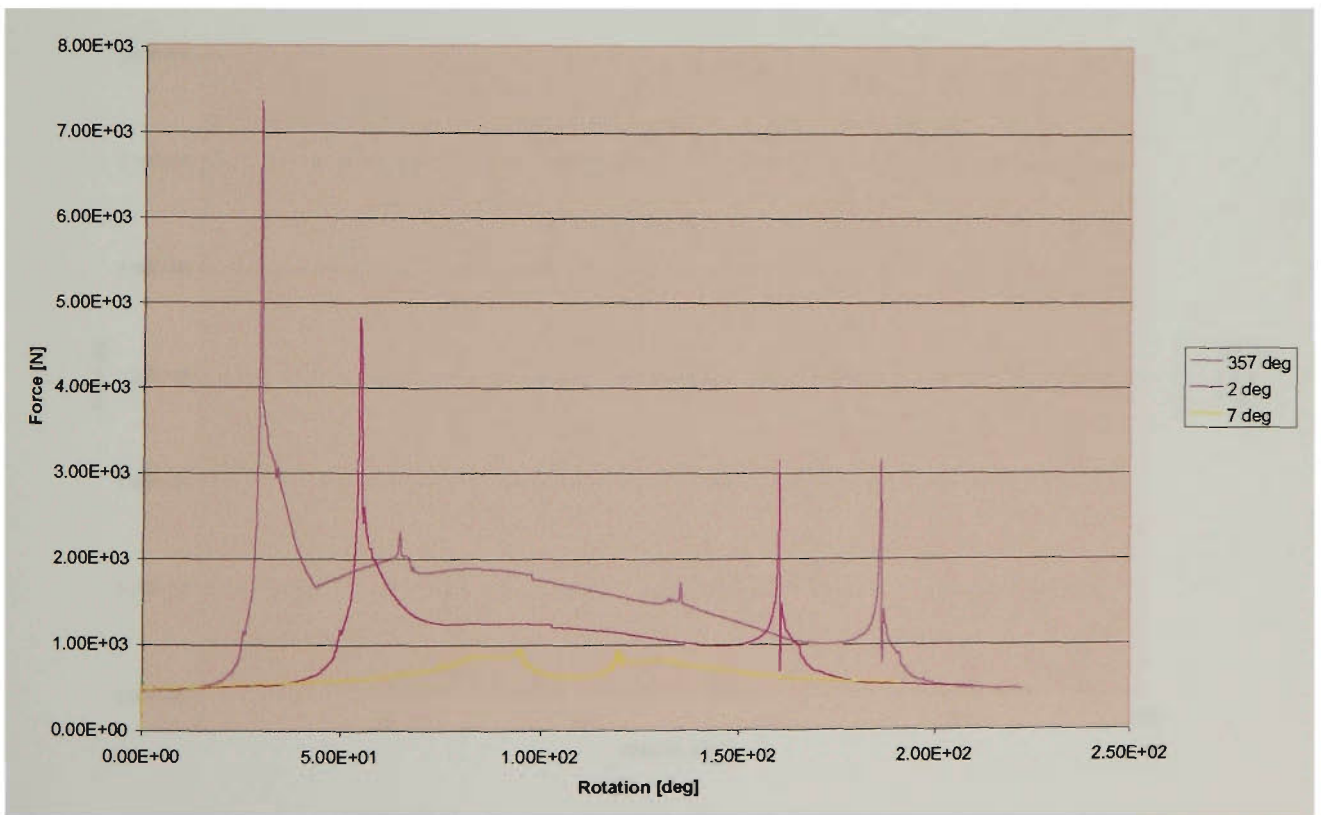


Figure 4.50 – Gudgeon Pin to Guideshaft Force at 18000 degrees/sec

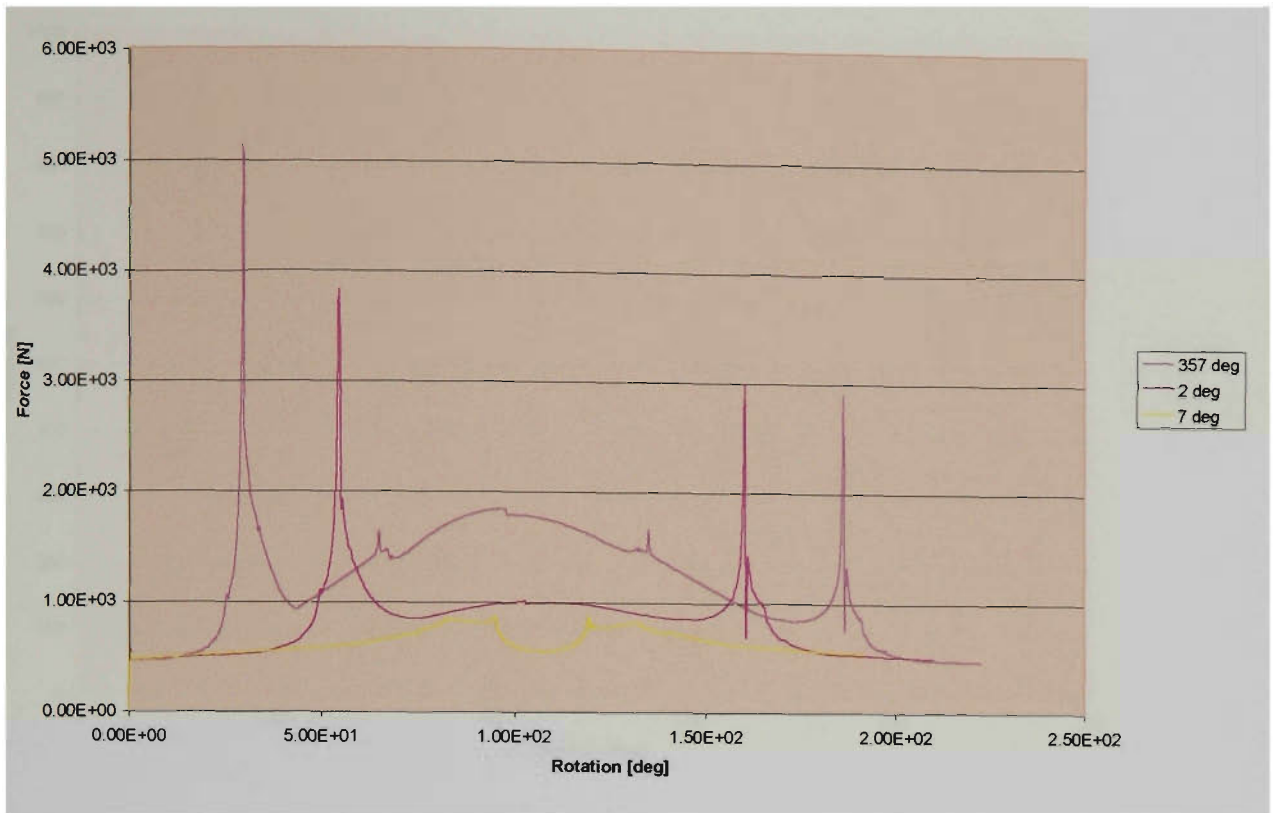


Figure 4.51 – Gudgeon Pin to Rocker Arm Force at 18000 degrees/sec

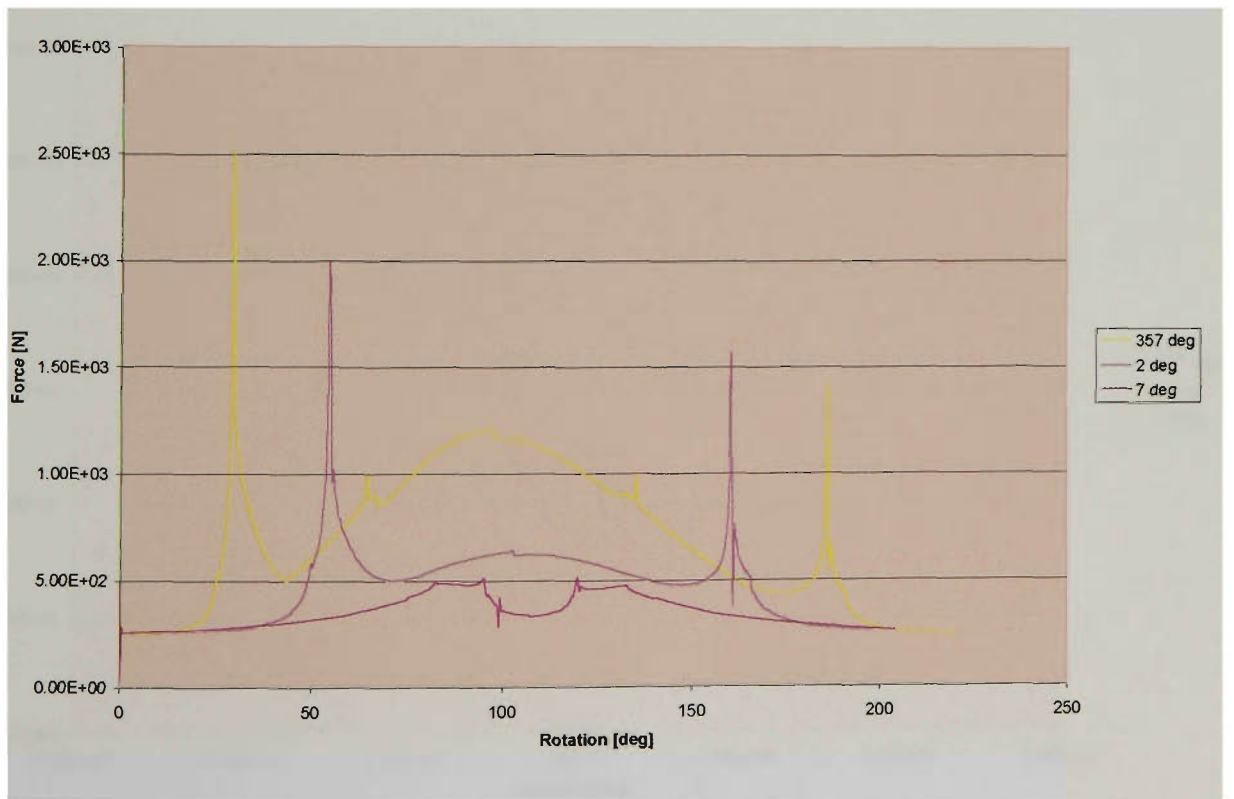


Figure 4.52 – Rockershaft Force at 18000 degrees/sec

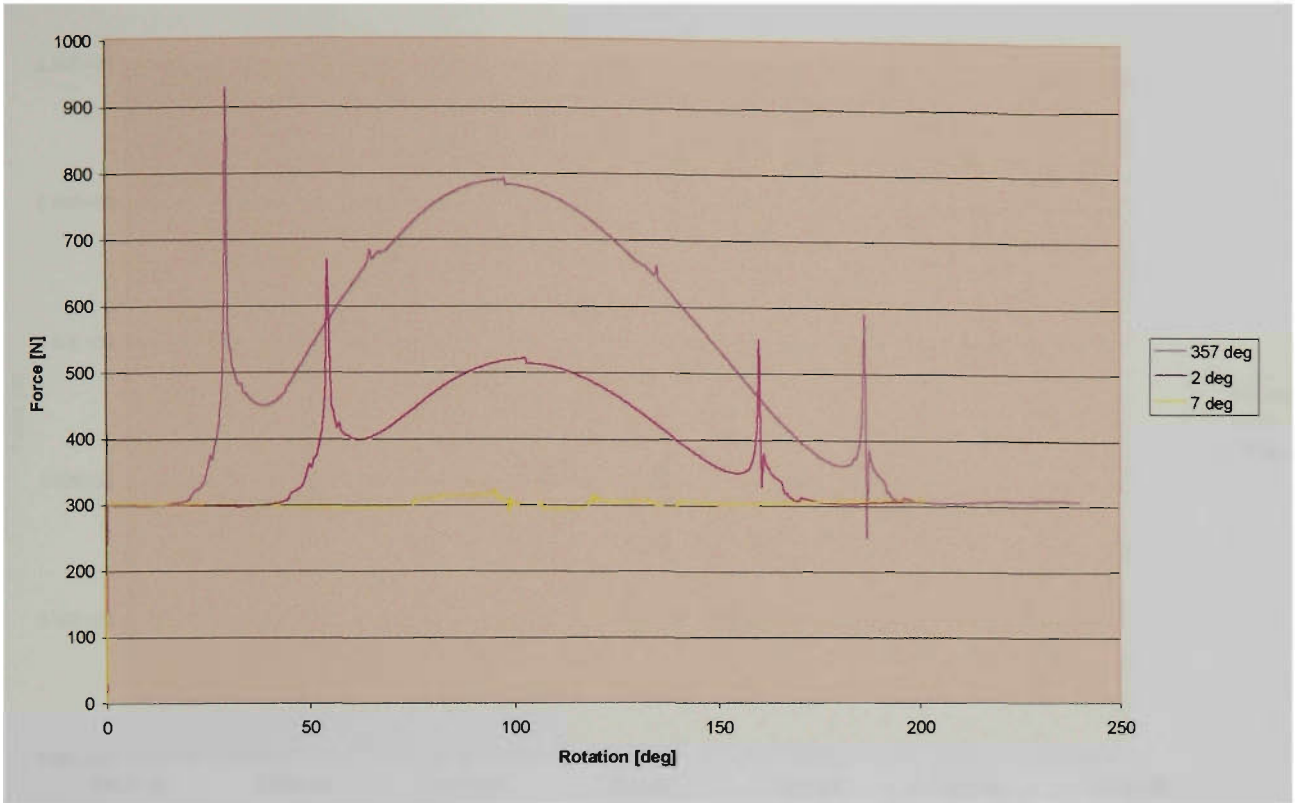


Figure 4.53 – Rocker Arm to Bucket Force at 9000 degrees/sec



Figure 4.54 – Gudgeon Pin to Guideshaft Force at 9000 degrees/sec

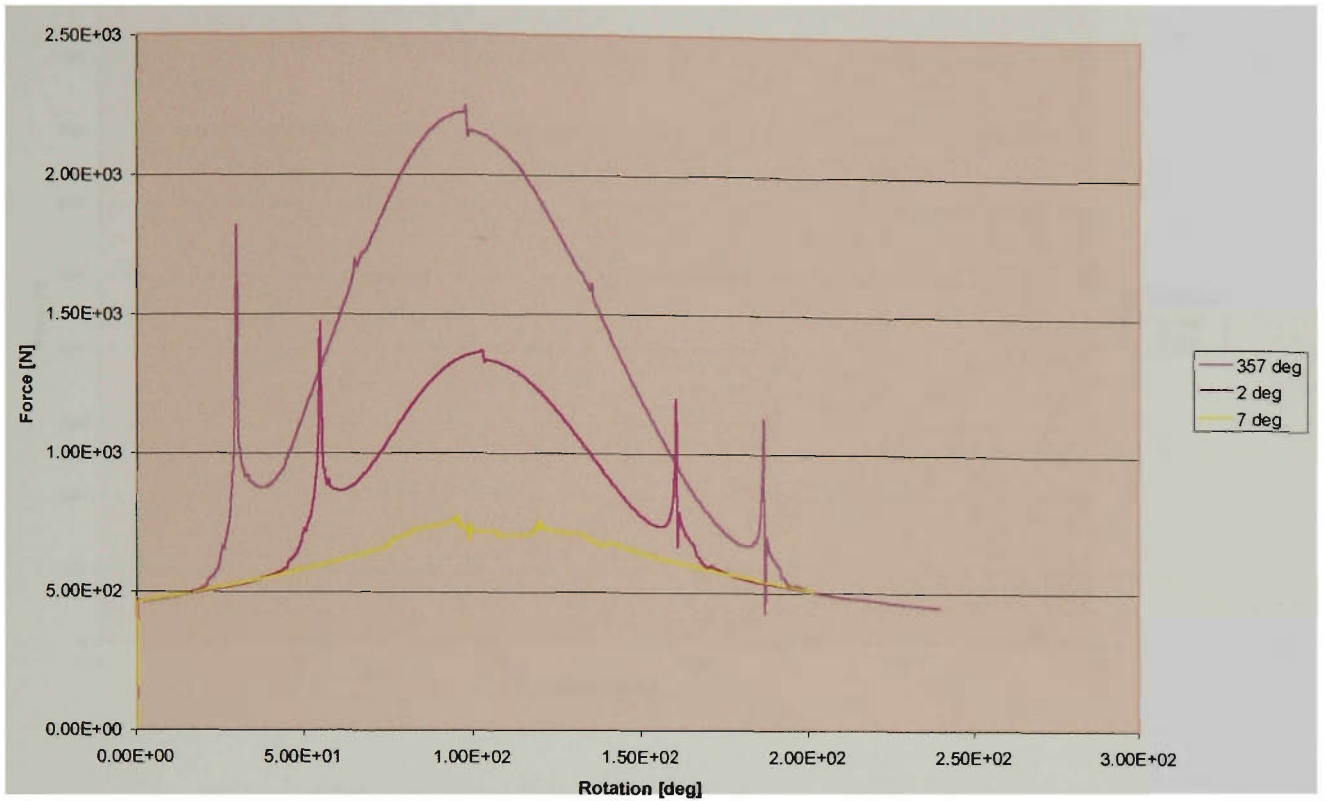


Figure 4.55 – Gudgeon Pin to Rocker Arm Force at 9000 degrees/sec

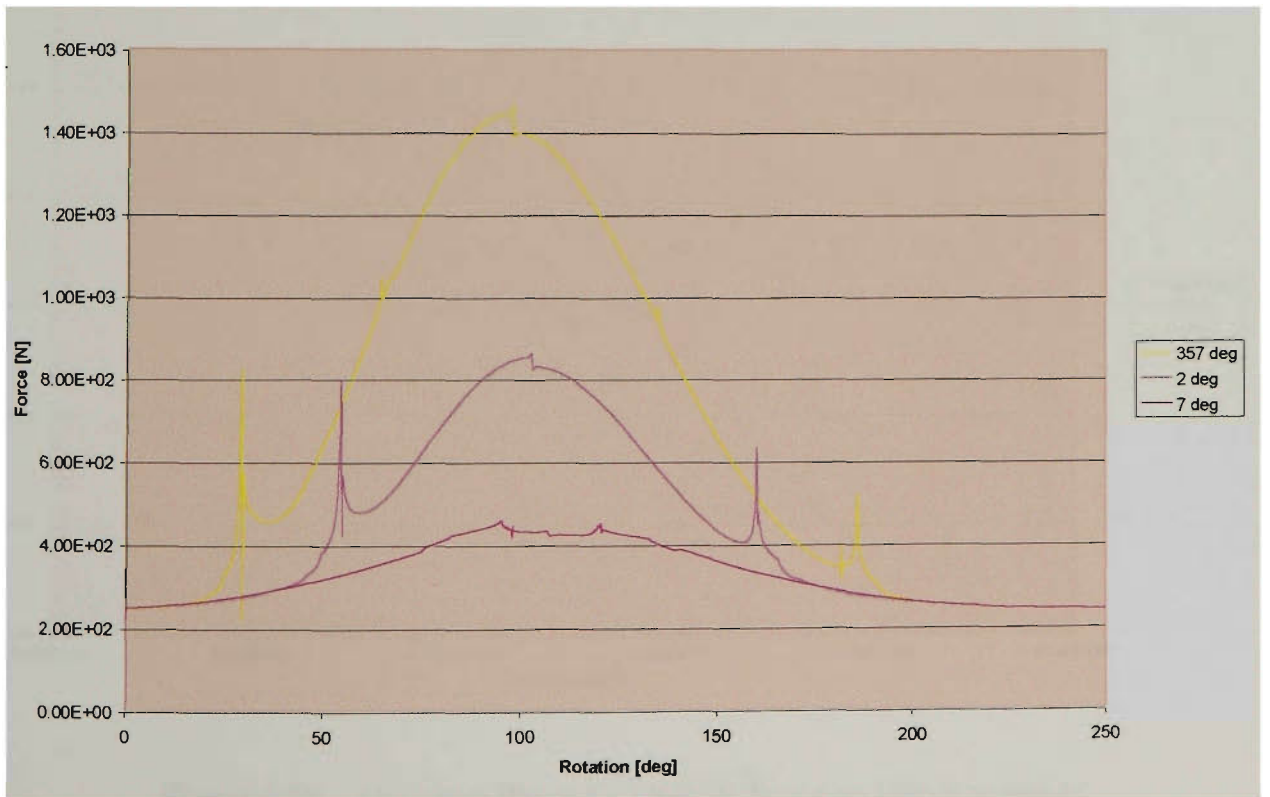


Figure 4.56 – Rockershaft Force at 9000 degrees/sec

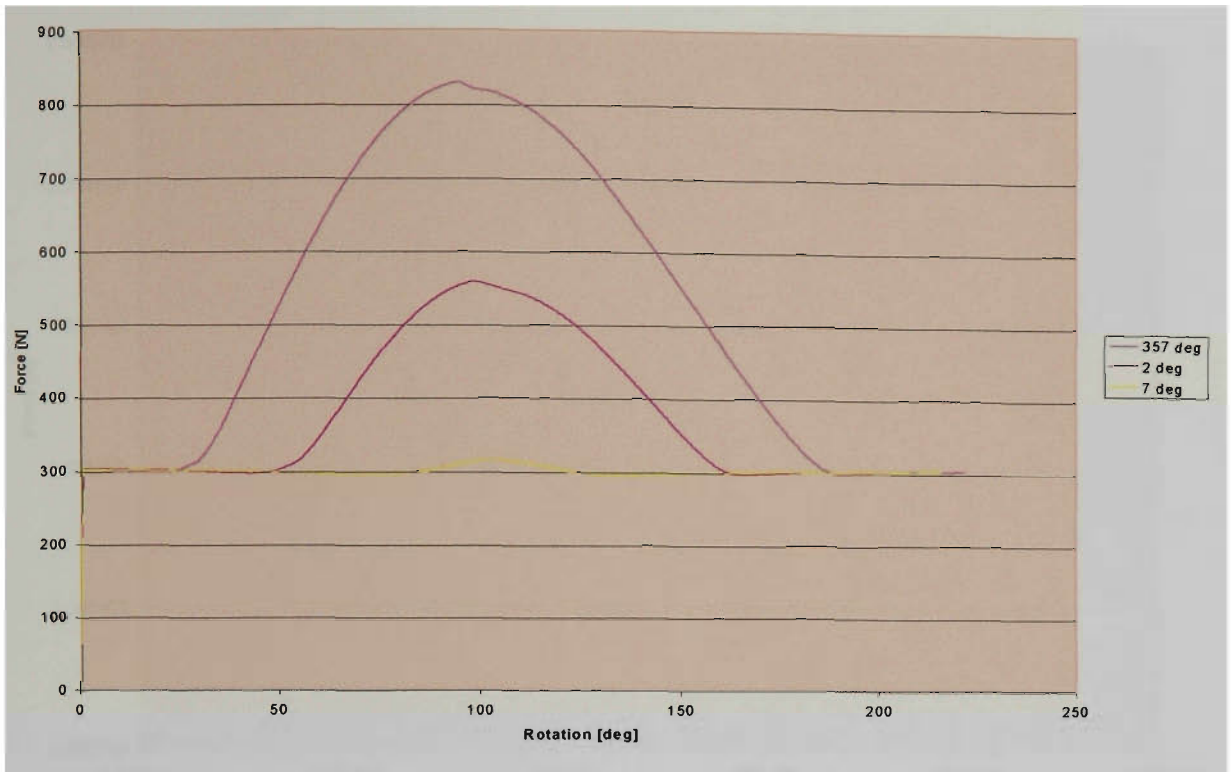


Figure 4.57 – Rocker Arm to Bucket Force at 180 degrees/sec

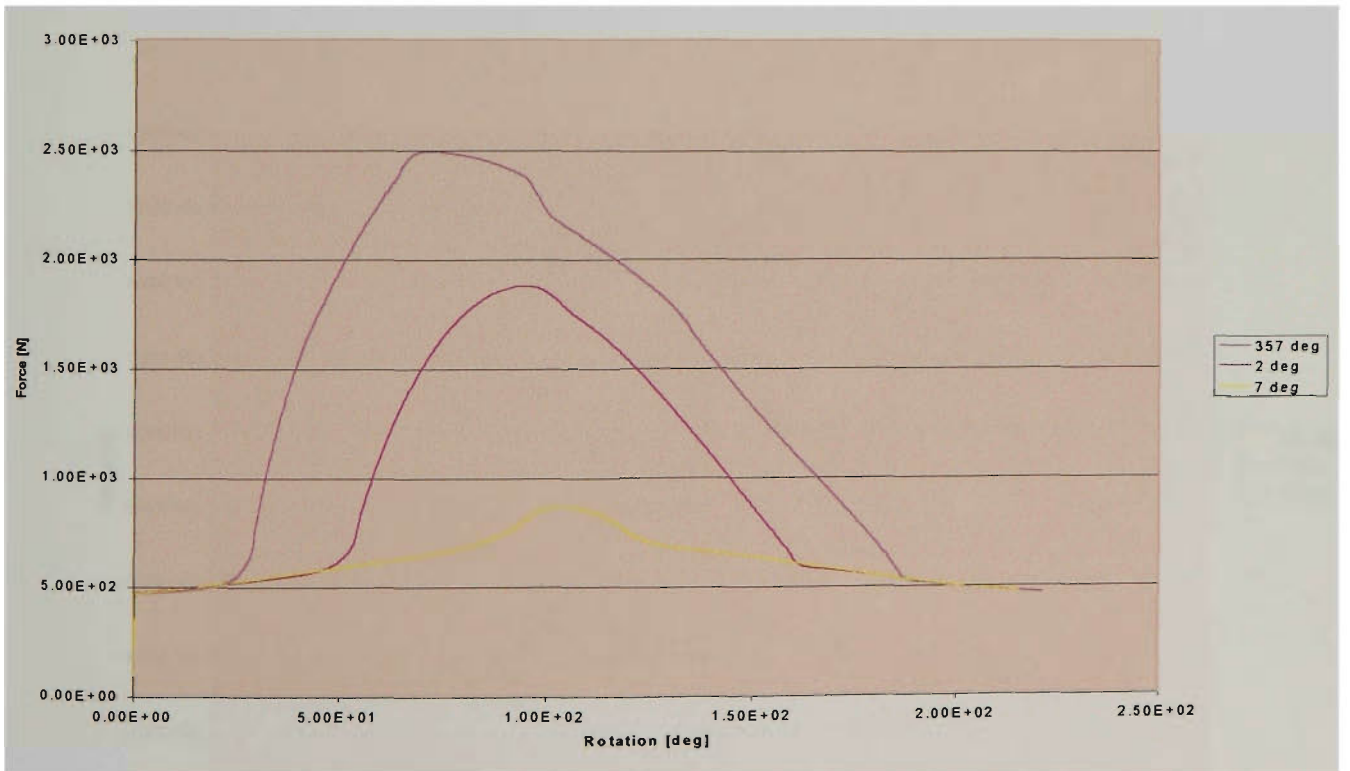


Figure 4.58 – Gudgeon Pin to Guideshaft Force at 180 degrees/sec

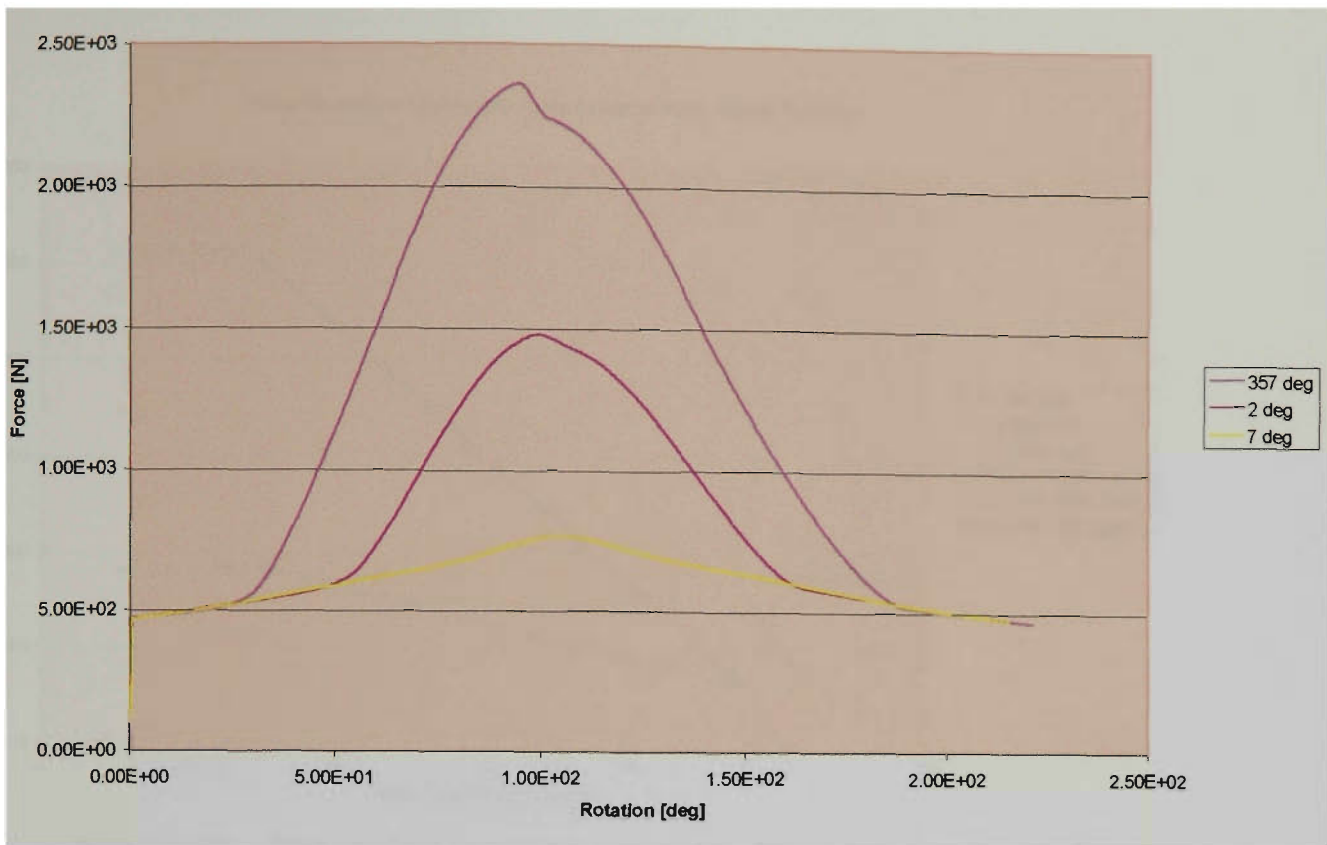


Figure 4.59 – Gudgeon Pin to Rocker Arm Force at 180 degrees/sec

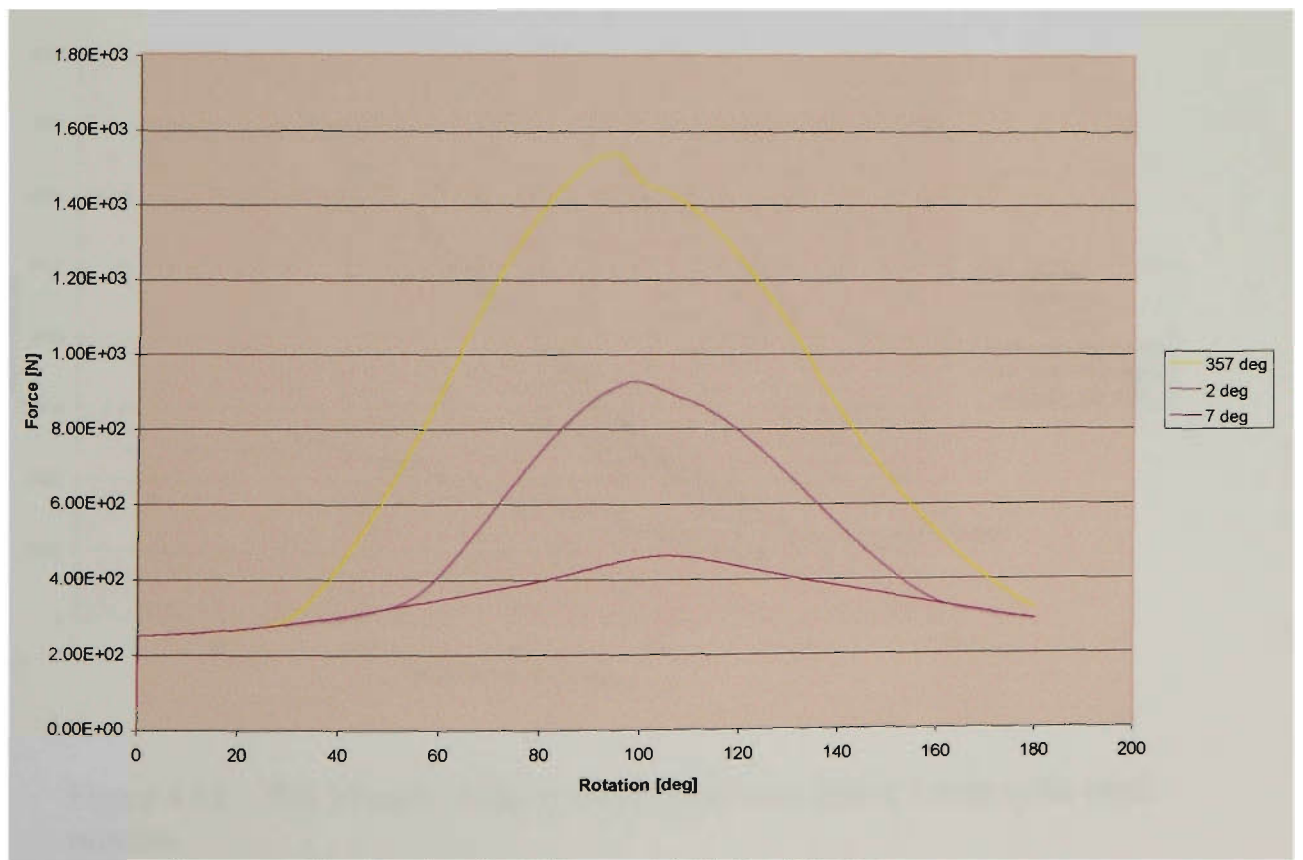


Figure 4.60 – Rockershaft Force at 180 degrees/sec

Peak Bucket to Rocker Tip Forces versus Valve Crank Rotation

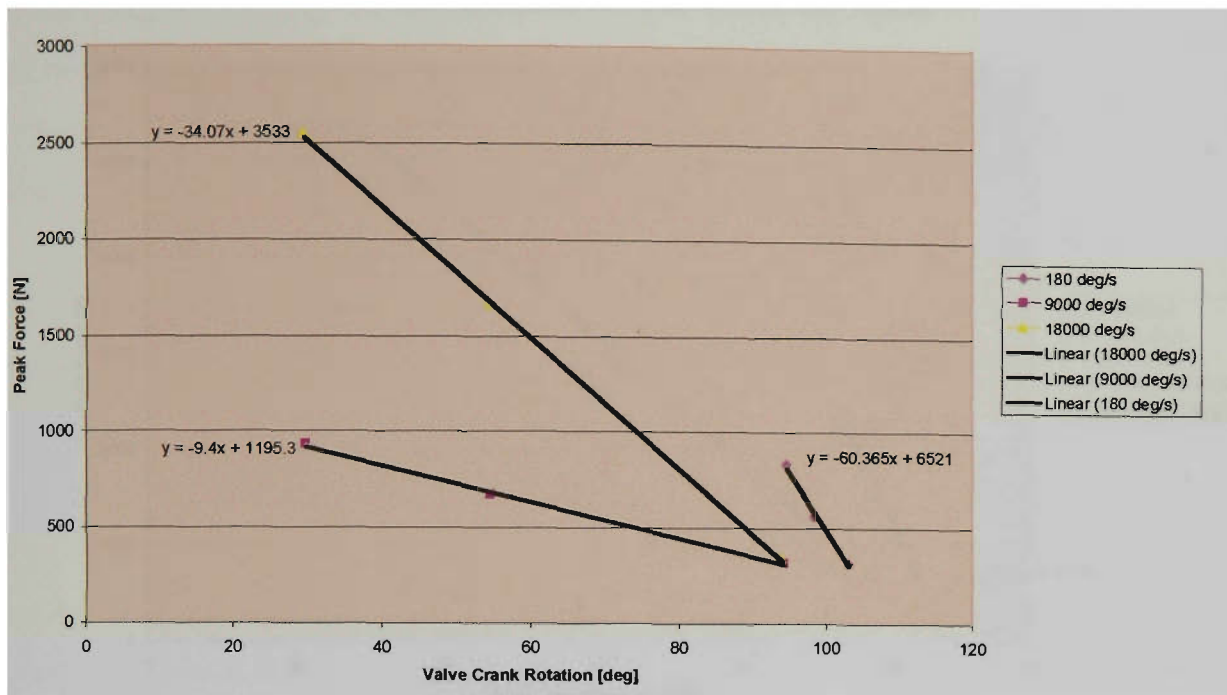


Figure 4.61 – Plot of peak bucket to rocker arm forces versus valve crank rotation

Peak Pin to Guide Forces versus Valve Crank Rotation

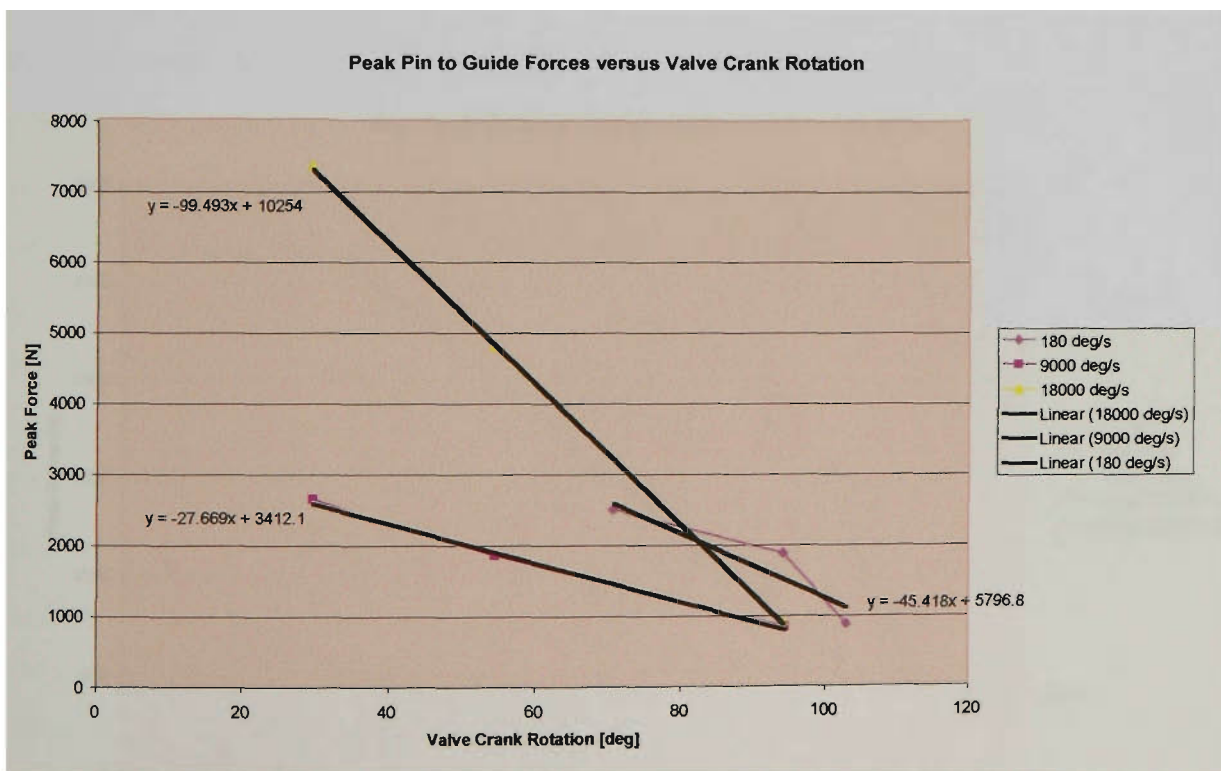


Figure 4.62 – Plot of peak gudgeon pin to guideshaft forces versus valve crank rotation

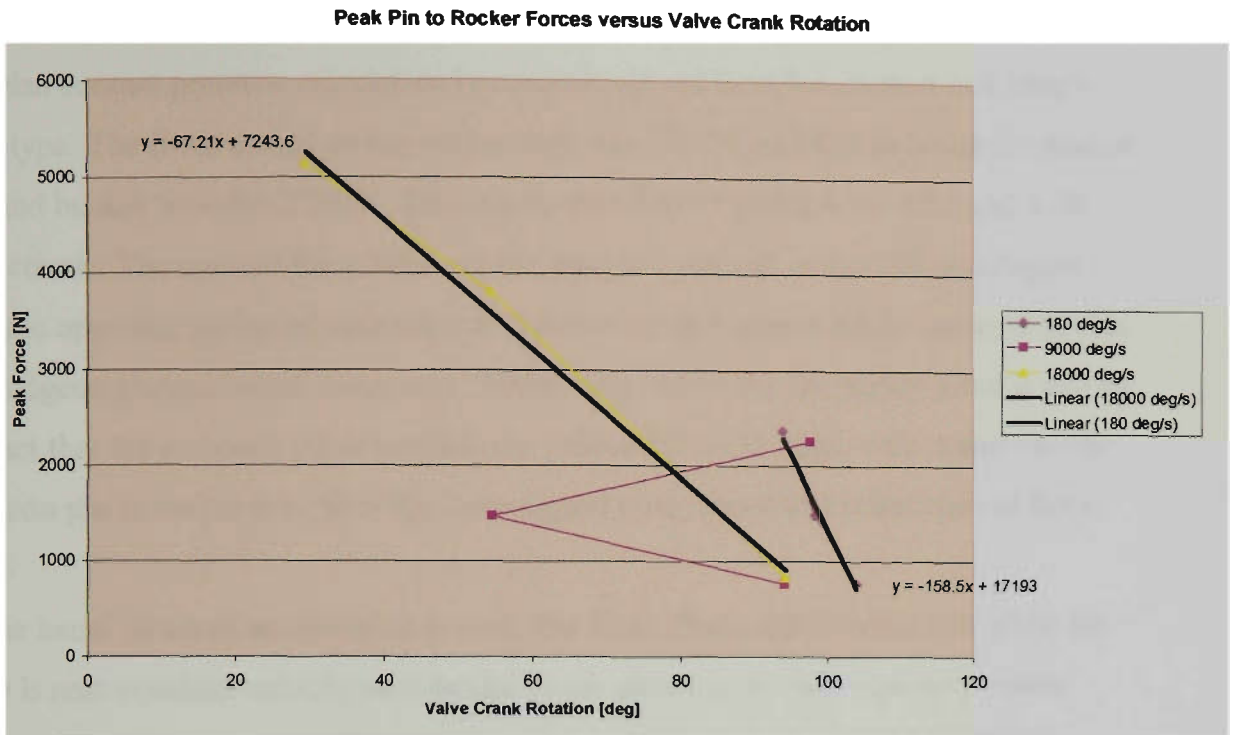


Figure 4.63 – Plot of peak gudgeon pin to rocker arm forces versus valve crank rotation

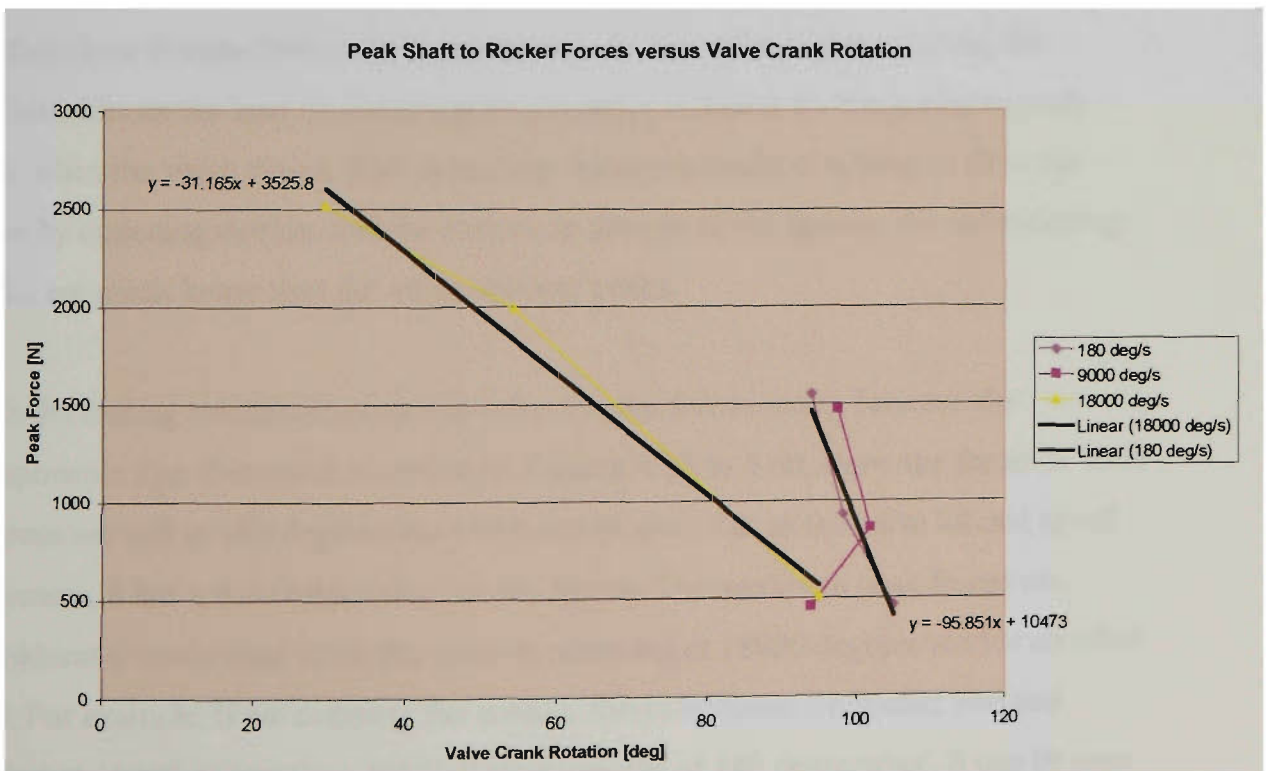


Figure 4.64 – Plot of peak rockershaft forces versus valve crank rotation

At maximum speed of 18000 degrees/sec and maximum lift, a maximum gudgeon pin/rocker arm contact force of 5000N was obtained. This force is necessary for determining the bending load on the rocker arm. It has not been considered for Hertzian contact pressure calculation because it will not be a line contact in a future prototype. The force acting on the rockershaft was 2500N and that between the rocker arm and bucket was also 2500N. This can be seen from Figures 4.51, 4.52 and 4.49 respectively. The contact force between the gudgeon pin and guideshaft was higher than the opposing gudgeon pin/rocker arm force. From Figure 4.50, it can be seen that the gudgeon pin/guideshaft force was 7300N. The reason for the higher force is due to the fact that the gudgeon pin is pushing the guideshaft on an angle with respect to the gudgeon pin to rocker arm. It is this non-aligned component that raises the net force.

As the initial thrust of acceleration is over, the force drops and remains low while the valve is near constant velocity as it begins to get closer to its fully opened position. When the valve reaches its fully opened position, an opening force of 650N was obtained between the rocker arm/bucket, 2000 N between gudgeon pin/guideshaft, 1800 N between gudgeon pin/rocker arm and 1200 N for the rockershaft. Fully open, the valve stops and then changes direction, therefore the force is not constant, due to the fact there is some friction to be overcome. As the valve begins to close, the friction reduces the load on the gudgeon pin and it is harder for the spring to push back when the valve closes. This is because friction actually is helping to slow the valve by opposing motion, and the reason, as seen in all the figures, the valve closing peaks are much lower than the valve opening peaks.

With decreasing rotational speed and valve lift, the forces acting between the components also decreased accordingly. Figures 4.53 to 4.60, show the forces at 9000 degrees/sec and at 180 degrees/sec and it can be seen that as the valve lift and speed decreases, it has a noticeable effect on the forces. The maximum peak forces are considerably lower than when the valve is operating at 18000 degrees/sec for all valve lifts. For example, if we compare the contact forces between the rocker arm and bucket at 18000 degrees/sec, 9000 degrees/sec and at 180 degrees/sec, it can be seen

that the contact forces are much lower at decreasing speeds. The contact force between the rocker arm and bucket at 18000 degrees/sec, as mentioned previously was 2500 N. From Figure 4.53, it can be seen that at 9000 degrees/sec, the contact force between the rocker arm and bucket is 920 N. At the maximum speed of 18000 degrees/sec, the contact force obtained between the gudgeon pin and guideshaft was 7300 N, while at 9000 degrees/sec, the contact force decreased to 2700 N. The contact force between the gudgeon pin and rocker arm at 9000 degrees/sec was 1600 N, while at 18000 degrees/sec it was 5000 N. The force acting on the rockershaft at 9000 degrees/sec was 800 N, as compared to 2500 N at 18000 degrees/sec.

At 180 degrees/sec, it can be seen from the figures that for all the components, the only contact force acting is the spring force of 300 N, as the system is virtually operating at idle, and inertia is nearly zero.

The guideshaft position also affects the contact forces. The lower the valve lift the less the contact force between the components. For example the contact force obtained between the rocker arm and bucket, when the guideshaft is at maximum lift (357 degrees), was 2500 N, as shown in Figure 4.49. While when the guideshaft was at mid-range lift (2 degrees), the contact force was 1600 N. The contact force obtained between the gudgeon pin and guideshaft at maximum lift, was 7300 N, while at mid-range lift, the force decreased to 4800 N, as shown in Figure 4.50. While the contact forces acting between the gudgeon pin and rocker arm and on the rockershaft also decreased between maximum lift and mid-range lift.

At 9000 degrees/sec, again the contact forces are lower at lower valve lifts, than at maximum valve lift. Figure 4.53 shows the contact force between the rocker arm and bucket, and it can be seen that the contact force at maximum lift, was 920 N, while at mid-range lift, it was 660 N. The contact force between the gudgeon pin and guideshaft at maximum lift was 2600 N, while at mid-range lift, it was 1700 N, as seen in Figure 4.54. The contact force between the gudgeon pin and rocker arm at maximum lift was 1750 N, while at mid-range lift it was 1450 N. While the contact force acting on the rockershaft at maximum lift was 800 N and at mid-range lift 780 N.

At minimum lift (7 degrees anti-clockwise guideshaft adjustment), it can be seen from all the figures, that at 18000 degrees/sec and at 9000 degrees/sec, the only force acting was the spring force because the valve lift is virtually zero. While at 180 degrees/sec as seen from Figures 4.57 to 4.60, whether at maximum lift or at minimum lift, the only force acting was the spring force because inertia was low.

The results show that the forces vary with valve lifts and speeds, a higher valve lift and speed produces higher forces. The reason that the forces are lower at decreasing speeds and valve lifts, is due to the fact that once the valve begins to move off its seat the change in momentum is not as great, as it is at higher speeds and higher valve lifts.

The highest contact force peaks between all the components occur as the valve is beginning to open. This is due to the fact that as the valve begins to be pushed open, it must accelerate off the valve seat and in addition during opening the friction resists the acceleration.

From the peak force figures it can be seen that the forces acting between the components are linear except for the peak force of the rockershaft when the system is operating at 9000 degrees/sec. Also the peak gudgeon pin to the rocker arm force when the system is also operating at 9000 degrees/sec is not linear. This can be seen from Figures 4.64 and 4.63 respectively. The non-linearity is due to the fact that the peaks occur at different phases of motion. This is probably due to friction on the valve and also the way in which the gudgeon pin moves along the guideshaft and rocker arm.

4.5.2 Stress Analysis

The stress analysis of the rocker arm was conducted using Cosmos/DesignStar. Cosmos/DesignStar is a FEA package that allows stress analysis on components created in any of the major CAD packages.

The rocker arm, as previously stated was created in SolidWorks, and subsequently it was imported into Cosmos/DesignStar in a first attempt to evaluate whether it could withstand the loads acting on it. The rocker arm as imported into Cosmos/DesignStar is shown in Figure 4.65.

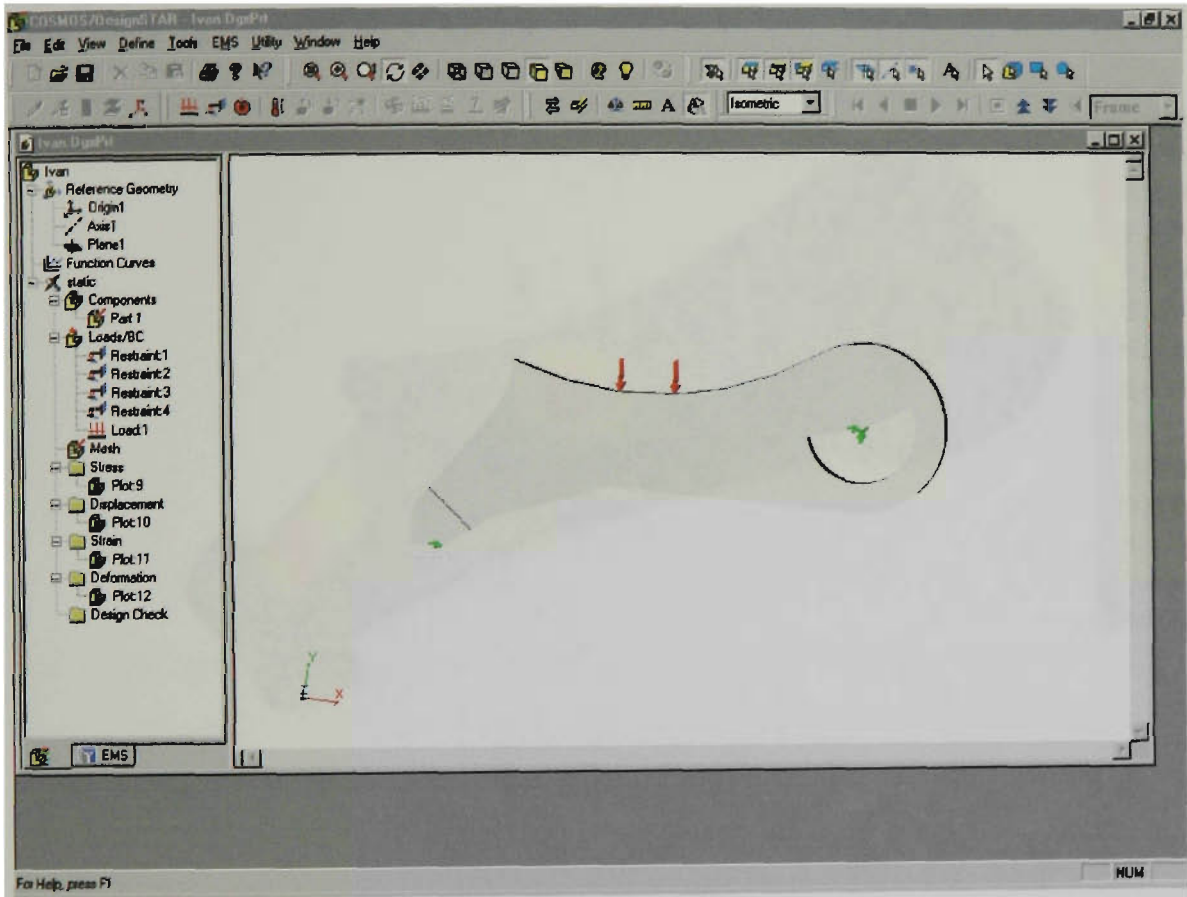


Figure 4.65 – FEA of rocker arm in Cosmos/DesignStar

Once the rocker arm was imported into Cosmos/DesignStar, the type of analysis performed needed to be selected and the material of the component defined. Static analysis was selected and the material for the rocker arm selected was ASTM 40-41 alloy steel.

Once the material and type of analysis were selected, the rocker arm had to be constrained. A load of 5000 N acting on the top of the rocker arm was defined, with a fixed constraint acting on the pivot, and a prescribed constraint which allowed

translation in the x direction only, acting at the tip of the rocker. Once the constraints on the rocker arm were defined, the component was meshed, and the analysis of the rocker arm was completed. The FEA results of the rocker arm can be seen in Figures 4.66 to 4.67.

Ivan-static :: Static Nodal Stress
Units : N/m² Deformation Scale 1 : 5.87864

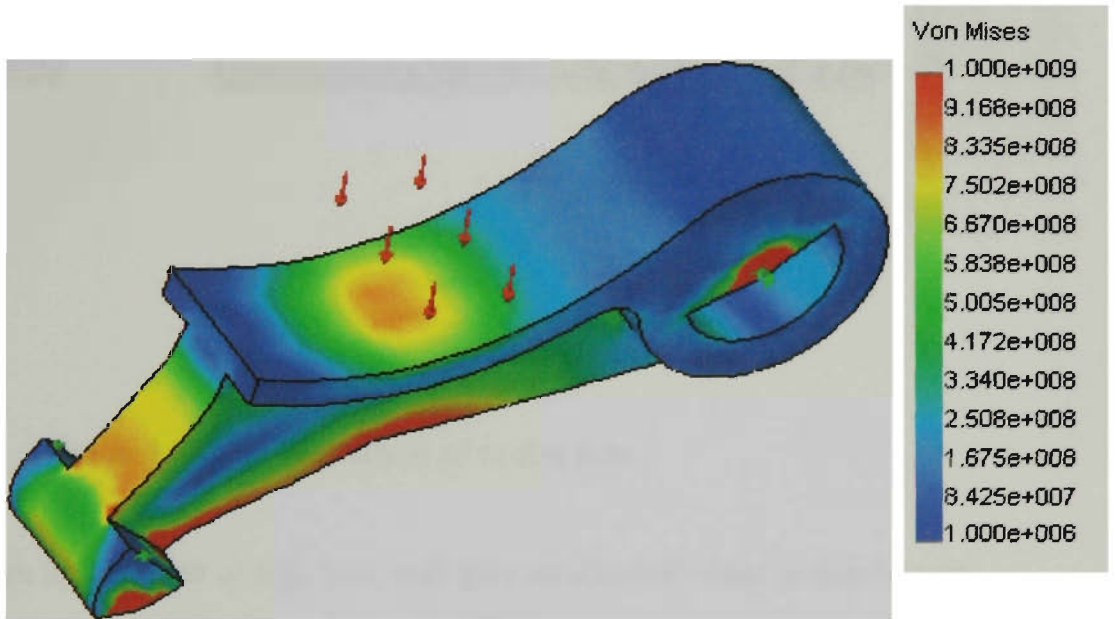


Figure 4.66 – FEA Analysis of rocker arm

Ivan-static :: Static Nodal Stress
Units : N/m² Deformation Scale 1 : 5.87864

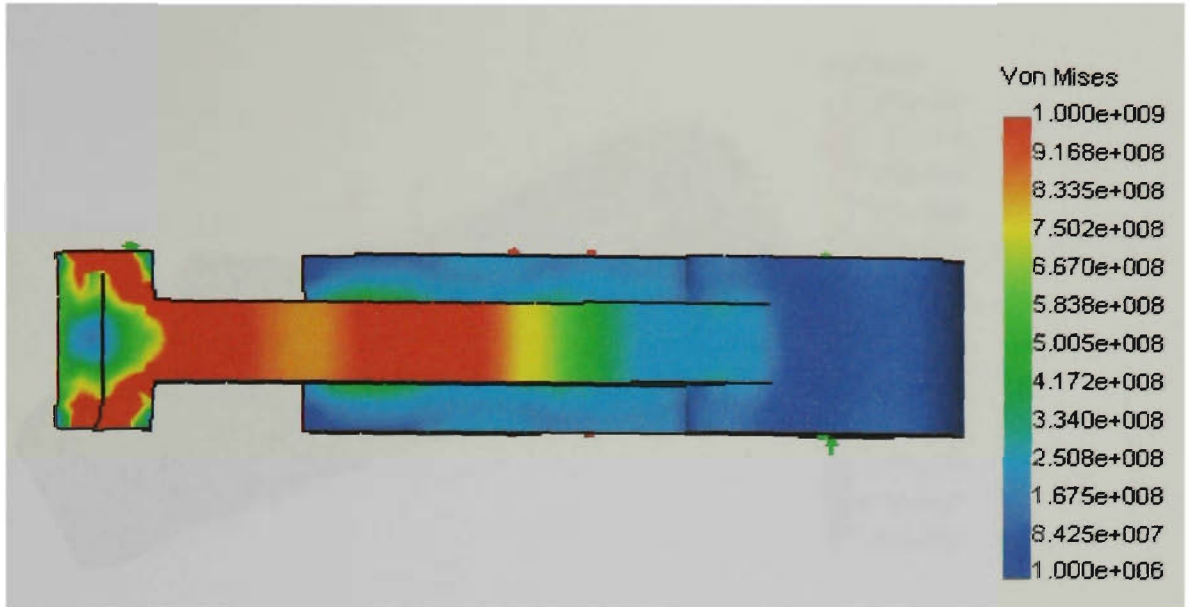


Figure 4.67 – FEA Analysis of rocker arm

The maximum fatigue limit of fully reversed alloy steel is 500 Mpa. As can be seen from Figures 4.66 and 4.67, the rocker arm exhibits excessive stress, especially in the centre on the non-contact side, as seen in Figure 4.67.

Component design and FEA analysis is an iterative process and in order to reduce this stress, gradual changes such as strengthening the non-contact side of the rocker arm, by thickening the rocker vertical and adding a flange to the non-contact side, were tried and the resulting stress patterns, as seen in Figure 4.68 to 4.69 are shown.

ROCKERFEA15-cosi :: Static Nodal Stress
Units : N/m² Deformation Scale 1 : 8.78259

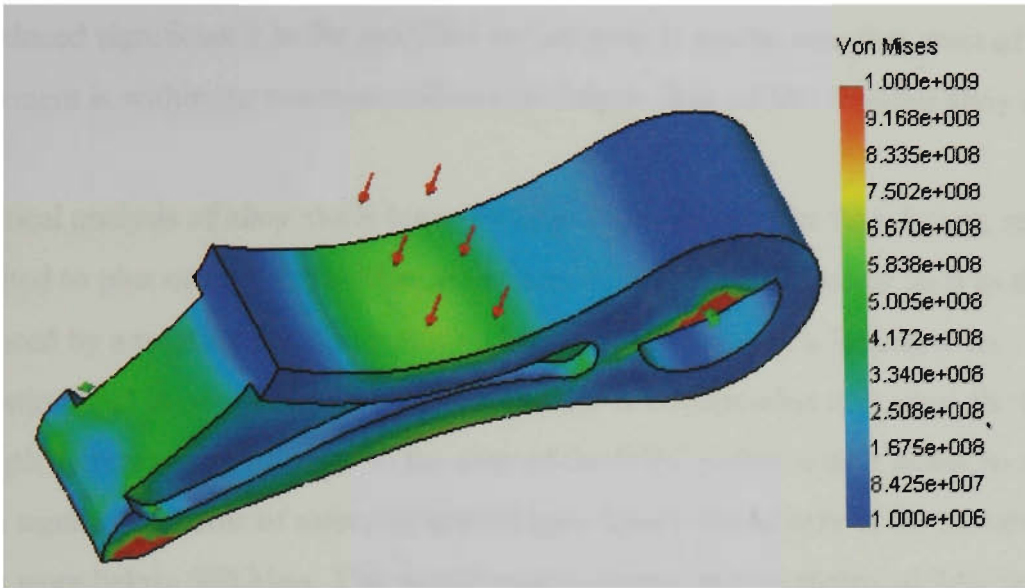


Figure 4.68 – FEA Analysis of modified rocker arm

ROCKERFEA15-cosi :: Static Nodal Stress
Units : N/m² Deformation Scale 1 : 8.78259

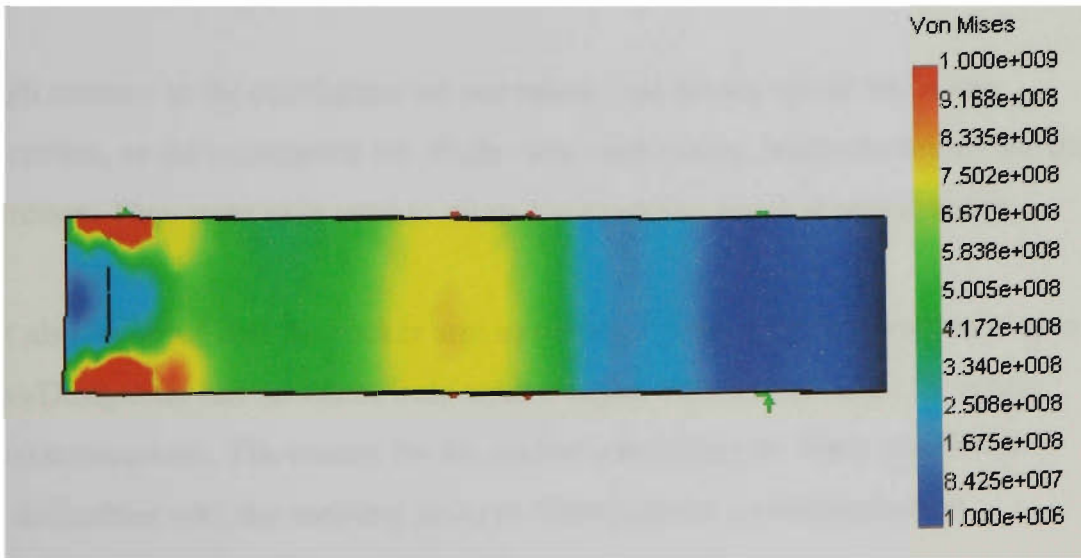


Figure 4.69 – FEA Analysis of modified rocker arm

As can be seen from Figures 4.68 and 4.69, the stress concentrations of the rocker arm are reduced significantly in the modified rocker arm. It can be seen that most of the component is within the maximum allowable fatigue limit of 500 Mpa for alloy steel.

Statistical analysis of alloy steels (case hardened) has shown that their fatigue strength is limited to plus or minus 500 Mpa in the case of fully reversed stress such as that produced by a rotating beam in bending. However if the stress is limited to an oscillating load in one direction of either tension or compression only, then the fatigue strength increases to 800 Mpa. In the case of the DVC rocker arm, it could be argued that a significant factor of safety against fatigue failure would arise if the maximum stress were below 500 Mpa. This would guard against any possibility of fully reversed stress. However, due to the limited space available for the rocker arm in the standard Vectra cylinder head, the stress due to bending across the restricted centre section remained above 500 Mpa through several design iterations, as seen in Figure 4.69. Given the nature of the rocker arm's operation, it is unlikely that the stress will be reversed. Therefore, it is likely that the rocker arm will not suffer a fatigue failure because the maximum stress is below 800 Mpa.

The high stresses at the constraints are unrealistic and should not be taken into consideration, as the constraints are single dimension points, hence the reason for the high stresses. They were only used to allow the model to function appropriately.

It must also be noted that the rocker arm as modeled using ADAMS and analysed in Cosmos/DesignStar has no fillets, only square edges, which is not ideal for actual stress concentrations. The reason for the rocker arm having no fillets was that it avoids difficulties with the meshing process. However the actual production component would have fillets and the rocker arm would be stronger.

4.5.3 Hertz Contact Pressure

The preferred standard production cylinder head material is nodular iron, for high stress surfaces such as camshafts. According to Gaffney and Redington (1998), nodular iron can withstand contact pressures of up to 1700 MPa.

The maximum Herztian contact pressure obtained between the gudgeon pin and guideshaft was 996 MPa (refer to Appendix C). However, the guideshaft and gudgeon pin will be made from ASTM 40-41 alloy steel, which is a stronger material than nodular iron. The alloy steel would be case hardened, which would give it a satisfactory contact resistance.

5 CONCLUSIONS AND RECOMMENDATIONS

5.1 Conclusions

A cylinder head test rig was constructed to measure the valve lift profile of the standard Vectra engine cylinder head. The DVC system was successfully simulated using ADAMS software for its valve lift profile and loads acting on the components. The stress analysis of the key component of the DVC system, the rocker arm was carried out.

The following conclusions can be drawn from the research reported here:

- The valve lift profile of a standard Vectra engine was determined using the test rig constructed for that purpose.
- Simulation of the proposed DVC system demonstrated that the system has variable lift characteristics which can achieve any valve lift between maximum and minimum, according to engine speed.
- According to the results of the DVC simulation, a maximum valve lift of 10.70 mm was attained compared to a maximum of 9 mm for the standard Vectra engine.
- The minimum lift obtained during simulation of the DVC system was practically zero, therefore it seems reasonable to infer that a throttle would not be required with the proposed system.

- Analysis of the rocker arm indicated that the loads imposed on it would not lead to failure under repeated bending loads, while the Hertzian contact pressure between the gudgeon pin and the guideshaft was within the maximum allowable contact pressure.

5.2 Recommendations for Future Work

The following recommendations are proposed for future research:

- A DVC system should be designed, constructed and fitted to the existing Vectra engine.
- Performance tests on the Vectra engine with the DVC system including fuel consumption and emission tests, should be carried out and compared with results obtained from the standard Vectra engine.

6 REFERENCES

Ashley, C., (1995), Powertrain Development, *Automotive Engineer*, Vol. 20, pp. 20

Bassett, M.D., Blakey, S.C. and Foss, P.W., (1997), A Simple Two-State Late Intake Valve Closing Mechanism, *Proc. I. Mech.* Vol. 211.

Brauer, K, (1999), Valve Timing is Everything, *www.edmunds.com*

Crohn, M. and Wolf, K., (1990), Variable Valve Timing in the New Mercedes-Benz Four-Valve Engines, *SAE 891990*

Deeg, E.W., (1992), New Algorithms for Calculating Hertzian Stresses, Deformations, and Contact Zone Parameters, *AMP Journal of Technology*, Vol.2, pp.14 – 22

Desantes, J., Payri, F. and Corberan, J., (1988), A Study of the Performance of a SI Engine Incorporating a Hydraulically controlled Variable Valve Timing System, *SAE 880604*

Douglas, E., (1997), EVA Meet Demands for Performance and Economy, *Southwest Research Institute*

Edgar, J, (2001), BMW Valvetronic, *www.autospeed.com*

Gaffney, J. and Redington, P., (1998), Things to Know about Cam Grinding, *Automotive Design and Production*, www.autofieldguide.com

Griffiths, P. and Mistry, K.N., (1988), Variable Valve Timing for Fuel Economy Improvement – The Mitchell System, *SAE 880392*

Hannibal, W. and Bertsch, A., (1998), VAST: A New Variable Valve Timing System for Vehicle Engines, *SAE 980769*

Hara, S. and Kumagai, K., (1989), Application of a Valve Lift and Timing Control System to an Automotive Engine, *SAE 890581*

Hara, S., Nakajima, Y. and Nagumo, S., (1985), Effects of Intake-Valve Closing Timing on Spark-Ignition Engine Combustion, *SAE 850074*

Hatano, K., Iida, K., Higashi., H. and Murata, S., (1993), Development of a New Multi-Mode Variable Valve Timing Engine, *SAE 930878*

Herrin, R. and Pozniak, D., (1984), A Lost-Motion, Variable Valve Timing System for Automotive Piston Engines, *SAE 840335*

Heywood, J., (1988), *Engine Fundamentals*, McGraw-Hill

Hosaka, T. and Hamazaki, M., (1991) Development of the Variable Valve Timing and Lift (VTEC) Engine for the Honda NSX, *SAE 910008*

Hu, H., (1996), Four-Cycle Internal Combustion Engine with Two-Cycle Compression Release Braking, *SAE 961123*

Kreuter, P., Heuser, P. and Reinicke, J., (1998), The Meta VVH System – A Continuously Variable Valve Timing System, *SAE 980765*

Lee, J., Lee, C. and Nitkiewicz, J., (1995), The Application of a Lost Motion VVT System to a DOHC SI Engine, *SAE 950816*

Leone, T.G., Christenson, E.J. and Stein, R.A., (1996), Comparison of Variable Camshaft Timing Strategies at Part Load, *SAE 960584*

Lenz, H.P. and Wichart, K., (1988), Variable Valve Timing – A Possibility to Control Engine Load without Throttle, *SAE 880388*

Ma, T.H., (1988), The Effect of Variable Engine Valve Timing, *SAE 880390*

Maekawa, K. and Ohsawa, N., (1989), Development of a Valve Timing Control System, *SAE 890680*

Matsuki, M., Nakano, K., Amemiya, T., Tanabe, Y., Shimizu, D. and Ohmura, I., (1996), Development of a Lean Burn Engine with a Variable Valve Timing Mechanism, *SAE 960583*

Moriya, Y., Watanabe, Uda, H., Kawamura, H. and Yosioka, M., (1996), A Newly Developed Intelligent Variable Valve Timing System – Continuously Controlled Cam Phasing as Applied to a New 3 Litre Inline 6 Engine, *SAE 960579*

Nakayama, Y., Maruya, T., Oikawa, T. and Fujiwara M. (1994), Reduction of HC Emission from VTEC Engine During Cold-Start Condition, *SAE 940481*

Ohya, Y. and Fujieda, M., (1995), A New Engine Control System Using Direct Fuel Injection and Variable Valve Timing, *SAE 950973*

Payri, F., Boada, F. and Macian V., (1994), Reduction of Pumping Losses by the use of a Variable Valve System, *Proc. I. Mech Vol. 198*,

Saunders, R.J. and Abdul-Wahab, E.A., (1989), Variable Valve Closure Timing for Load Control and the Otto Atkinson Cycle Engine, *SAE 890677*

Schechter, M. and Llevin M. (1996), Camless Engine, *SAE 960581*

Shigley, J., (1989), Mechanical Engineering Design, *McGraw-Hill Kogakusha*

Steinberg, R., Lenz, I. and Koehnlein, G., (1998), A Fully Continuous Variable Cam Timing Concept for Intake and Exhaust Phasing, *SAE 980767*

Titolo, T., (1991), The Variable Valve Timing System – Application on a V8 Engine, *SAE 910009*

Tuttle, J., (1982), Controlling Engine Load by Means of Early Intake-Valve Closing, *SAE 820408*

Urata, Y., Umiyama, H., Shimizu, K., Fujiyoshi, Y. and Fukuo, K., (1993), A Study of Vehicle Equipped with Non-Throttling S.I Engine with Early Intake Valve Closing Mechanism, *SAE 930820*

U.S Department of Energy, (2001), Conserve Resources for Future Generations, *Why is Fuel Economy Important*, www.fueleconomy.com

U.S Department of Energy, (1998), Climate Change, *Why is Fuel Economy Important*, www.fueleconomy.com

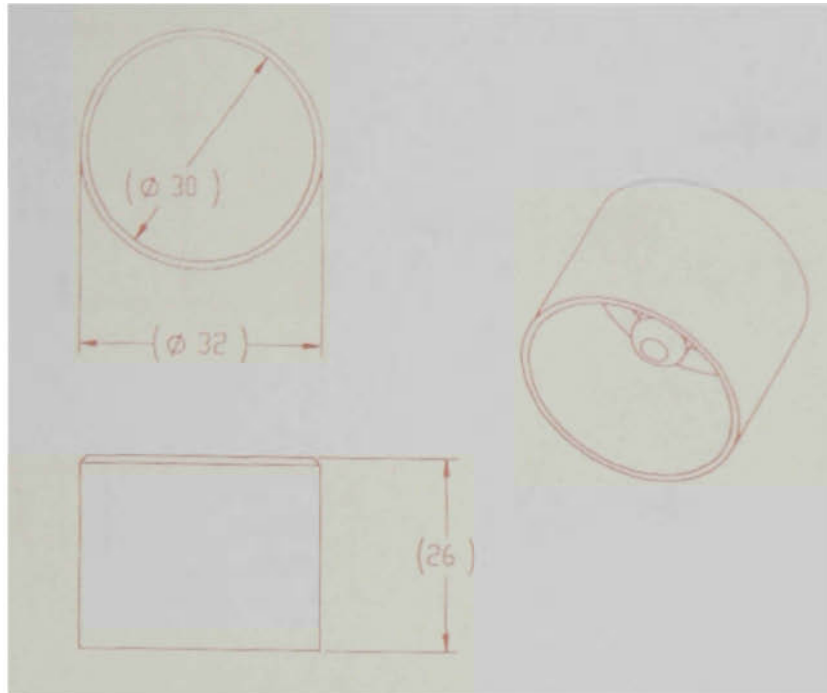
Vogel, O., Roussopoulos, K., Guzzella, L. and Czekaj, J., (1996) An Initial Study of Variable Valve Timing Implemented with a Secondary Valve in the Intake Runner, *SAE 960590*

Wilson, N., Dobson, C. and Mudell, G., (1993), Active Valve Train, *Automotive Engineer*, Vol.18, pp. 42-46

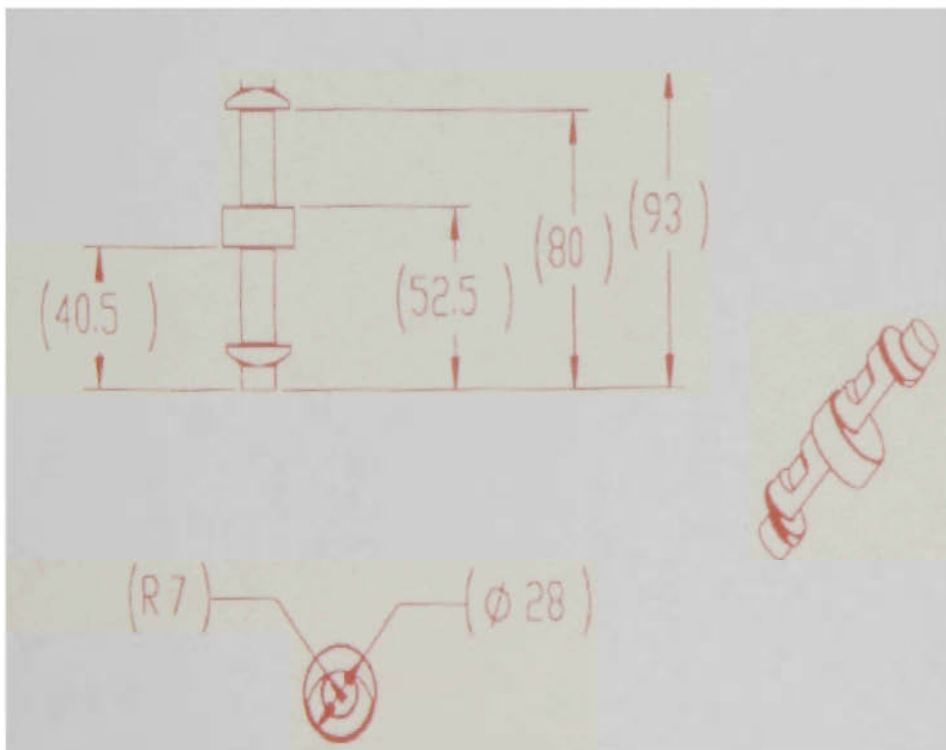
Yagi, S., Miura, S., Satoh, I., Ishibashi, Y. and Nishi, K., (1992) A New Variable Valve Engine applying Shuttle Cam Mechanism, *SAE 920451*

Appendix A – Component Measurements

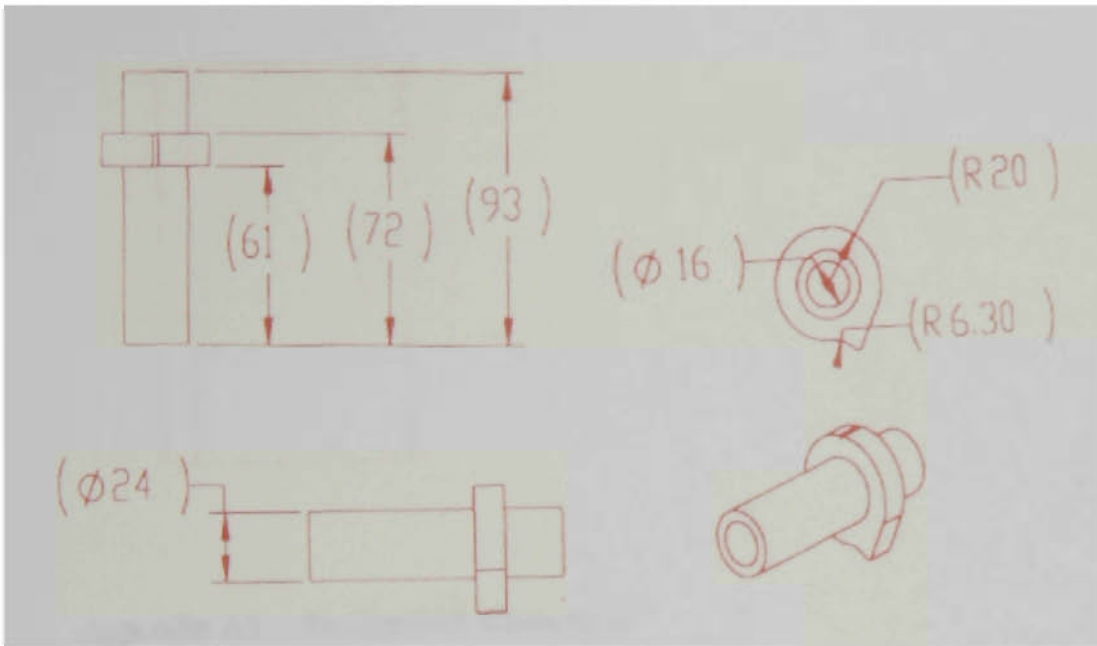
The dimensions of the DVC components (millimetres) are shown from Appendix A1 to A8.



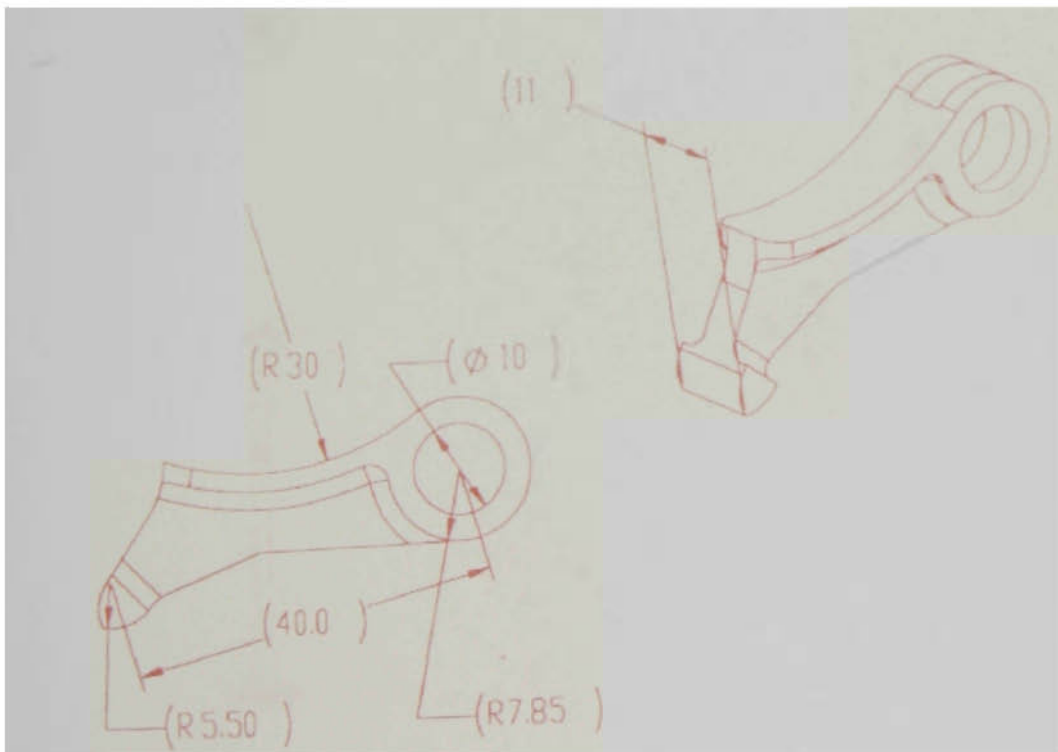
Appendix A1 – Bucket dimensions



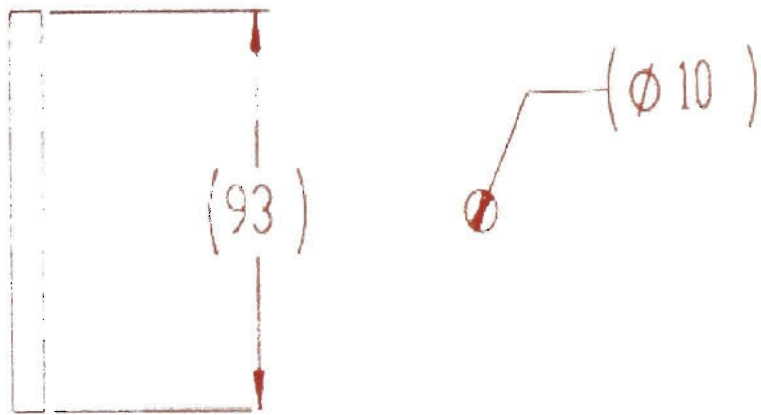
Appendix A2 – Valve Crank dimensions



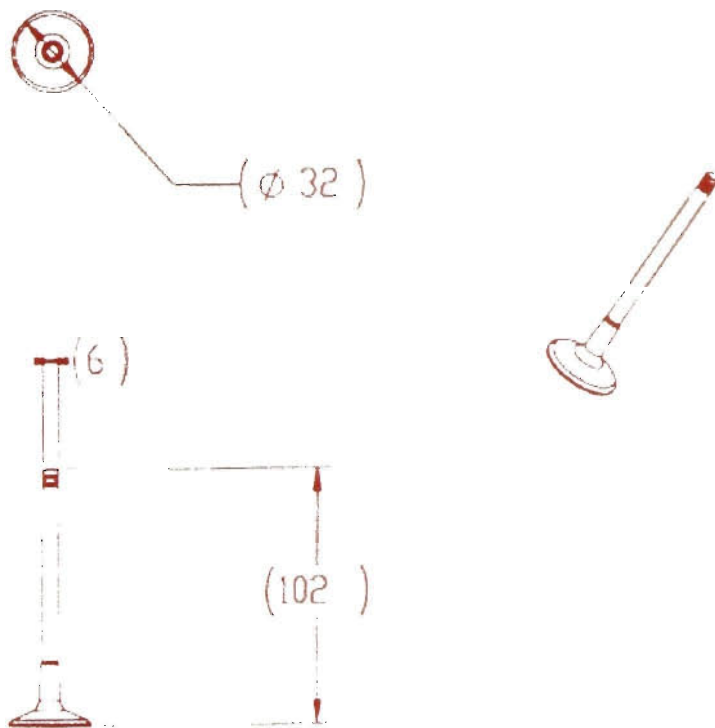
Appendix A3 – Guideshaft dimensions



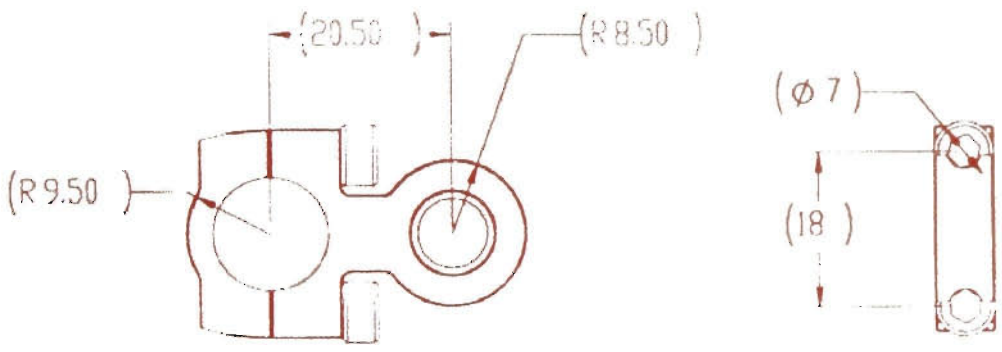
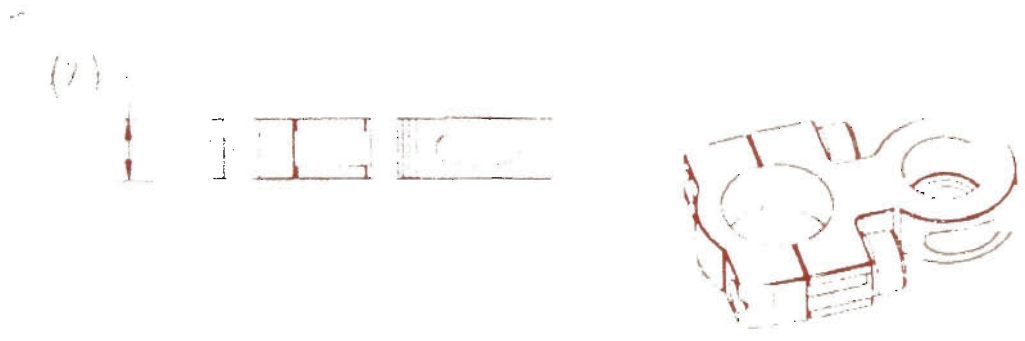
Appendix A4 –Rocker Arm dimensions



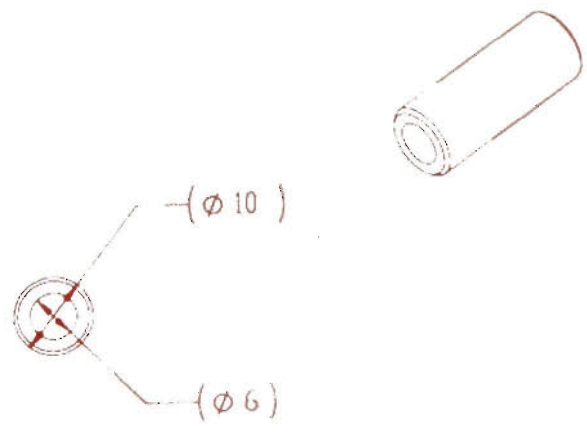
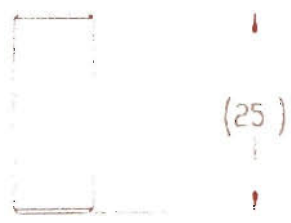
Appendix A5 – Rockershaft dimensions



Appendix A6 – Valve dimensions



Appendix A7 – Conrod dimensions



Appendix A8 – Gudgeon Pin dimensions

Appendix B – Constraint Descriptions

The descriptions of the constraints that were used in ADAMS to constrain the DVC components is shown in Table B1.

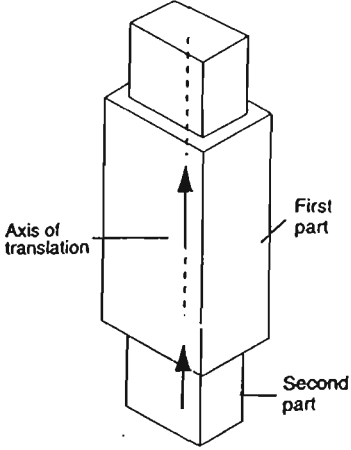
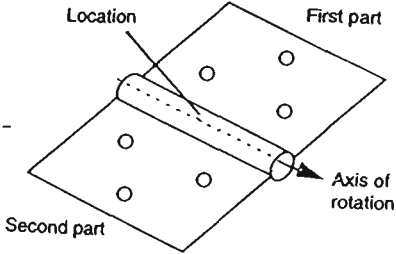
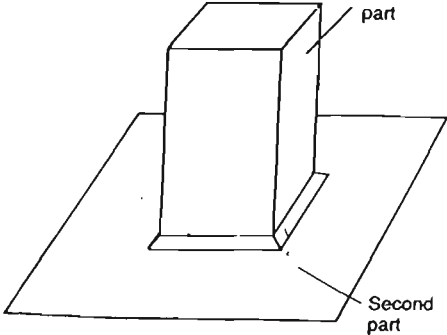
Constraints	Description
<p>Translational Joint</p> 	<p>A translational joint allows one part to translate along a vector with respect to another part. The parts can only translate, not rotate, with respect to each other.</p>
<p>Revolute Joint</p> 	<p>A revolute joint allows the rotation of one part with respect to another about a common axis. The revolute joint can be located anywhere along the axis about which the joint's parts can rotate with respect to each other.</p>
<p>Fixed Joint</p> 	<p>A fixed joint locks two parts together so they cannot move with respect to each other.</p>

Table B1 – Description of constraints

Appendix C – Hertzian Stress Calculations

The Hertzian stress calculations between the Guideshaft and Gudgeon Pin is shown in Table C1

Calculation of Hertzian Contact Pressure p_{max} of Pin to Guide Based on Adams Simulation of Maximum Contact Force		
Includes estimate of required Hardness [HB] for Endurance Strength, S_e , for reliability 0.99 to 0.999% and life $>10^8$ cycles		
<u>Calculation of contact patch half width</u>		
$1 - 0.3^2$	0.91	Poisson's Ratio equals 0.3
$(1 - 0.3^2)/E_1$	4.39614E-12	Elastic Modulus equals 207 [Gpa]
$1/d_1$	100	Pin Diameter equals 0.01 [m]
$1/d_2$	-79.36507937	Guide Diameter equals -0.0126 [m]
$1/d_1 + 1/d_2$	20.63492063	
$[(1-0.3^2)/E_1]+[(1-0.3^2)/E_2] / [(1/d_1)+(1/d_2)]$	4.26087E-13	
$2F([(1-0.3^2)/E_1]+[(1-0.3^2)/E_2] / [(1/d_1)+(1/d_2)]) / \pi L$	1.80015E-07	Force, F equals 7300 [N] & Guide Width, L equals 0.011 [m]
$SQRT(2F([(1-0.3^2)/E_1]+[(1-0.3^2)/E_2] / [(1/d_1)+(1/d_2)]) / \pi L)$	0.000424282	Contact Half Width, b [m]
<u>Calculation of contact pressure</u>		
$2F / \pi b L$	996	Maximum Contact Pressure, p_{max} [MPa]
<u>Calculation of fully reversed Shear Stress</u>		
$0.3p_{max}$	299	Maximum sub surface reversed Shear Stress, T_{max} [Mpa]
<u>Calculation of required surface hardness</u>		
$(S_e + 70) / 2.76$	386	Required Hardness [HB] (Brinell Hardness number)

Table C1 – Calculation of the Hertzian stress between the gudgeon pin and guideshaft